

THE UNIVERSITY OF MANITOBA

SCOUR AT CONSTRICTIONS DUE TO
ICE JAMMING

by

DARWIN ALEXANDER DONACHUK

A THESIS

SUBMITTED TO THE FACULTY OF GRADUATE STUDIES
IN PARTIAL FULFILLMENT OF THE REQUIREMENTS FOR THE DEGREE
OF MASTER OF SCIENCE

DEPARTMENT OF CIVIL ENGINEERING

WINNIPEG, MANITOBA,

FEBRUARY, 1975.

SCOUR AT CONSTRICTIONS DUE TO
ICE JAMMING

by

DARWIN ALEXANDER DONACHUK

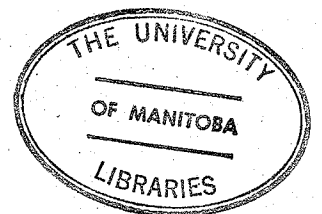
A dissertation submitted to the Faculty of Graduate Studies of
the University of Manitoba in partial fulfillment of the requirements
of the degree of

MASTER OF SCIENCE

© 1975

Permission has been granted to the LIBRARY OF THE UNIVER-
SITY OF MANITOBA to lend or sell copies of this dissertation, to
the NATIONAL LIBRARY OF CANADA to microfilm this
dissertation and to lend or sell copies of the film, and UNIVERSITY
MICROFILMS to publish an abstract of this dissertation.

The author reserves other publication rights, and neither the
dissertation nor extensive extracts from it may be printed or other-
wise reproduced without the author's written permission.



ABSTRACT

The scour phenomenon has been investigated for various types of scour: at bends, constrictions and confluences. The influence of an ice cover on the ultimate scour, however, has not received similar attention. Observed severe thickening of ice jams at constrictions meant that higher velocities prevail beneath them. It was felt that any scour which resulted would not be accounted for in existing equations. A model was used to observe location, depth, and Froude number of jamming and resulting scour. Spill-through constrictions of varying widths were placed in a sand bed flume representing a small gravel bed river approximately 150 feet wide and 10 to 20 feet in depth. Polyethylene blocks representing ice were added and location of jamming and depth of thickening were observed. Ice jamming was found to occur downstream of the constriction with single thickening through and upstream of the constriction. Scour in the majority of runs representing gravel bed rivers was found to occur below the hanging dam and only as random pothole scour. However, in tests run with walnut shells representing sand bed rivers, extensive scour occurred at the downstream toe of the abutments similar to scour without ice, but at much lower Froude numbers. It was therefore concluded that scour due to ice can take place at Froude numbers much lower than those observed without ice conditions.

ACKNOWLEDGEMENTS

The writer wishes to express his sincere gratitude to Prof. V. Galay for the encouragement and helpful advice given to the writer in the preparation of this thesis.

Thanks are also due to my wife, Margaret, for her understanding and participation in this endeavour.

TABLE OF CONTENTS

	<u>Page</u>
Title Page	i
Abstract	ii
Acknowledgements	iii
Table of Contents.	iv
List of Tables	viii
List of Figures.	ix

CHAPTER I

INTRODUCTION

1.1 Introduction	1
1.2 Scour at Spill-Through Abutments.	1
1.3 Scour at Spill-Through Abutments Due to Ice	1
1.4 Purpose and Scope	2
1.5 Outline of Contents	3

CHAPTER II

REVIEW OF LITERATURE ON SCOUR AND BACKWATER

2.1 Reported Scour Under Ice	6
2.2 Maximum Backwater at Constrictions on Rigid Beds	11
2.3 Constrictions on Alluvial Channels.	14
2.4 Literature Review of Flow Patterns and Velocity Distribution Through Constrictions	14

REVIEW OF LITERATURE ON ICE JAMS

3.1	Reported Scour Under Ice	19
3.2	Causes of Ice Jams	20
3.3	Criterion for Progression of Ice Cover	22
3.4	Maximum Backwater Due to Ice Jams.	28
3.5	Hanging Dam Formation	28
3.6	Conclusion	30

CHAPTER IV

EXPERIMENTAL EQUIPMENT, MATERIALS AND PROCEDURE

4.1	General	32
4.2	Material	34
4.3	Procedure	37
4.4	Data Taken.	38
4.5	Ice Feeding	39
4.6	Model Setup	39

CHAPTER V

COMPARISON OF EXPERIMENTAL RESULTS ON SCOUR WITHOUT ICE

5.1	General	40
5.2	Scour Patterns.	40
5.3	Analysis of Scour at Spill-Through Abutments.	43
5.4	Analysis of Backwater at Spill-Through Abutments	49
5.5	Analysis of Flow Patterns and Velocity Distribution.	51
5.6	Conclusion.	55

CHAPTER VI	<u>Page</u>
------------	-------------

ICE JAMMING STUDIES

6.1	Description of Jamming.	56
6.2	Flow Patterns and Scour Under Ice Conditions.	62
6.3	Comparison With Other Experimenters	74
6.4	Preliminary Tests	77
6.5	Bed Material Affect on Scour and Hanging Dam Formation	85
6.6	Conjectures	87
6.7	Conclusions	89

CHAPTER VII

CONCLUSIONS AND RECOMMENDATIONS

7.1	Introduction.	91
7.2	Conclusion.	92
7.3	Recommendations	93

LIST OF REFERENCES	95
------------------------------	----

APPENDIX A

EXPERIMENTAL DATA ON TESTS WITHOUT ICE

A.1	Scour At Spill-Through Abutments.	103
-----	---	-----

APPENDIX B

EXPERIMENTAL DATA ON ICE JAMMING TESTS

B.1	Hanging Dam	104
B.2	Effect of Detergent	106

APPENDIX C

Page

HANGING DAM ILLUSTRATIONS

107

LIST OF TABLES

<u>Table</u>		<u>Page</u>
I	Characteristics of Bed Material	36
II	Comparison of Design Curves of Laursen, Komura and Das With This Study . .	48
III	Maximum Froude Number and Velocity at the Constriction.	74
IV	Comparison of F_2 and Thickness of Ice With Pariset and Uzuner	80

LIST OF FIGURES

Figure

- 2.1 Definition Diagram For Spill-Through Abutments
- 2.2 Definition Diagram For Flow Expansion And Contraction
- 2.3 Non-Dimensional Profiles Of Live Stream Boundary Das (1972)
- 3.1 Definition Diagram For Underturning
- 3.2 Analytical Predictions Of Conditions For Upstream Propagation Of Leading End Of Ice Cover
- 3.3 Lazier (1973) Depth Vs. Velocity For Stable Jamming (Model Study Of Moira River)
- 4.1 Model Layout
- 4.2 Size-Distribution Curve For Bed Materials
- 5.1 Scour Patterns Obtained By Das (1972) End-Dump Closure
- 5.2 View Of Scour Holes At Downstream Corner Of Abutments
- 5.3 At High Constriction Ratios Spill-Through Abutments Effect Scour Patterns
- 5.4 Comparison Of This Study With Laursen's (1963) Analysis For Scour At Isolated Abutments
- 5.5 Comparison Of This Study With a) Laursen (1963) and b) Komura (1960) Analysis For Scour In Long Contractions
- 5.6 Comparison Of Garde Et Al's (1961) Data On Scour At Spill-Through Abutments With This Study
- 5.7 Comparison Of Das (1972) Design Curve For Scour At End-Dump Constrictions With This Study

Figure

- 5.8 Comparison Of H/h Vs. m Obtained By Das (1972) With This Study
- 5.9 Comparison Of Relationship $(H/h)^3$ and $F^2 (1/M^2 - 1)$ Obtained By Das (1972) and Liu Et Al (1957) With This Study
- 5.10 Relationship For Maximum Backwater Depth On Mobile Beds Correlating C, F, and M
- 5.11 Flow Patterns At Constrictions As Shown By Dye
- 5.12 Flow Expanding Uniformly After Scouring The Bed
- 5.13 a) Typical Live Stream Boundary For This Study On Tests Without Scour b) Velocity Distribution For End-Dump Closure Das (1972)
- 6.1 Hanging Dam Formation
- 6.2 Effect Of Solid Ice Cover Near Constriction On Hanging Dam Formation
- 6.3 Typical Dry Jam Formed By Failure Of Hanging Dam
- 6.4 Water Surface Profile For Dry Jam Formed In Test HD-18
- 6.5 Expanding Flow Beneath Hanging Dam
- 6.6 Unusual Flow Patterns
- 6.7 HD-11 Scour Below Maximum Ice Accumulation For Runs Partially Lacking In 1' x 1' x 1' Blocks.
 $F = .08$ $d = .2$ $m = .46$
- 6.8 Solid Ice Cover Effect On Scour At Constrictions
- 6.9 Dry Ice Jams
- 6.10 Scour Within Constrictions a) Photo Of Block Jammed Against C.P.R. Bridge At Riverton, Manitoba, 1974. b) Photo Of Scour Within Constriction Caused By Blocks Jammed Between Ice Cover And Abutments

Figure

- 6.11 From Kivisild (1959) a) Curve Showing The Average Depth From Underside Of Ice Cover To River Bed As A Function Of Flow Per Unit Width At Maximum Ice Deposits In Hanging Dam. b) Curve Shows The Gradient Of Energy Head As A Function Of Flow Per Unit Width Under An Ice Cover At Maximum Possible Ice Deposits In Hanging Dam
- 6.12 Use Of Detergents To Reduce Surface Tension
- 6.13 Rate Of Feeding Effect On Hanging Dam Formation Run HD-14
- 6.14 Unusual Scour Observed Below Hanging Dam Supported By Downstream Ice Cover And Lacking In Small Ice Floes
- 6.15 Test Run With Walnut Shells As Bed Material

LIST OF SYMBOLS

a	= length of closure dam normal to flow
B	= average width of approach channel
b_b	= width of opening measured at normal bed level
b_c	= average flow width (between live stream boundaries) at vena-contracta
b_{bs}	= width of opening measured at scoured bed level
b_w	= width of opening measured at water surface
C	= discharge coefficient (synonymous with C_d and C_m)
C_D	= drag coefficient
C_K	= Kindsvater and Carter's discharge coefficient
C_c	= coefficient of contraction = b_c/b
C_d	= discharge coefficient for constriction on rigid bed
C_m	= discharge coefficient for constriction on mobile bed
C_s	= square of the surface-velocity coefficient
d	= representative size of bed material = d_{50} for sizes up to 2 mm
d_{50}	= grain size of which the given percent by weight of the bed material is finer
d_s	= limiting depth of scour below original bed level
e	= ice cover porosity

- F = Froude number of normal (approach) flow = V/\sqrt{gh} (scour equations)
- F = upstream Froude number (V_u/\sqrt{gh}) (ice studies)
- F_2 = upstream modified Froude number ($V_u/\sqrt{2gh}$)
- F_b = bed factor of Blench
- f_l = Lacey's silt factor
- g = acceleration due to gravity
- H = water depth in the upstream stagnation zone (considered equivalent to depth of maximum backwater)
- H = depth of upstream flow (ice studies)
- H_D = height of spill-through abutments above original bed
- ΔH = head loss at the constriction
- h = average depth of normal flow, a characteristic length in scour
- h_1, h_2, h_3 , and h_4 = depth of flow at sections 1-1, 2-2, 3-3 and 4-4 along centre line
- h_{f13} = head loss in friction between sections 1-1 and 3-3
- h (x) = depth of flow under the cover
- i, i_n = representative energy gradient or water surface slope
- J = a variable coefficient for bed sediment in Garde's scour equation
- j_3, j_4 = exponents in " $\tau_{o_{max}}/\tau_o^{-m}$ " relationship

- K_m = a multiplying factor in scour relationship
 L = length of leading edge blocks
 L_{23} = length of contraction of live stream from dump line to vena-contracta
 L_{34} = length of expansion of live stream beyond vena-contracta
 M = opening ratio = $l - m$
 m = contraction ratio = $(B-b)/B$
 n = Manning's roughness coefficient
 p = an exponent in Garde's scour equation
 Q = normal (approach) discharge
 q = unit normal discharge
 $q_1, q_2, q_3,$ and q_4 = unit discharges at sections 11, 22, 33 and 44 respectively
 r = ratio of depth of local scour at a constriction to depth of scour in equivalent long contraction (Laursen)
 S_u = submergence of blocks due to the pressure reduction in accelerated flow
 t = thickness of the ice cover
 t_1 = part of the cover above the water surface
 t_2 = part of the cover below the water surface
 V = mean velocity of normal (approach) flow
 $V_1, V_2, V_3,$ and V_4 = velocities at section 1-1, 2-2, 3-3 and 4-4
 V_s = surface velocity of the free stream
 V_u = mean velocity of the free stream

w	= fall velocity
X_c, Y_c	= Cartesian co-ordinates for live stream contraction
X_e, Y_e	= Cartesian co-ordinates for live stream expansion
Y_1, Y_2	= overall angle of contraction and expansion of the live stream boundary with flow direction
Y_{1L}	= local angle of contraction at the dump line
Y_{2L}	= local angle of expansion just downstream of the vena-contracta
α_e	= energy correction coefficient
β	= normalized half length of separation zone
γ_s	= unit weight of bed material
γ_w	= unit weight of water
ρ'	= specific density of ice cover
ρ_s	= specific density of bed material
ρ_w, ρ	= specific density of water
σ_g	= geometric standard deviation of particle size
τ_c	= critical shear stress for granular material on horizontal bed
$\bar{\tau}_0$	= average intensity of shear stress on uncontracted channel periphery
ϕ	= empirical coefficient in backwater rise equation for rigid-bed channels, due to Liu, Bradley and Plate (1957)
δ	= angle of rotation

CHAPTER I

1.1 Introduction

Since bridgework generally costs much more per unit length than earthwork, maximum economy is usually achieved by making the effective width of a waterway opening no greater than is necessary to meet basic hydraulic requirements. C. R. Neill (1967) lists usual constraints on shortening of bridgework as scour, backwater, and velocities.

1.2 Scour At Spill-through Abutments

Scour at spill-through abutments at ice free conditions is the result of local and general scour. Three approaches have been used to determine maximum scour depth.

- a) Regime type analysis Khosla (1936) and Blench (1957).
- b) Empirical correlations, Garde Subranamya and Nambudripad (1961). Izzard and Bradley (1957) Ahmad (1953) and Das (1972) scour at end dump constrictions.
- c) An analysis taking into account increased bed shear stress. Straub (1934) Laursen (1960) and Komura (1966).

1.3 Scour At Spill-through Abutments Due To Ice

Accounts of ice jams attaining great depths downstream of constrictions and narrows indicate that high

velocities below these ice jams cause scour. There is no equation relating scour during ice jams to existing flow conditions. Theoretical and laboratory work on ice have been limited to uniform flow in straight channels. Field investigations have been limited because of the difficulty in obtaining data. A valid prediction of possible back-water and scour from ice jams can only be done by past experience and intuition.

1.4 Purpose and Scope

It can be seen from the foregoing that scour at constrictions has received a fair amount of attention, but as yet design charts differ in the predicted scour depths. For spill-through abutments on small rivers, it is necessary to know which design curves are applicable. Scour due to ice jamming at constrictions is, however, an unresearched phenomenon. The purpose of the testing programme will be to indicate

- location of jamming,
- Froude numbers at which jamming and instability takes place,
- the role floe size and porosity play in jamming,
- the effect of a solid ice cover downstream of the constriction,
- surface tension effects in modeling,
- possible depths of jamming,
- resulting scour.

This study was confined mainly to gravel bed rivers approximately 150 feet wide and 10 to 20 feet in depth. One test was performed with walnut shells for the bed material representing a sand bed. Spill-through abutments provided three constriction ratios at which ice jams were formed. Time involved in testing prevented a wider range of testing in respect to depth of flow, constriction ratio, bed material size and porosity of ice. The small number of tests prevented dimensional plotting and the results can only be used as an indication of the location and depth of scour with and without ice.

1.5 Outline of Contents

Previous studies on scour and backwater at constrictions are reviewed in Chapter II. Investigations of local scour such as due to bridge abutments or spur-dikes, and on general scour due to channel constrictions, are reviewed.

Studies on backwater due to different constriction geometry both on rigid bed and alluvial channels are reviewed.

In Chapter III a review is made of reported scour under ice near constrictions. Causes of ice jams and the increase in backwater due to ice jams are also reviewed. The criterion for the progression of an ice cover is reviewed in detail since it explains limitations on thickening and

upstream progression. Hanging dam formation is reviewed and other tests on ice jamming in which constrictions were involved. The literature review indicates lack of information on ice conditions at constrictions and none whatsoever on scour possibilities.

The experimental equipment materials and procedure are detailed in Chapter IV. The tests were run in a three foot wide flume and comprised over 50 runs with and without ice, using a bed material size of .5 mm in all but one test. Three main constriction ratios of .46, .40, and .36 were used and bed material was not added to the flow in any of the runs.

Chapter V compares the scour depths and patterns of this study with those of previous experimenters. The resulting maximum scour depth and backwater from this study are plotted on various design curves in order to determine which design curves are applicable to spill-through abutments on small rivers.

In Chapter VI, the results of all experiments with ice are discussed. Froude number of overturning and thickening are compared with previous experimenters, and the use of detergents for the elimination of surface tension is discussed.

Hanging dam formation at three constriction ratios were observed with respect to scour depth, location and their dependence on Froude number of flow and porosity.

A short conclusion and recommendation for further studies is contained in Chapter VII. The complete experimental data is detailed in tabular form in Appendix A and B.

CHAPTER II

REVIEW OF LITERATURE ON SCOUR AND BACKWATER

2.1 Bed Scour Due To Constrictions

Bed scour due to channel constrictions results from:

1) Obstruction or local scour - Piers, abutments or short spur dikes effect flow only in their vicinity. A vortex system forms near the obstacle and the increased bottom velocities associated with the vorticies, increase drag and lift on bed particles which in turn cause local erosion.

2) Contraction scour or general scour - A new flow regime is caused by a gradual contraction in a channel over a sufficient length causing a general degradation of the channel in this reach. Scour depth is determined from the increased bed shear in the contracted reach. Scour at spill-through abutments involve both types.

Three approaches have been used in the development of formula for predicting maximum scour depth:

1) Analysis of scour due to increased discharge intensity (a regime type analysis) applying empirical coefficients:

Khosla (1936) based on Lacey's studies on scour in alluvial rivers in regime, derived a relationship between d_s , the scour depth below the original bed and q , the discharge intensity per foot width of the main channel as

$$h + d_s = .90 \left(\frac{q^{2/3}}{f_l^{1/3}} \right) \quad (2.1)$$

where d_s = depth of scour, h = depth of flow, and f_l is Lacey's silt factor, a function of bed sediment. A coefficient of 1.0 to 3.5 to account for flow concentration is used to apply this to bridge piers, bends, or spur dikes.

Blench (1957) reported an empirical correlation between $(h + d_s)$ and q developed from prototype data by Andre (1956) in the form $(h + d_s) F_b^{1/3} = 1.35 q^{.74}$ where F_b is the bed factor equal to v^2/d .

2) Empirical correlations involving relevant non-dimensional variables:

Garde, Subramanya and Nambudripad (1961) studied scour around a spur dike made of a vertical steel plate. They showed that the Froude number, the opening ratio, and the average drag coefficient of the sediment particle adequately account for maximum scour depth by verifying the dimensional analysis with the help of experimental data. They concluded that

$$\frac{(h + d_s)}{h} = J \left(\frac{1}{M} \right) F^p \quad (2.2)$$

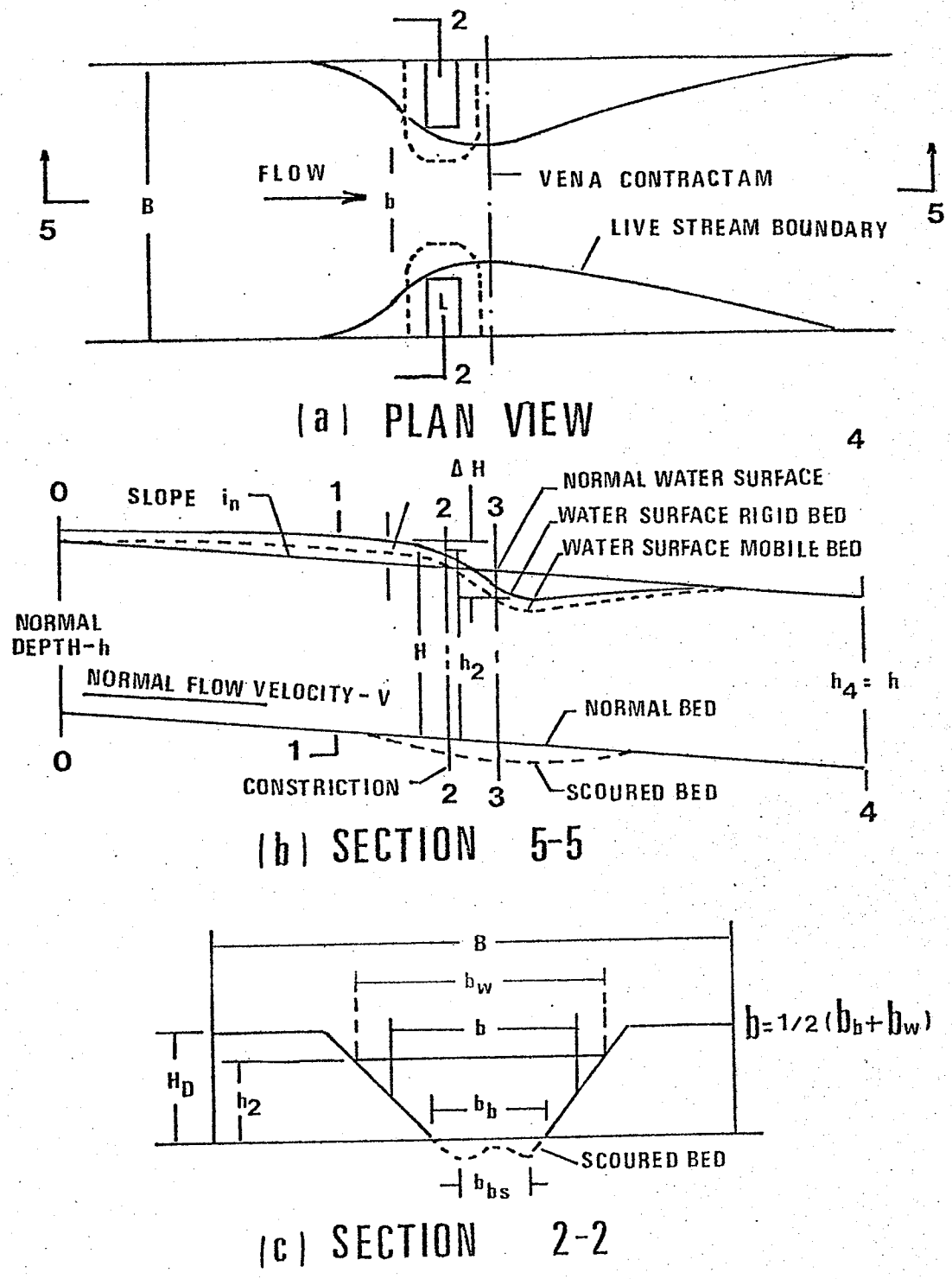


Fig. 2.1. DEFINITION DIAGRAMS FOR SPILL-THROUGH ABUTMENTS.

J and p are functions of C_D which is the drag coefficient of the bed sediment.

$$C_D = \{4/3 (\gamma_S - \gamma_W) d\} / w^2 \rho_W \quad (2.3)$$

M = opening ratio.

They found J varied in the range 2.75 to 5 and p varied in the range .67 to .9 for bed sediment ranging from .29 to .25 mm. Neill (1962) contended that C_D does not adequately account for the sediment. Beyond a median size of 1.5 mm, the fall velocity being proportional to the root of size, C_D would be independent of the size and thus depth of scour would be the same for large boulders.

Liu Chang and Skinner conducted experiments on vertical wall, wing-wall and spill-through abutments. They also found that the Froude number and opening ratio M are the most essential non-dimensional terms influencing scour, however, the effect of sediment size was not analysed.

Izzard and Bradley (1957) and Ahmad (1953) suggested relationships in the form

$$(h+d_s) = K_m (q_2)^{2/3} \quad (2.4)$$

in which K_m , a multiplying factor, is primarily a function of the spur dike configuration and q_2 is the discharge intensity at the constriction ($q_2 = q/l-m$).

Das (1972) proposed design curves for maximum scour due to end-dump constrictions F , m , ρ_s/ρ_w , d/h and $(d_s + h)/h$ were the essential inter-related non-dimensional variables describing scour where ρ_s , ρ_w are the specific densities of bed material and water respectively. The resulting equation is

$$\frac{(h+d_s)}{h} = 0.695 F^{0.85} \left(\frac{h}{d}\right)^{0.29} \left(\frac{\rho_w}{\Delta\rho_s}\right)^{0.43} 10^{0.43(j_3 m + j_4)} \quad (2.5)$$

j_3 and j_4 are coefficients primarily dependent upon F .

3) Analysis of erosion due to increased bed shear stress:

Straub (1934), Laursen (1960), and Komura (1966) analysed scour in a long contraction.

For the case of sediment transporting flow, scour in a constriction would obtain equilibrium after the sediment inflow balances the sediment outflow.

In the case of the clear water flow, the boundary shear stress in the scoured region is the critical shear stress for the material.

Laursen and Komura proposed:

$$\frac{(h+d_s)}{h} = \left(\frac{\bar{\tau}_0}{\tau_c}\right)^{3/7} \left(\frac{B}{b}\right)^{6/7} \quad (2.6)$$

for scour in clear water flow for a long contraction $\bar{\tau}_0$ and τ_c are the boundary shear stress in the normal channel

and the critical shear stress for the bed material respectively. Laursen also reasoned that when the clear opening is more than $5.5 d_s$ interference is minimal and scour holes due to the individual abutments do not overlap. For this case he proposed:

$$\frac{a}{h} = 2.75 \frac{d_s}{h} \left\{ \frac{1}{r} \left(\frac{d_s}{h} \right) + 1 \right\}^{7/6} \left(\frac{\bar{\tau}_0}{\tau_c} \right)^{1/2} - 1 \quad (2.7)$$

for clear water scour.

a = length of encroaching abutment.

r = ratio of depth of scour at an abutment to depth of scour in a fictitious long contraction of width as $a + 2.75 d_s$.

$$\left(\frac{h + d_s}{h} \right)_{\text{limiting}} = 12.5 \frac{(F)}{M} \quad (2.8)$$

They also showed the affect of constriction shape on depth of scour.

2.2 Maximum Backwater At Constrictions On Rigid Beds

Lane (1920) experimenting with sharp edged vertical constrictions revealed that the Weisback formula applies to sudden constrictions whereas the d'Aubuisson formula applies to gradual contracting flow. He mentioned, but unfortunately did not give any relationship with, maximum backwater.

Kindsvater and Carter (1953) and Tracy and Carter (1953) performed extensive investigations of open channel flow through abutments of various shapes and geometry using dimensional analysis.

A discharge equation was derived from the energy and continuity equations

$$Q = C_K b h_3 \left(2g(\Delta H + \alpha_e V_1^2 / 2g - h_{f_{1-3}}) \right)^{1/2} \quad (2.9)$$

Q = discharge in cfs.

C_K = Kindsvater's discharge coefficient.

b = mean width of the contracted opening.

h_3 = flow depth at section 3-3.

$\alpha_e \frac{V_1^2}{2g}$ = weighted velocity head at section 1-1 where the mean velocity is V_1 and α_e is the energy coefficient.

$h_{f_{1-3}}$ = head loss in friction between sections 1-1 and 3-3.

From dimensional analysis C_K is primarily dependent upon F_3 , the Froude number of the flow at section 3-3 ($F_3 = Q/bh_3\{gh_3\}^{1/2}$), m , the contraction ratio and L/b the ratio of the length of the contraction in the flow direction to the opening width.

Curves have been presented for various shaped abutments, in order to predict discharge knowing h_3 and Δh .

Tracy and Carter have presented curves for a

dimensionless backwater as $h^*/\Delta h$. By dimensional analysis $h^*/\Delta h$ was empirically correlated with the constriction ratio m and the Mannings roughness factor n for vertical faced constrictions with square edged abutments and other shapes. The shortcomings of this method is that it cannot estimate directly the maximum backwater h^* from $h^*/\Delta h$ relationships because h is dependent upon Q , h_c and C_K has to be evaluated in the first instance by a trial and error procedure.

Liu, Bradley and Plate (1957) conducted studies for vertical board, wing-wall and sloping spill-through abutments. Energy momentum and continuity principles led to an equation for H , the depth of maximum backwater section given by

$$(H/h)^3 = \frac{3}{2} F^2 \left(\frac{9\phi}{4M^2} - 1 \right) \quad (2.10)$$

F = the Froude number of unconfined normal flow.

ϕ = empirical coefficient.

M = opening ratio = $1-m$.

The empirical coefficient ϕ was observed to depend upon the model type F , M and b empirically correlated for a simple vertical board model as

$$\phi = 1.33 \left\{ 1 - \frac{2}{3} M^2 \left(2 - M - \frac{1}{3F^2} \right) \right\} \quad (2.11)$$

The final equation was

$$(H/h)^3 - 1 = 4.83 F^2 \left\{ \frac{1}{M^2} - \frac{2}{3} (2.5 - M) \right\} \quad (2.12)$$

Valentine (1958) from a dimensional approach obtained

$$C_d = \frac{Q}{bH^{3/2}} \quad (2.13)$$

C_d = discharge coefficient function of F and m
by substituting for V and Q , it can be written as

$$\frac{H}{h} = (g^{1/2}/C_d)^{2/3} \cdot \left(\frac{F}{M}\right)^{2/3} \quad (2.14)$$

Biery and Delleur (1962) studied backwater rise through arch bridge constrictions.

Their studies resulted in an equation for any type of constriction

$$\frac{H}{h} = 1 + 0.47 \left\{ \left(\frac{F}{M}\right)^{2/3} \right\}^{3.39} \quad (2.15)$$

2.3 Constrictions On Alluvial Channels

Liu Chang and Skinner (1961) concluded that h for alluvial channels is about sixty percent of that in a rigid channel.

Sandover (1969) presented curves for h^*/h versus M with F as the variable.

2.4 Literature Review Of Flow Patterns And Velocity Distribution Through Constriction

Flow patterns through constrictions were observed by Das (1972) for end dump constrictions.

Kindsvater and Carter (1955) studied various constriction geometries and Biery and Delleur (1962) experimented with semi-circular arch bridge constrictions.

Das (1972) described rapid drop of water surface contours around the dump line in contrast to a flatter drop along the centre line indicates the flow to be accelerating more rapidly close to the advancing boundary.

The long contraction causes the flow to expand gradually over a longer length. He also noted the local angle of contraction Y_1 at the dump line to be larger than the local angle of expansion Y_2 .

Das measured the flow width at the vena-contracta b_c , the length of contraction L_{23} and the length of expansion L_{34} .

He concludes that the geometry of the constriction has a decisive influence on the coefficient of contraction from the fact that the contracting stream has a vertical edge upstream and downstream of the constrictions and hugs the sloping face in between. He assumed

$$C_c = f_1 (m, F, \tan \phi) \quad (2.16)$$

$\tan \phi =$ slope of end-dump face.

He expressed contraction length as

$$\frac{L_{23}}{b} = f_2 (m, F, \tan \phi) \quad (2.17)$$

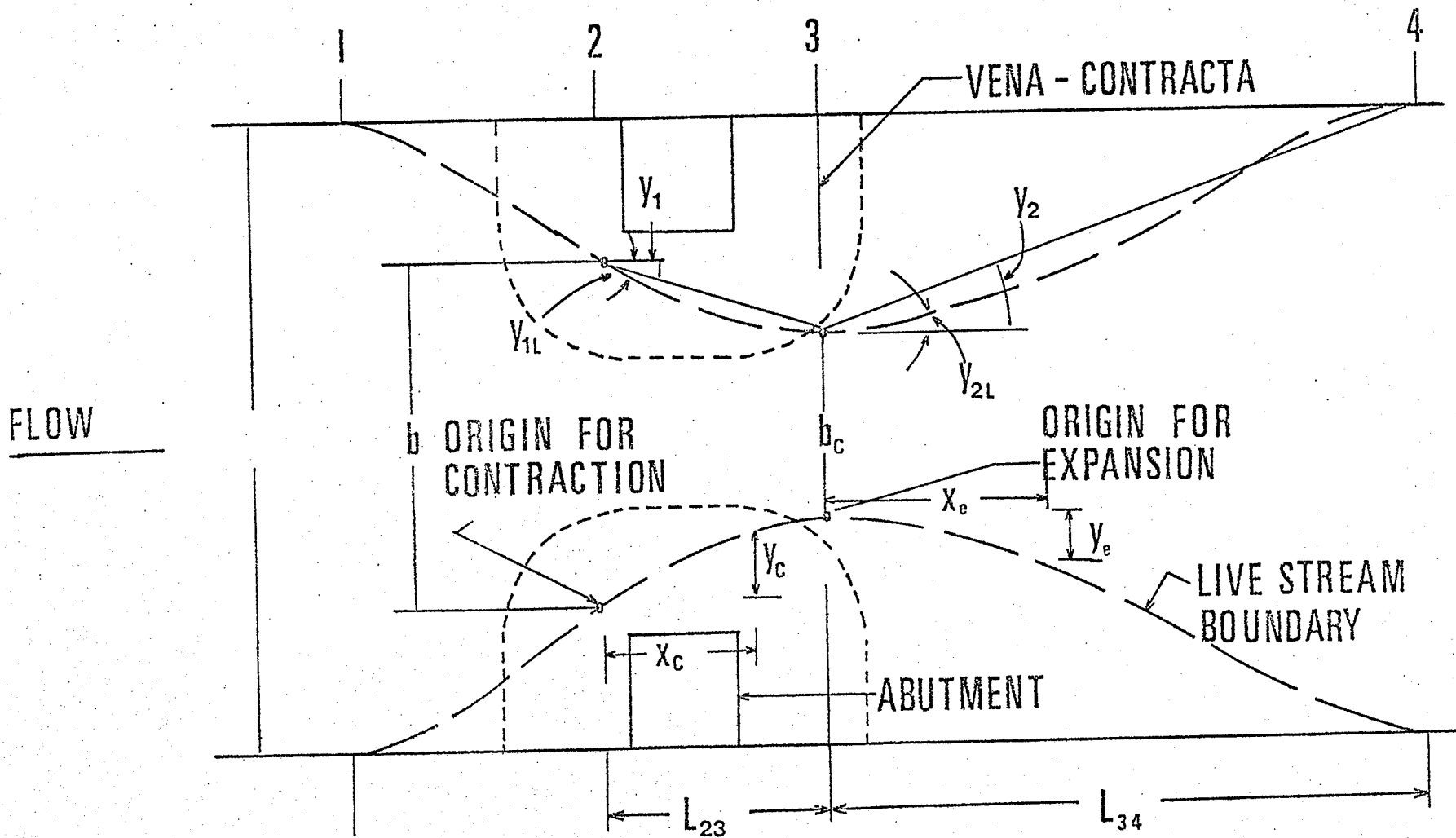


Fig. 2.2 DEFINITION DIAGRAM FOR FLOW CONTRACTION AND EXPANSION.

and expansion length

$$\tan \phi_2 = \frac{L_{34}}{(B-b)/2} = f_4 (M, F, \tan \phi) \quad (2.18)$$

Das concludes

- 1) C_c is primarily dependent upon M
- 2) Angle of contraction Y_1 varies between 5° and 25°
- 3) Angle of expansion Y_2 varies between 15° and 35° dependent primarily on Froude number of approach flow.

He also obtained non-dimensional plots of

$$\frac{x_c}{L_{23}} \text{ vs } \frac{2y_c}{B-b_c}$$

and

$$\frac{x_e}{L_{34}} \text{ vs } \frac{2y_e}{B-b_c}$$

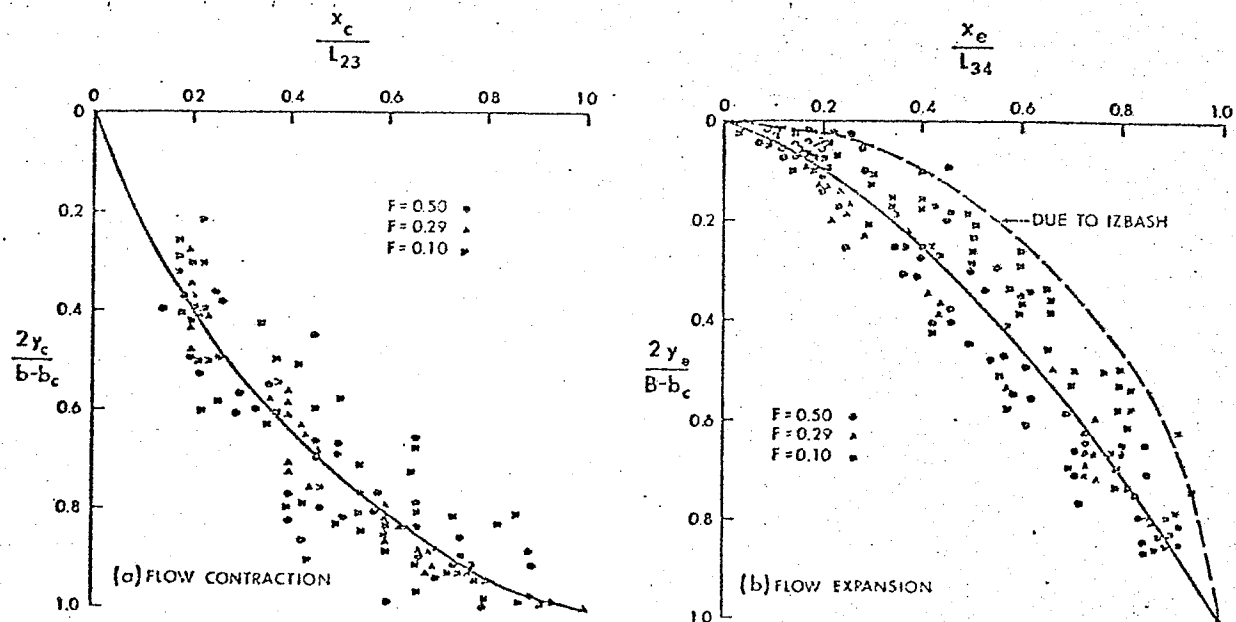


Fig. 2.3 NON-DIMENSIONAL PROFILES OF LIVE STREAM BOUNDARY DAS (1972)

indicating profiles are similar irrespective of Froude number and contraction ratio.

CHAPTER III

REVIEW OF LITERATURE ON ICE JAMS

3.1 Reported Scour Under Ice

Melin (1954) describes erosion in Scandinavian Rivers composed primarily of frazil.

"In places where barrages appear, the ice will often fill up a great part of the section right down to the bottom. Therefore, the water is forced to follow one or a few channels, flowing more rapidly than before, resulting in a great tendency of erosion.

Areas where such erosion is common are the upper part of the calm waters. Here big masses of soil and gravel have been deposited after having been brought from the rapids above, and the bottom constitutes a very good ground for erosion when the velocity of the water increases. Sometimes the flow will follow a channel along the riverside eroding it and causing big masses of sediment to plunge into the river."

3.2 Causes of Ice Jams

Ice Jams are of several different varieties and origin. Unfortunately, there are no universal definitions of ice jams, therefore it is necessary to state those used in this report.

Ice jamming is said to occur when a cover of loose chunks of ice begin to compact and become at least two layers in depth.

A dry jam is formed by the jamming of ice floes down to the river bottom at an obstacle which may be an existing ice accumulation or bed irregularity. Water has to flow by infiltration through the ice plug and its level increases rapidly upstream. This jam is practically unpredictable and unstable, and will go out when the upstream water level increases sufficiently.

A hanging dam is a stable jam which is greater than one-third the depth of flow. Two types can exist according to method of formation. The first type is caused by jamming of a cover which causes a reduction in flow and consequently a stable ice cover more than one-third the depth of flow. The second type occurs at channel expansions. Within the expansion, velocity and ice carrying capacity of the water are low and the ice cover can obtain great thickness by accretion.

For the formation of an ice jam there must be a discharge of fragmented solid ice or frazil ice, and an obstacle to impede the passage. Therefore, the meteorological and hydrological conditions which govern the stream discharge and the geometric properties of the channel could affect the passage of ice.

U. S. Army Corps of Engineers (1967) Bryce (1968) summarized the causes of jams (Uzuner 1971).

a) Obstructions Which Impede Ice Passage.

i) Channel constrictions, such as rapids, sharp bends, bridge piers, protruding abutments, flow regulating structures, islands, and border ice extending outward from the shore.

ii) Extreme cold resulting in extensive freezing and blockage of the channel by shorefast and/or bottomfast ice.

iii) Thick lake (or sea) ice forced to river mouth during high wind and storm periods where it is grounded in the relatively shallow river channels.

iv) Floes remaining in a river mouth after ebb tide.

v) Sudden streamwise decrease in depth along a channel accompanied by decreases in velocity and slope and/or increase in width of the channel.

b) Sources of Increase in River-Ice Discharge.

i) Production of excessive frazil ice, which adhere to

channel boundaries and/or structures and blocks the channel.

ii) Sudden releases of thick lake ice into a river, usually from collapse of a natural ice arch some distance upstream from the river entrance after a heavy storm can glut the river completely.

iii) Sudden temperature increase or injection of thermal pollution at upstream locations causing weakening and break-up of sheet ice which then moves downstream.

iv) Break up of ice sheet by increased river discharge.

v) Previous winter conditions (Michel).

vi) Surface flooding in winter.

There are of course other flow, hydrological and topographical conditions which can lead to ice jam formation.

3.3 Criterion For Progression Of Ice Cover.

The conditions under which the blocks at the leading edge of the cover reach a condition of incipient motion is known as the criterion for the progression of an ice cover.

Uzuner's (1971) example is as follows: "Imagine an ice block flowing downstream coming into contact with a stationary, continuous, or fragmentic, ice cover. If the ice block reaches a state of static equilibrium upon impact with the ice cover, the cover will propogate upstream. Under other conditions, the block will be swept under the cover

and come to rest or continue with the flow."

McLachlan (1927) wrote one of the first publications on the hydrodynamic conditions controlling the progression of ice covers based on field observations on the St. Lawrence River. He stated that ice covers may thicken and progress at velocities up to 2.25 feet per second without floes passing underneath.

Cossineau (1964) also concluded that a velocity of 2.25 feet per second is an upper limit which can only be obtained under ideal conditions. Field observations on the St. Lawrence were also the basis for his conclusions.

Estiveef (1958) from observations of ice cover progression in the northern rivers of the U.S.S.R. states frazil coming up to surface to develop into ice floes cannot form an ice cover at velocities higher than 2.3 to 2.6 feet per second.

Kivisild (1959) states that the criterion for the progression of an ice cover should be expressed in terms of the Froude number F of the flow upstream from the cover $F = \frac{Vu}{\sqrt{gH}}$ where Vu is the velocity and H is the depth upstream from the cover and g is the gravitational constant. He concluded on the basis of his observations of frazil ice on Canadian rivers that the upper limiting value of the Froude number for propagation of an ice cover is about .08. This value of .08 is dependent on the porosity of the ice accumulation. The average porosity value of Kivisild's tests

was .73.

Newbury (1968) also found from observations on the Nelson and Churchill Rivers that upstream progression of frazil ice occurs at a Froude number of approximately .08.

Cartier (1959) concluded from observations in a canal nine feet in depth and forty-six feet in width that it was possible to obtain upstream progression of an ice cover with big ice floes at velocities higher than 2.3 feet per second.

Pariset and Hauser (1961) developed a complete theoretical analysis for the stability of ice covers in rivers. This analysis applies to narrow rivers in which the tangential force exerted by the banks on the ice cover is adequate to support the flow induced and gravitational forces exerted on the cover in the streamwise direction. The thickness of the ice cover is governed by conditions at its upstream edge. The criterion for the progression of a cover is expressed in terms of the Froude number.

Pariset et al (1966) and Michel (1966) analysis of the leading edge blocks becoming unstable and being swept under are as follows:

Pressure supporting the block is reduced as the flow passes under the ice cover. The elevation of the block is lowered below that corresponding to the no flow condition. At the stagnation point at the leading edge of the ice cover, the local water surface elevation is increased by the amount of the velocity head.

When the water surface elevation at the leading edge becomes equal to that at the top of the block, an ice block becomes unstable and is swept under the ice cover.

$$F_2 = \left\{ \frac{t}{H} (1 - \frac{\rho'}{\rho}) (1 - e) \right\}^{\frac{1}{2}} (1 - \frac{t}{H}) \quad (3.1)$$

t = thickness of ice at leading edge.

H = depth of flow upstream of cover.

F_2 = modified Froude number.

ρ', ρ = density of ice and water respectively.

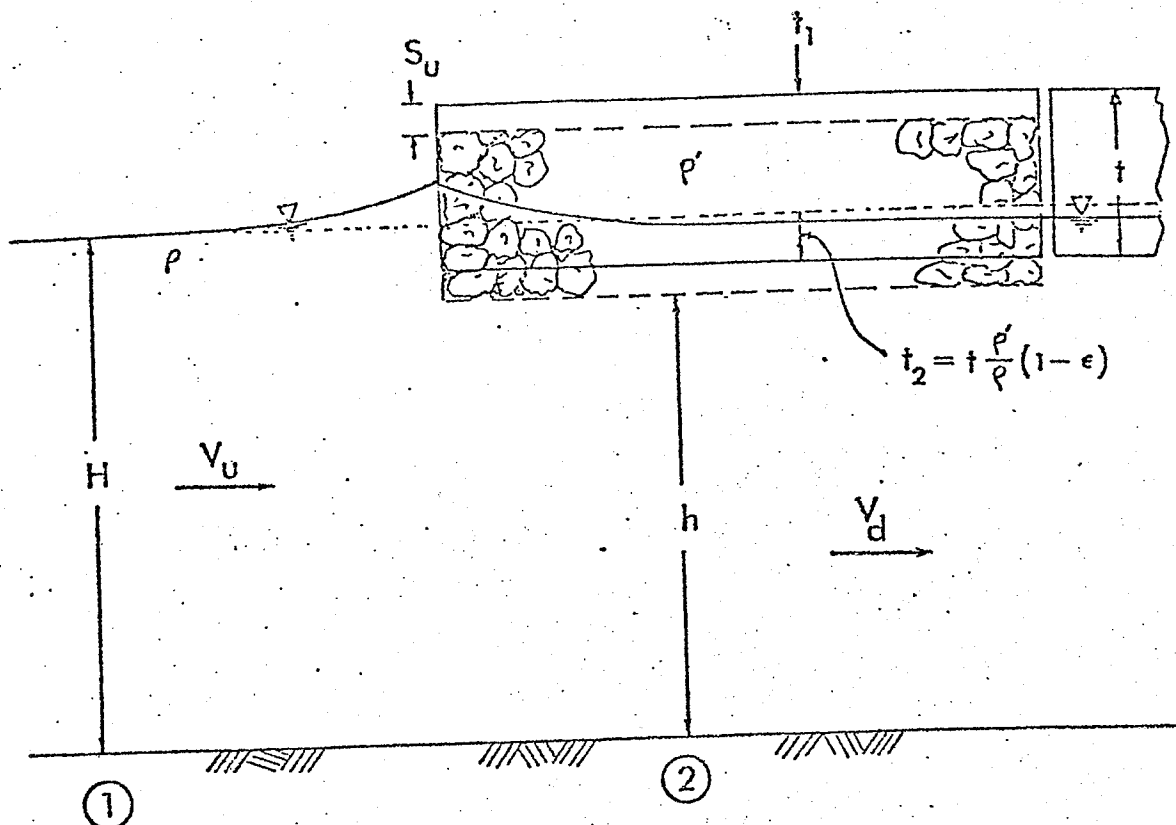
e = porosity of the ice.

This is the general equation derived by Michel (1966) taking porosity into consideration.

For $e = 0$ this reduces to the equation developed by Pariset et al (1966).

Uzuner (1971) provided a similar expression to Pariset et al and Michel, however, he used a much more realistic analysis of ice block submergence.

As the flow passes under the leading edge of the upstream block, it is accelerated because of the reduced flow area under the ice cover. The vertical acceleration as the flow passes around the lower upstream corner of the block produces local separation and further reduction of pressure in this vicinity. The block rotates about its downstream lower edge until equilibrium is reached between



a) UNDERTURNING ANALYSIS PARISET ET AL (1966)

b) UNDERTURNING ANALYSIS UZUNER (1971)

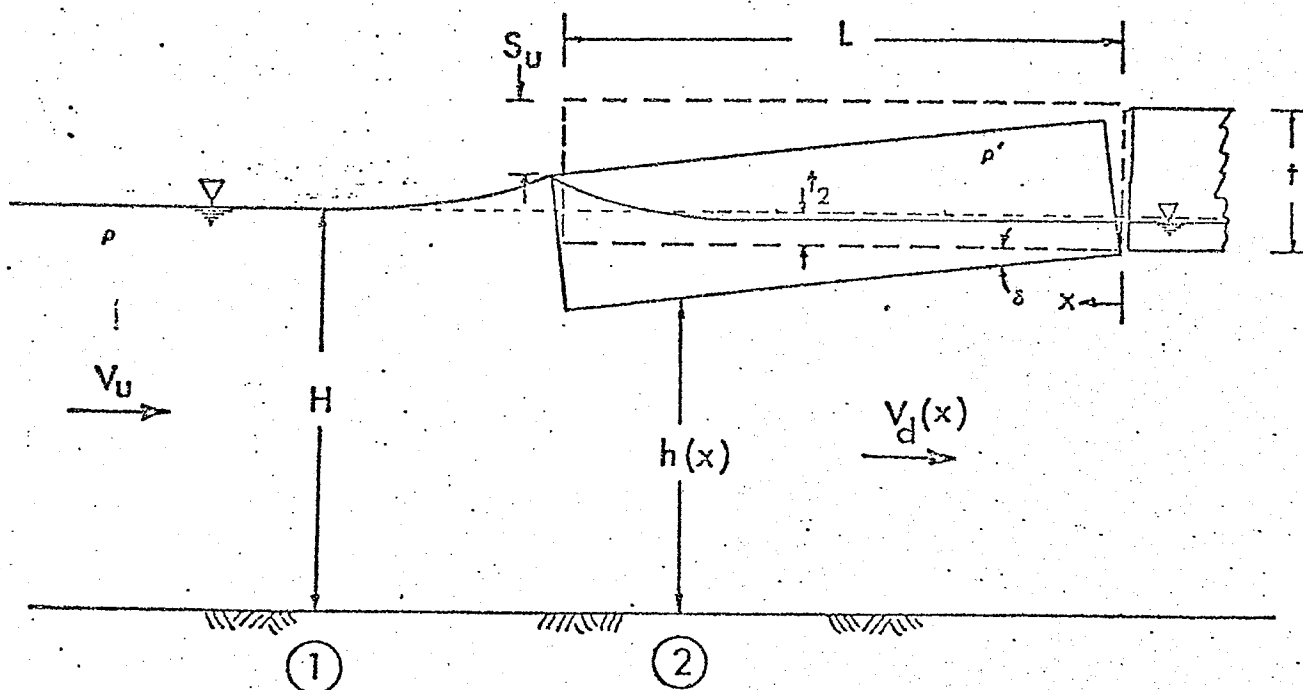


Fig. 3.1. DEFINITION DIAGRAM FOR UNDERTURNING.

the moments due to the blocks weight and the pressure distribution at the bottom of the block:

$$F_2^2 = \frac{\frac{t}{H} (1 - \frac{\rho'}{\rho})}{C_s + \frac{1}{1 - \frac{t}{H}} (1 + \beta)} \quad (3.2)$$

C_s = square of ratio of surface velocity to mean velocity.

B = normalized half length of separation zone.

For $C_s = 1$ and $\beta = 0$, this is the same as the equation derived by Pariset et al.

$\beta = 0$ for long blocks with no rotation.

Uzuner shows that rotation of blocks occurs at t/L values of .1 to .8.

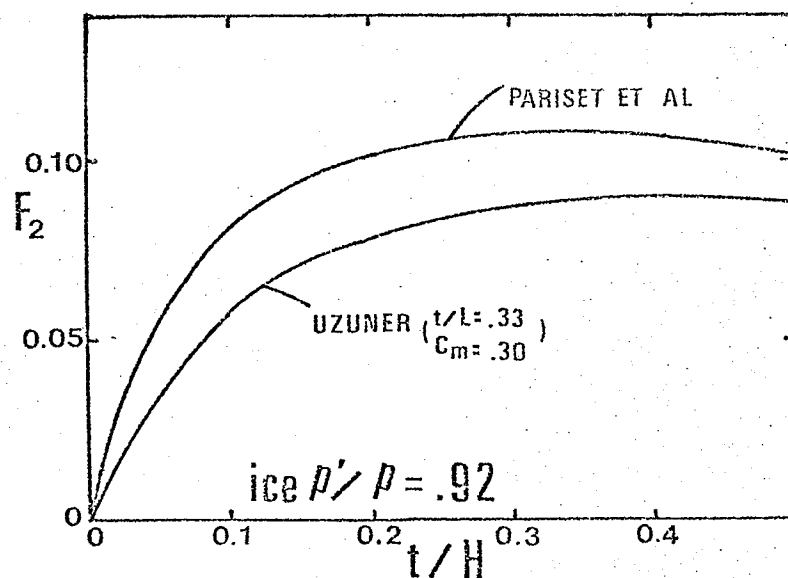


Fig. 3.2 ANALYTICAL PREDICTIONS OF CONDITIONS FOR UPSTREAM PROPAGATION OF LEADING END OF ICE COVER.

t = thickness of block

L = length of square block.

Uzuner takes into account C_s and β in his more realistic model and predicts lower F_2 values than Pariset et al.

3.4 Maximum Backwater Due To Ice Jams.

The main factors determining the maximum level during ice jams are as follows: (Bolsegna S.J. 1968).

- 1) Character of river bed and valley in sector where the jam occurs.
- 2) The thickness of ice cover and its firmness.
- 3) The intensity of influx of flood water (intensity of rise in water level) and the ice movement connected with it.
- 4) The height of water level in the sector below the jam.
- 5) Weather conditions during the formation of the ice jam.

The rise in water level as a result of the ice jam at a definite point in the river will also depend upon the distance of the point from the place where the jamming occurs.

When considering a particular location, such as a constriction, all of these factors will have an effect on backwater.

3.5 Hanging Dam Formation.

Pariset et al (1966), Morton, Michel (1966), and

others have mentioned hanging dams as a unique type of ice jam formed when high velocities are encountered, but Kivisild (1959) was the first to try and explain hanging dam formation in qualitative terms.

Kivisild (1959) gives a relationship between Froude number and depth of flow, depth from hanging dam to bed vs. discharge per foot width, for hanging dams formed by frazil flow.

Lazier's (1973) model study on the Moira River show relationships between velocities and depth for incipient and stable jamming. Although the model had a slight constriction and a jam downstream of the constriction, jamming depths and a Froude number relationship were not obtained.

Charbonneau (1973) undertook a model study on closure of the Reviere des Roches by formation of a hanging dam downstream of a constriction. The resulting report is mainly descriptive, but it does give an indication as to where the dam will form and possible depths, the effect of a solid ice cover on hanging dam formation and description of formation .

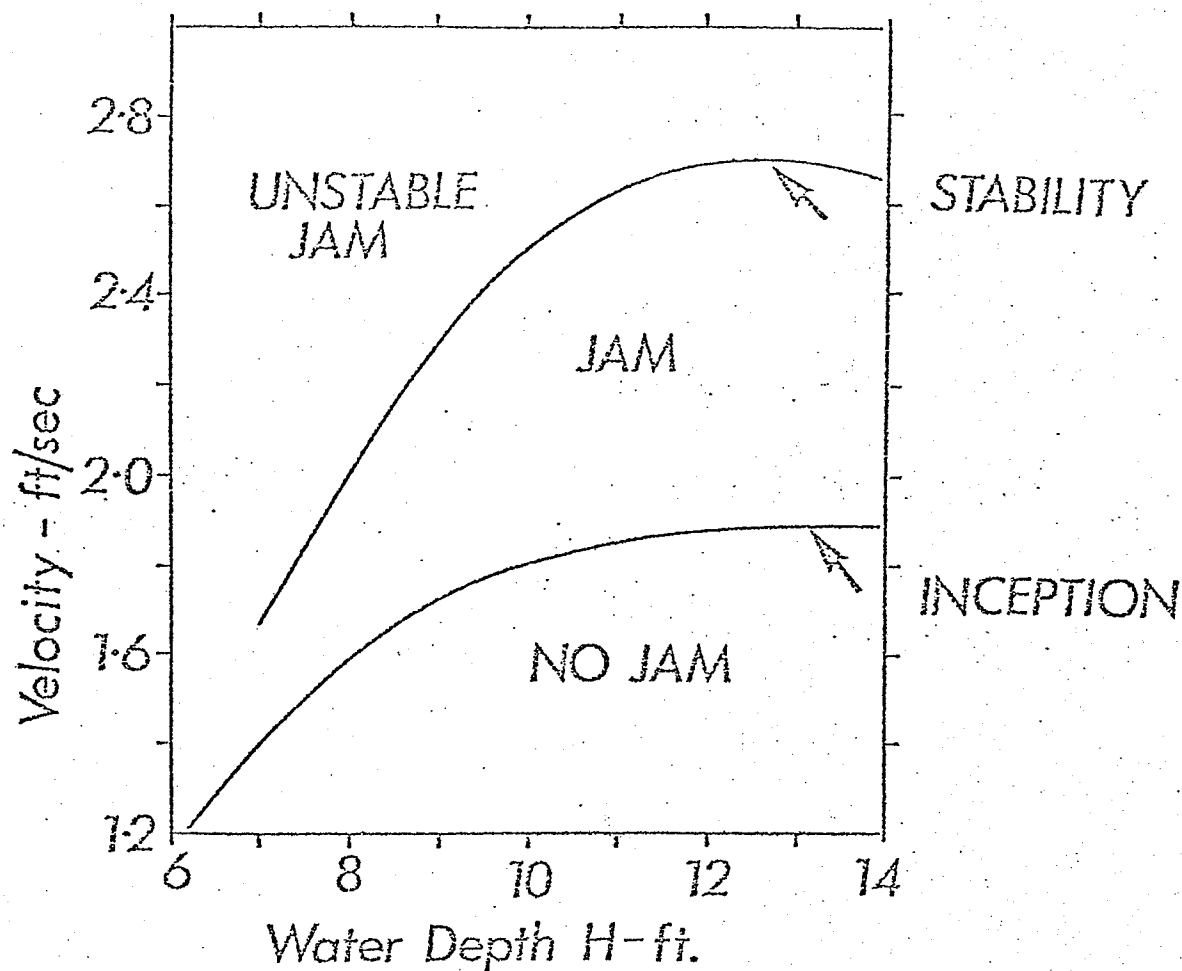


Fig. 3.3. LAZIER (1973) DEPTH VS. VELOCITY FOR STABLE JAMMING (MODEL STUDY OF MOIRA RIVER).

3.6. Conclusion.

As seen from the literature review of ice processes, scour below ice jams has not been studied. Ice jams are only predictable in straight uniform channels although Kivisild (1959) has made an attempt to predict depths and slopes from discharge per foot width for frazil ice accumulations. The following model study will compare thickening in a straight

uniform channel with that predicted by Pariset et al (1966) and Uzuner (1971). The resulting hanging dams formed with constrictions will be used for the determination of scour depth, and locations of hanging dam and scour. The Froude number of formation will be compared with those observed by Lazier (1973) and Charbonneau (1973), and depths and slopes will be compared with Kivisild's (1959) charts.

CHAPTER IV

EXPERIMENTAL EQUIPMENT, MATERIALS AND PROCEDURE4.1.1 General

The equipment used consisted of -

- 1) flume and flow system and
- 2) the measuring devices.

4.1.2 Flume and Flow System.

Experiments were carried out in a 39 foot recirculating flume 3 feet wide and 3 feet deep with a horizontal bottom. The side walls were glass from station -2 to station 18. Of the 3 foot depth available in the flume, the bottom 8 inches were filled with the bed material from station -2 to station 14. A head tank and an upstream stilling screen between the head tank and the flume took up six feet.

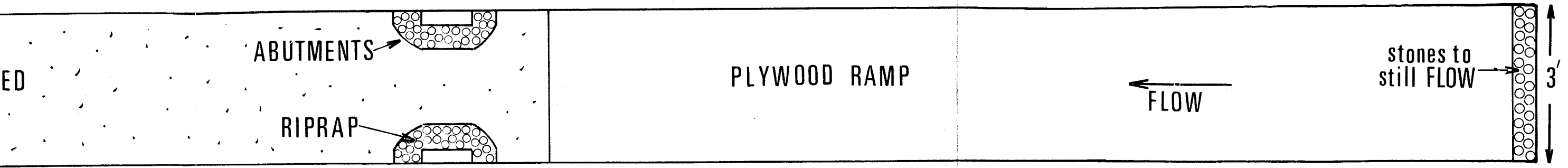
The downstream end was designated as station 18 and the upstream end designated as station -21. Station 0 was reserved for the centre of the constrictions. The bed elevation was arbitrarily designated as 1.1 feet.

Flow in the system to the extent of .5 cfs. was provided by a centrifical pump which drew supply from an

FIGURE 4.1

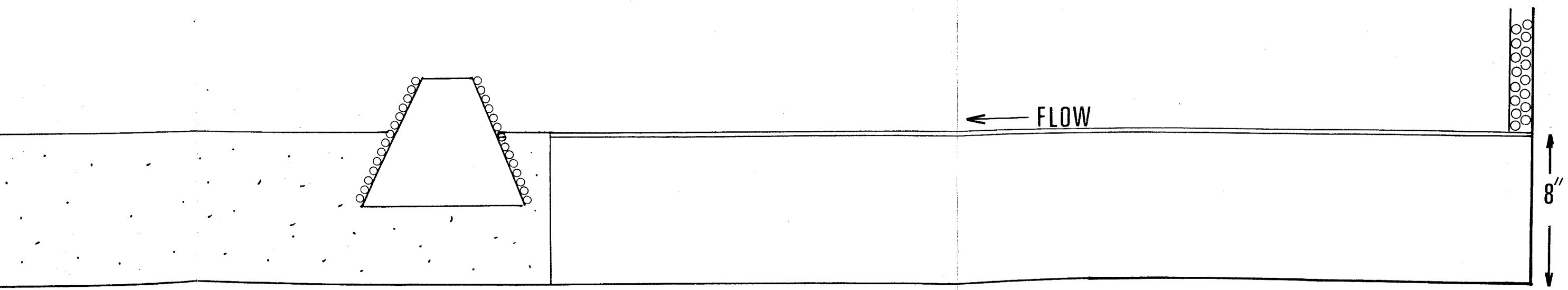
MODEL LAYOUT

FLUME LAYOUT

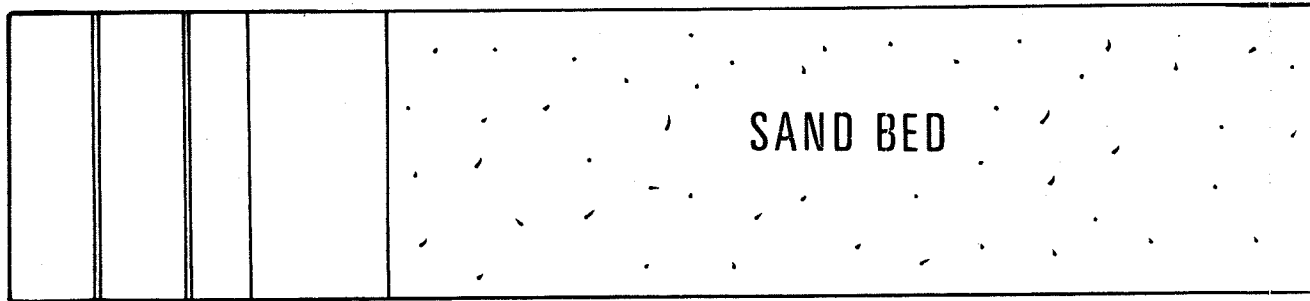


8 6 4 2 0 -2 -4 -6 -8 -10 -12 -14 -16 -18 -20

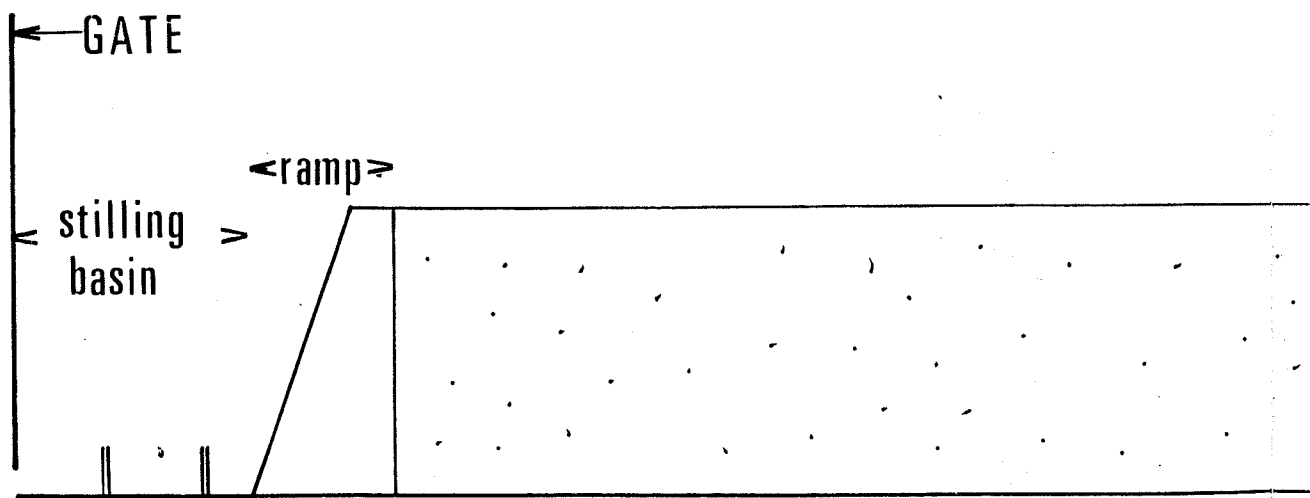
STATION (ft.)



SIDE VIEW



18 16 14 12 10 8 6



underlying sump. The flow was received in a head tank and the discharge was measured by timing the volume accumulated in the holding tanks.

The downstream end of the flume was provided with a tailgate which could be cranked up or down. This tailgate regulated the stage discharge pattern of the flow required in the study.

4.1.3 Measuring Devices

The principal recording instruments included;

- 1) A point gauge for measuring the water surface elevations and the static bed elevation at any point within the flume. The point gauge was equipped with a vernier to measure to the nearest 0.001 foot.
- 2) An electronically sensed propeller meter for velocity measurements.
- 3) Stop watch for discharge and velocity measurements.

4.2 Material

- 1) Sand - one size of sand of .5 mm median diameter was used as bed material in the main testing program.
- 2) Walnut shells - one test was run with walnut shells .65 mm median diameter.

U. S. Bureau of Reclamation recommends the sieve size passing 75% of the material by weight as the representative

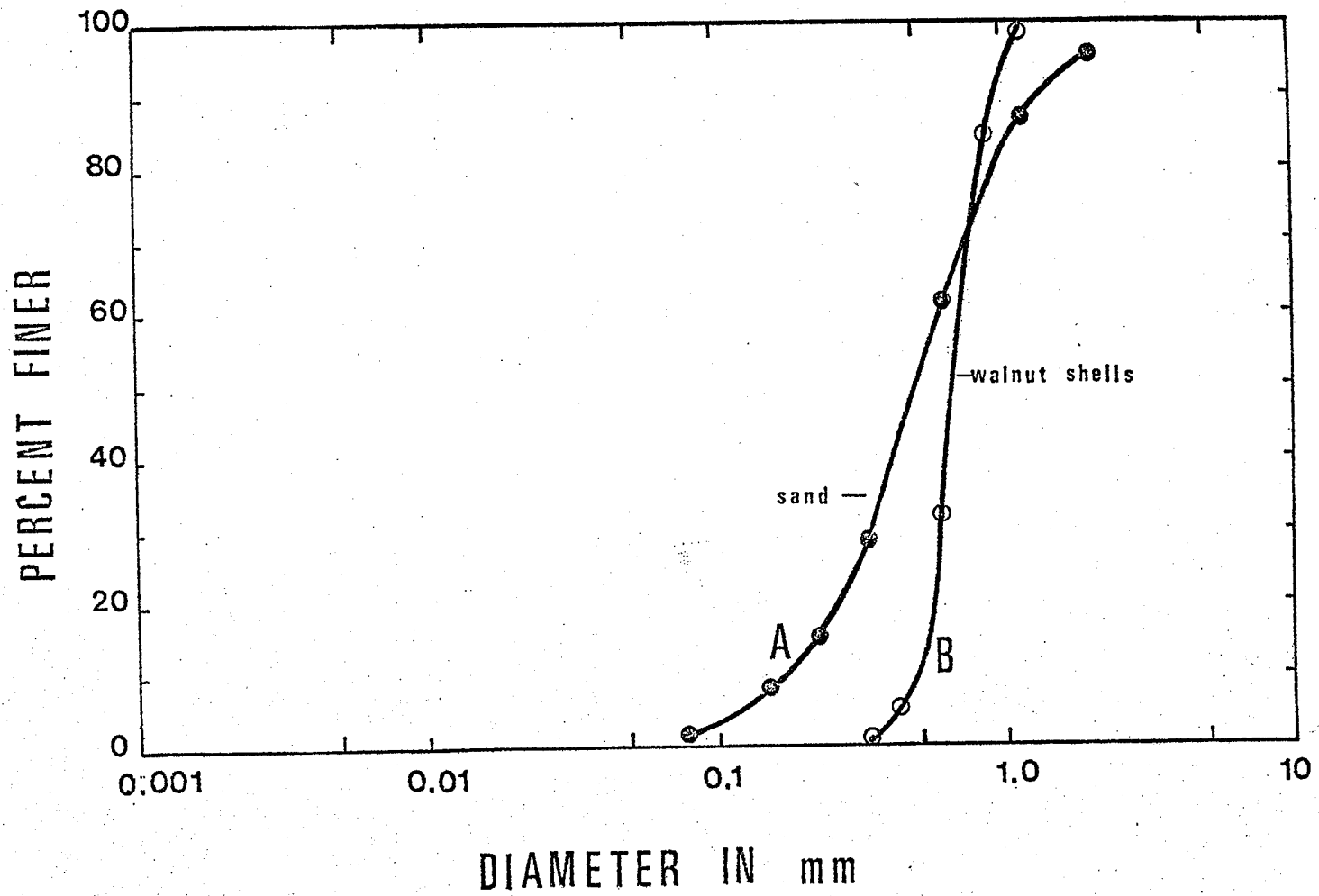


Fig. 4.2 SIZE-DISTRIBUTION CURVE FOR BED MATERIALS.

size for course non-cohesive materials above .2 inch. For the .5 mm material it was arbitrarily decided to accept the median size in this study.

The size distribution curve is shown in Fig. 4.2.

TABLE I
CHARACTERISTICS OF BED MATERIAL.

Distribution Curves	Material	d_{50} in mm.	Specific Gravity	σ_{gd}
A	Sand	.5	2.65	2.01
B	Walnut Shells	.65	1.3	1.25

- 3) Abutments - Top width of the abutments represented a 24 foot roadway approximately. Side and front slopes were both two to one with a circular sloping face joining the front and sides. The abutments were always continued below the maximum scour depth. The complete abutments, except for the top, were covered with riprap.
- 4) Abutment Riprap - One size of material was used which passed through a 3/8 and remained on a 1/4 inch sieve.
- 5) Ice Material - Low density polyethylene was used as ice material. Sizes ranged from 1/4" x 1/4" to 2 1/4" x 2 1/4". This represented 1' x 1' to 9' x 9' floes. Two thicknesses were also used 1/4" and 3/8" representing 1' and 1 1/2'. The

thicker ice usually being larger in size than the thin ice.

4.3 Procedure

In order to determine flow patterns, scour depth and pattern, velocities and backwater effects, runs A1 to A8 were performed without any ice. These were meant to assess the applicability of design curves for scour at constrictions in the model.

Run J7, J8, and J9 with five locations of a solid ice cover were performed with ice floes in order to gain some insight into Froude numbers at which ice jams occur at constrictions and the location effect of a solid ice cover downstream of the constriction.

C1 to C14 were run without any constrictions. These were intended to determine affect of detergent on underturning and to study mode of underturning. Ice floe size was also varied to test affect this had on Froude number at which they turned under.

The main testing program encompassed run HD1 to HD27. Three constriction ratios were tested .46, .40, .36, at depths of .2 and .33 feet. Studied in these runs were head loss due to the ice jam, depth of jams, backwater, scour, effect of solid ice cover, flow patterns, and the effect different rates of dumping had on the hanging dam.

4.4 Data Taken.

In the main tests, experimental procedure involved gathering data for varying approach flow conditions and constrictions in respect of -

- 1) flow pattern and velocity distribution through constriction.
- 2) maximum depth and pattern of scour at varying contraction ratios.
- 3) maximum backwater.
- 4) thickness of ice accumulation and volume of ice material used.
- 5) water elevations as affected by ice jamming.

The running of each test involved closing the tailgate and filling the flume to avoid scour at the constrictions at the beginning of testing. Before each run, the desired Froude number at 10 feet with depth of .2 or .33 was obtained by altering the discharge and tailgate. When this constant level was achieved, ice was added.

The slight difference in slope between bed and water surface was accepted because constricted flow is basically a local phenomenon.

By injecting dye from upstream and also using confetti, the flow pattern and eddy zones could be visualized.

Photographs of flow patterns, ice depths and forms, scour pattern and other pertinent features were taken during

the tests.

Flow was continued in runs A1 to A8 for six hours and in HD1 to HD27 for one-half hour after ice jamming.

The scour patterns were contoured while the water receded and scoured bed elevations were recorded.

4.5 Ice Feeding.

The usual method of ice feeding is as follows: 1 gallon cans were used as mixing containers. Pails were filled 1/2 full of ice, .08 cubic feet in volume, to the ice was added detergent and water. Each .08 cubic foot was dumped slowly over a large area upstream of the constriction.

4.6 Model Setup.

The model used represents a 150 foot river approximately 10 feet in depth. The scale ratios were based on the Froude Law Criterion; the scales were as follows -

Horizontal	1:50
Vertical	1:50
Velocity	1:7
Discharge	1:17,500.

CHAPTER V

COMPARISON OF EXPERIMENTAL RESULTS ON SCOUR WITHOUT ICE5.1 General

To determine whether scour hole depths and shapes, and backwater can be predicted on small rivers, experimental results from this study were compared with design curves of various abutment shapes and end-dump closure constrictions.

5.2 Scour Patterns

Maximum scour has been located at the vena-contracta section for end-dump constrictions by Das (1972) and Sandoyer (1970).

Liu Chang and Skinner (1961) and Tutt (1972) also observed scour downstream of the constriction for spill-through abutments. Shown in Fig. 5.1. are scour patterns obtained by Das for end-dump closure.

At lower contraction ratios, scour occurs around the face of the constriction whereas at higher degrees of contraction scour holes overlap and a general pothole scour pattern is observed. Deepest scour was noted to occur near the vena-contracta.

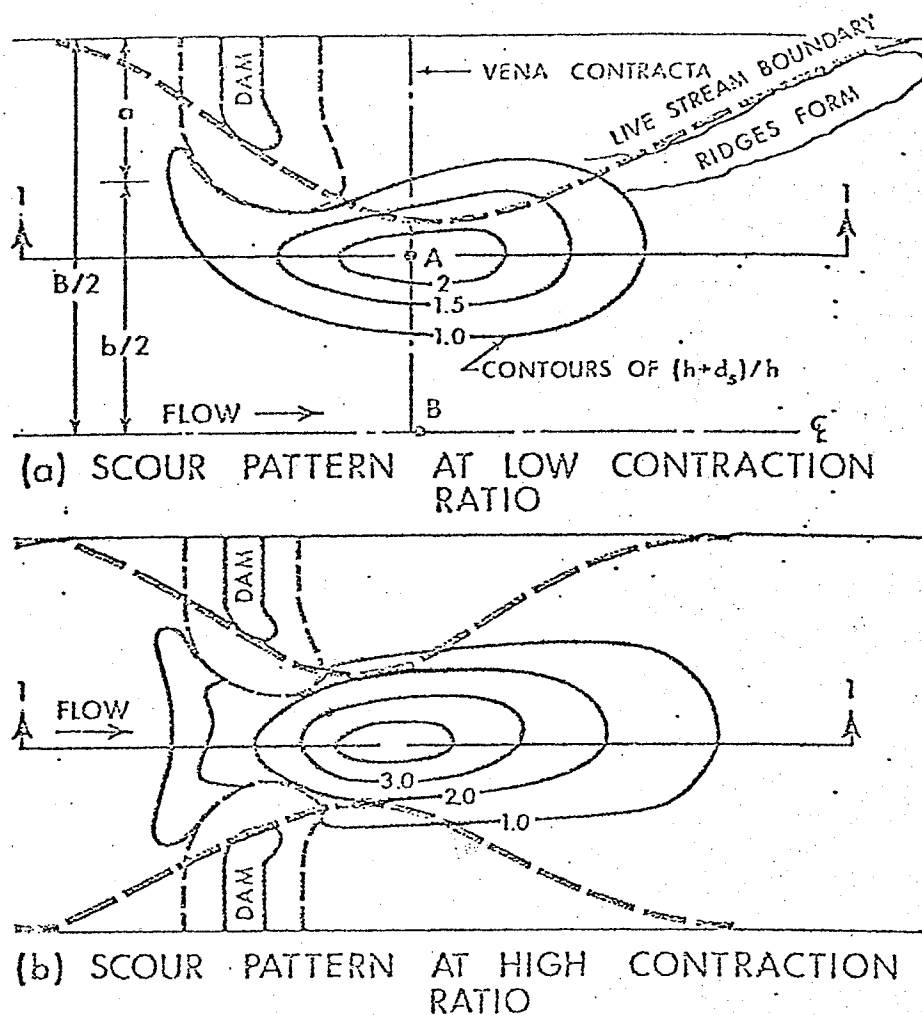
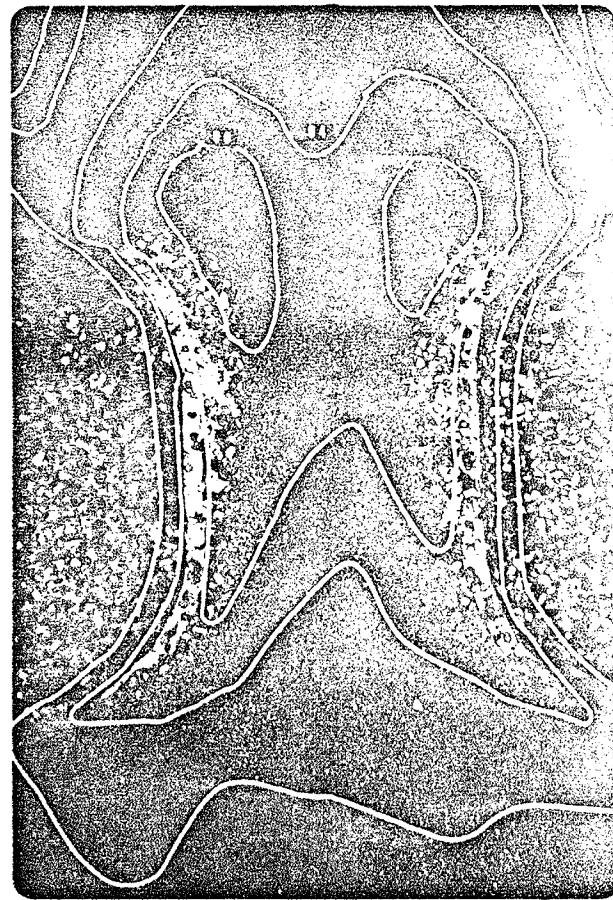


FIG. 5.1. SCOUR PATTERNS OBTAINED BY DAS (1972)
END DUMP CLOSURE

Spill-through abutments on small rivers appear in general to follow this type of scour pattern. Shown in Fig. 5.2 are scour patterns at low constriction ratios. The maximum scour occurs along abutments downstream of the constriction. Increasing the Froude number in these runs would cause the two scour holes to overlap and form a pothole downstream of the constriction.



a) RUN A-6 $F = .24$ $m = .45$



b) RUN B-6 $F = .25$ $m = .45$

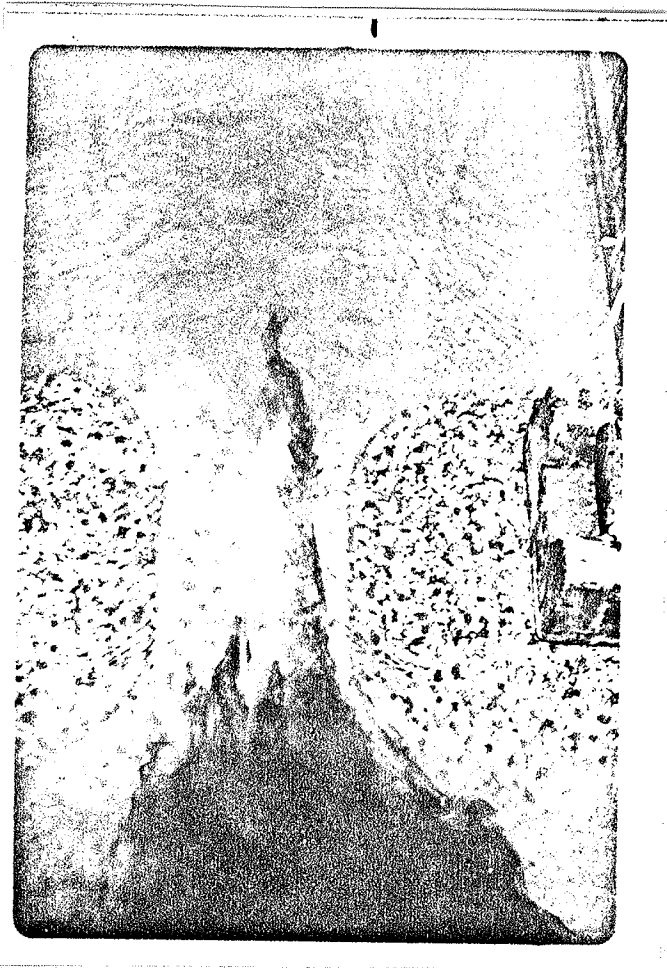
FIG. 5.2 VIEW OF SCOUR HOLES AT DOWNSTREAM CORNER OF ABUTMENTS

At very high constriction ratios, having the abutments continued below the maximum scour depth, results in them practically meeting in the centre of the channel. This will alter location and depth of scour. Therefore, constriction ratios much larger than .5 form different scour patterns at high Froude numbers than that described by Das (1972) for end-dump closure. See Fig. 5.3. An actual constriction ratio such as this does not seem practical.

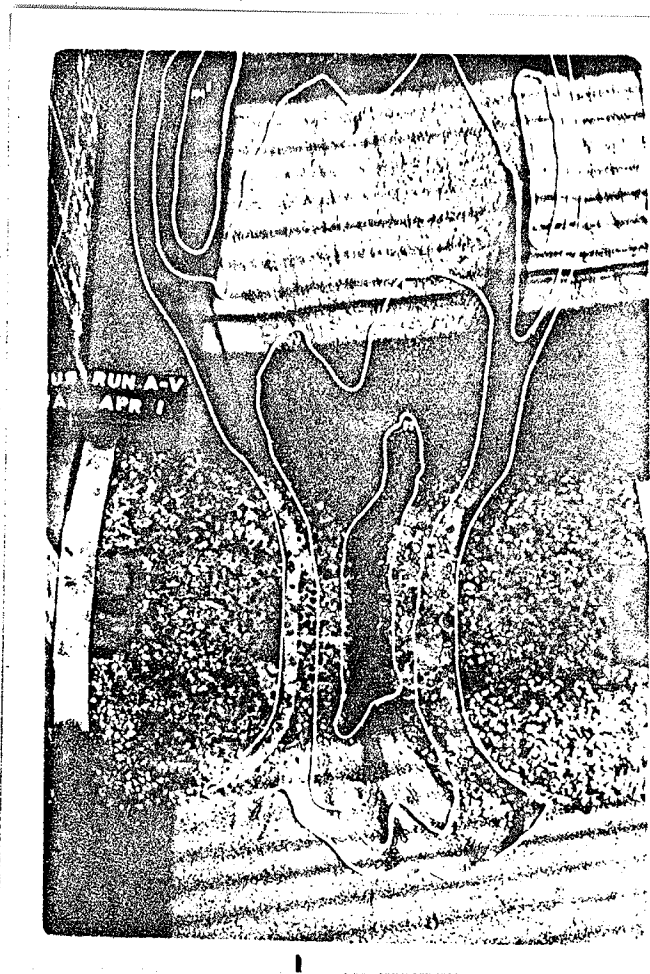
5.3 Analysis of Scour at Spill-through Abutments

In order to verify the amount of scour obtained during ice free conditions and to determine the design curves most suited to this situation, results from this study were compared with:

- a) Laursen's (1960, 1963) design curves for i) local scour at an isolated abutment and ii) general scour with opposing abutments.
- b) Komura's (1966) design curves for general scour at a long contraction.
- c) Garde et al (1966) maximum scour at vertical edge spur dikes.
- d) Liu et al (1961) maximum scour at bridge constrictions.
- e) Das (1972) design curves for scour at end-dump closure.



a) RUN A-2 $F = .25$ $m = .67$



b) RUN A-5 $F = .25$ $m = .53$

FIG. 5.3 AT HIGH CONSTRICTION RATIOS SPILL-THROUGH ABUTMENTS AFFECT SCOUR PATTERN

Check Against Laursen's and Komura's Analysis.

a) Isolated scour hole (Laursen 1963).

A comparison of \bar{d}_s/h for the runs with isolated scour holes is made in Figure 5.4 with Laursen's curves.

Laursen's curves predict much larger scour holes than those obtained in this study.

b) Overlapping scour holes due to Laursen (1960 and 1963) and Komura (1966).

Two tests with scour holes overlapping were plotted against Laursen's and Komura's curves. Figure 5.5. The scour holes obtained were larger than that predicted by Laursen and Komura.

Check of Garde et al's and Liu et al's Data.

Along with Garde et al's and Liu et al's data are plotted Das' results. Figure 5.6. This experiment seemed in best agreement with Das' study on scour at end-dump closure. Because contraction ratios in this study were not identical to any in Liu et al's and Garde et al's study, no direct comparison can be made.

Check with Das' Proposed Design Curve for Scour at End-Dump Closure.

The tests run in this experiment were at Froude numbers .22 to .25. The results plotted on Das' design curves, Fig. 5.7,

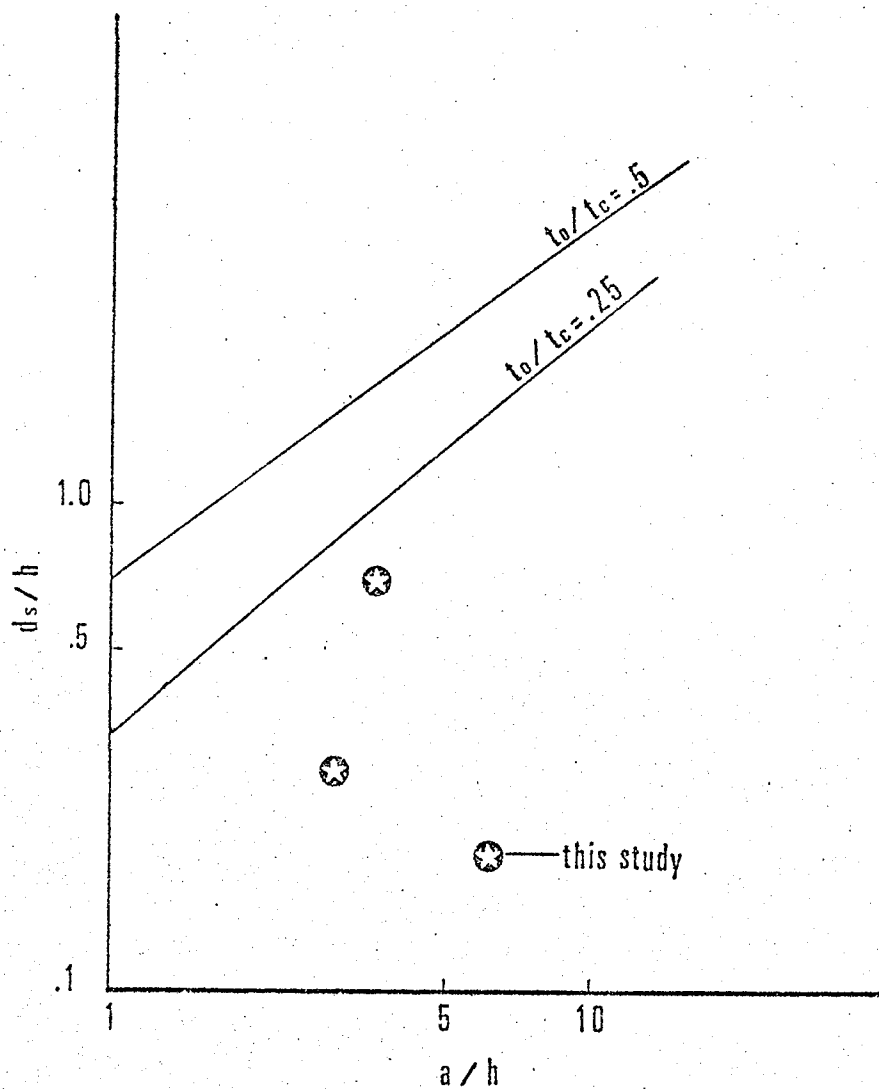


Fig. 5.4 COMPARISON OF THIS STUDY WITH LAURSEN'S (1963) ANALYSIS FOR SCOUR AT ISOLATED ABUTMENTS.

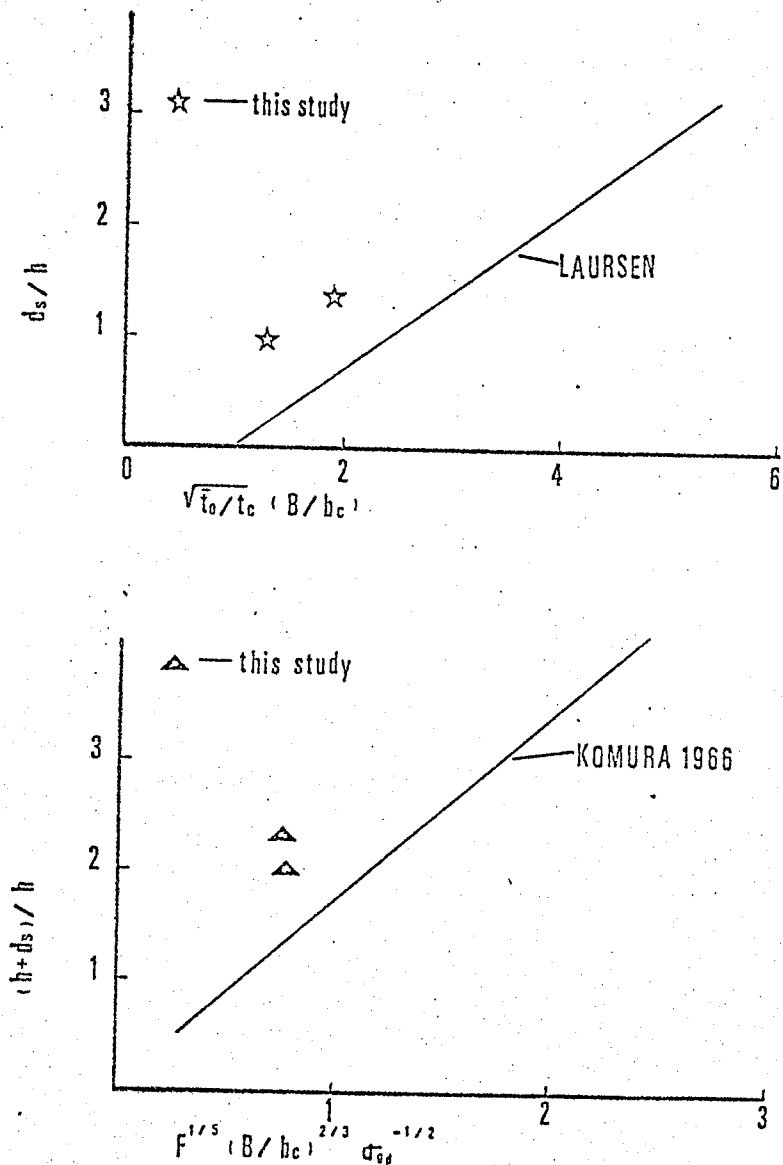


Fig. 5.5 COMPARISON OF THIS STUDY WITH a) LAURSEN AND b) KOMURA (1966) ANALYSIS FOR SCOUR IN LONG CONTRACTIONS.

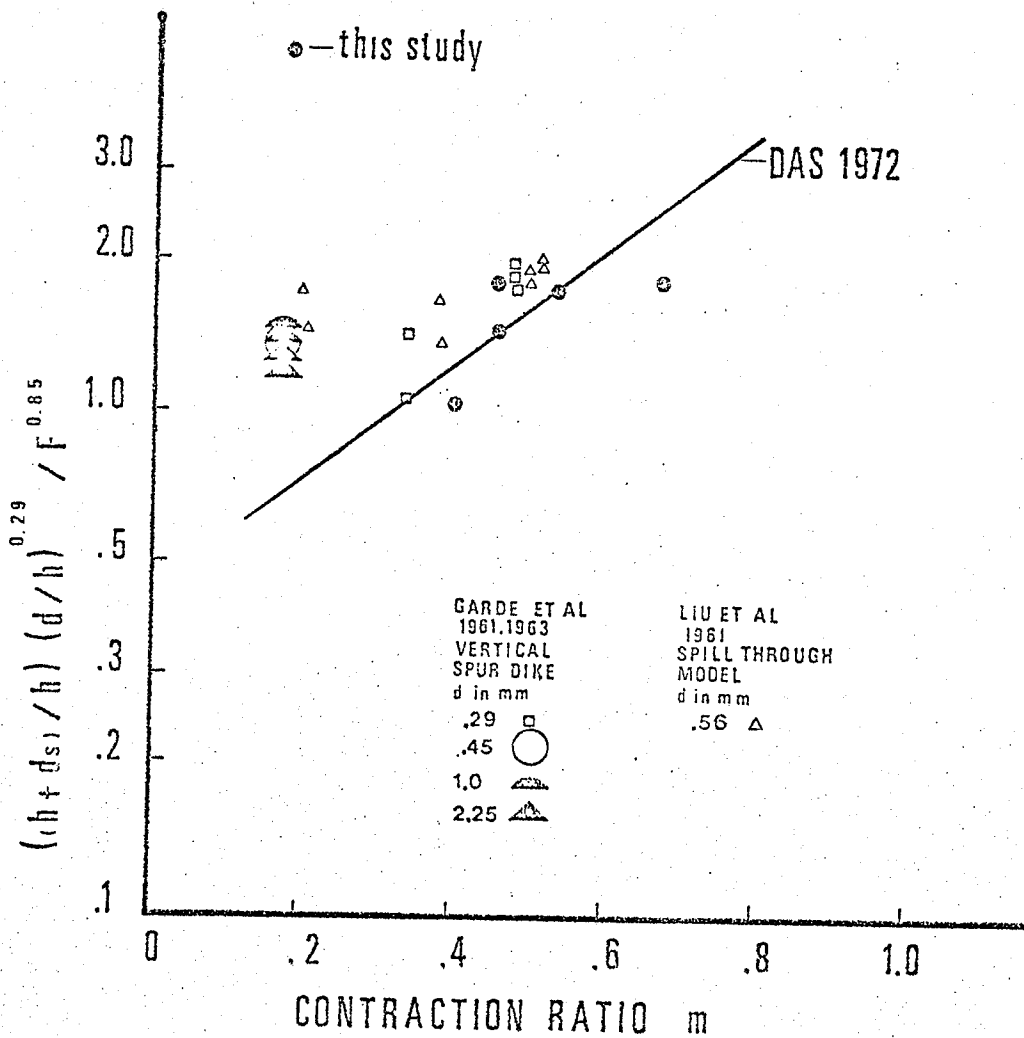


Fig. 5.6. COMPARISON OF GARDE ET AL'S (1961) DATA ON SCOUR AT VERTICAL SPUR-DIKES AND LIU ET AL'S (1961) DATA ON SCOUR AT SPILL-THROUGH ABUTMENTS, WITH THIS STUDY.

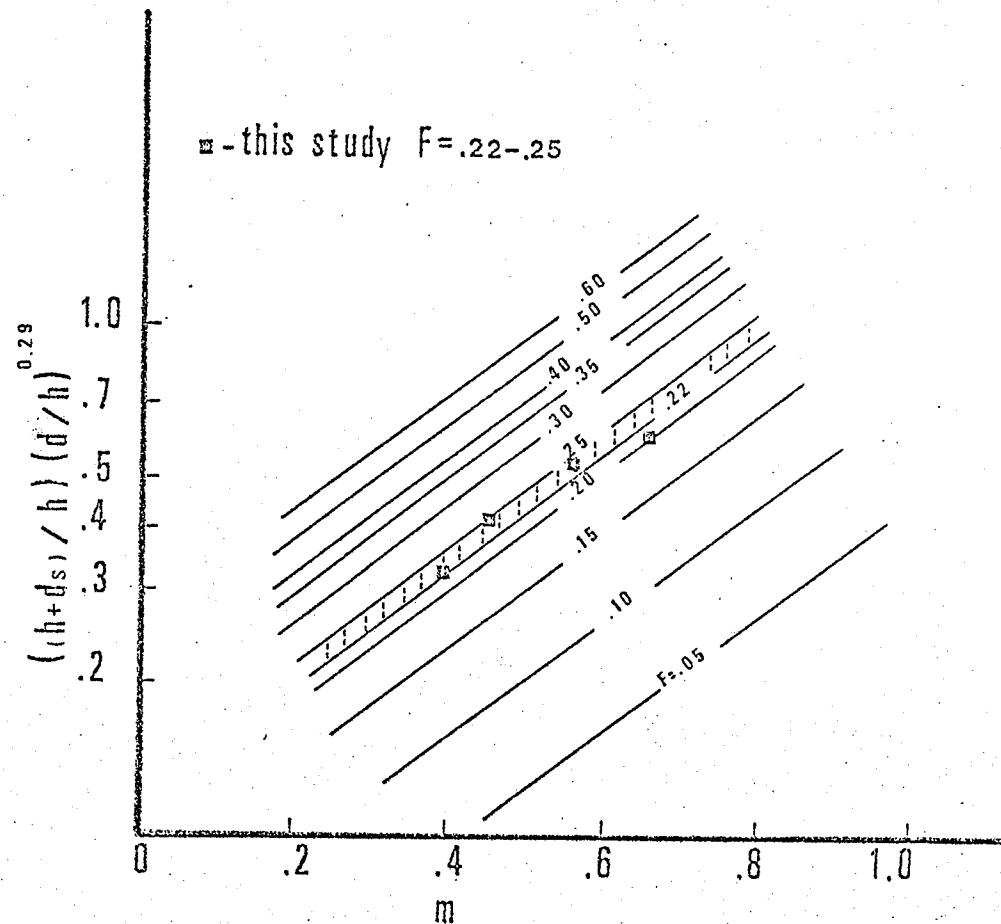


Fig. 5.7. COMPARISON OF DAS (1972) DESIGN CURVE FOR SCOUR AT END-DUMP CONSTRICTIONS WITH THIS STUDY.

TABLE II
COMPARISON OF DESIGN CURVES OF LAURSEN, KOMURA
AND DAS WITH THIS STUDY

Run No.	Froude No of normal flow	Depth of Flow	M Contraction Ratio	Depth of Scour Observed	Depth from Das end dump closure	Depth from Laursen Isolated Abutments	Depth from Laursen Constriction abutments	Depth from Komura long Constriction
A - 2	.25	.19	.67	.26	.35		.04	.06
A - 4	.22	.21	.4	.06	.07	.23		
A - 5	.23	.2	.53	.20	.23		.13	.07
A - 6	.24	.2	.45	.14	.14	.25		

show excellent agreements.

Table II shows a comparison of observed scour depths with those predicted by the above experimenters. The agreement with Das is very striking. Possible deviation of A-2 could result from abutments continuing under the bed limiting scour. Although tests were too few for any definite conclusions, scour at spill-through abutments on small rivers seem to be similar to that at end-dump closures. Reasons for this might be that the L/b ratio of abutments is large in small rivers. This tends to give more streamlined flow through the constrictions and a reduction in scour depth.

5.4 Analysis of Backwater at Spill-through Abutments

The maximum backwater will be taken as the elevation just upstream of the constriction.

Variation of H/h with M and F .

Liu et al (1957) Valentine (1958) Biery and Delleur (1962) Das (1972) and Sandover (1970) have considered

$$\frac{H}{h} = f \left(F, m, \frac{d}{H} \right)$$

from dimensional analysis to be the governing variables influencing the maximum backwater.

The results of this study plotted against Das' curves for H/h vs. M with F as a third variable show considerable agreement in Fig. 5.8.

Variation of $(H/h)^3$ with $F^2 (1/M^2 - 1)$

A plot of $(H/h)^3$ with $F^2 (1/M^2 - 1)$, Fig. 5.9. is made for rigid spill-through abutments and Das' backwater due to end-dump closure. The resulting plot agrees fairly well with Das.

Variation of C_m with F and M

Discharge coefficients C_m for all runs with bed scour were computed. These were plotted along with Valentine's coefficients for a rigid bed and Das' coefficients for end-dump closure.

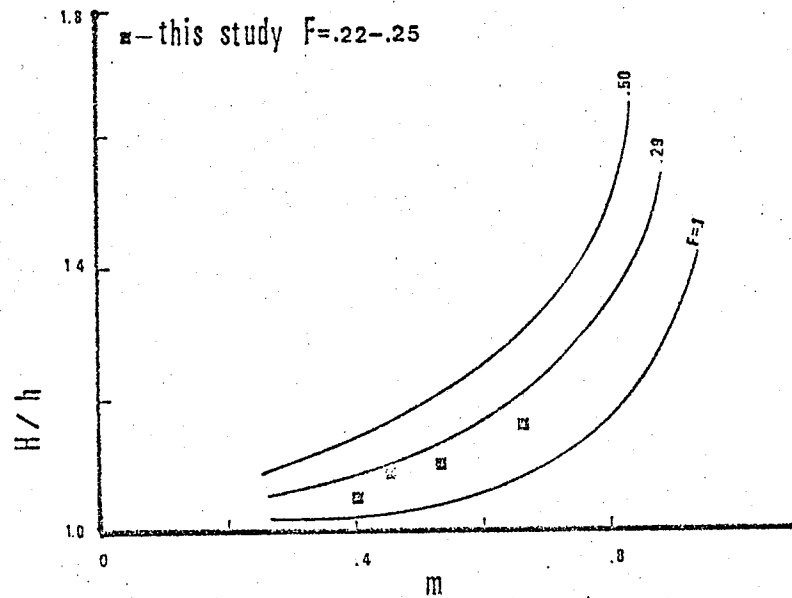


Fig. 5.8 COMPARISON OF H/h VS. m OBTAINED BY DAS (1972) WITH THIS STUDY.

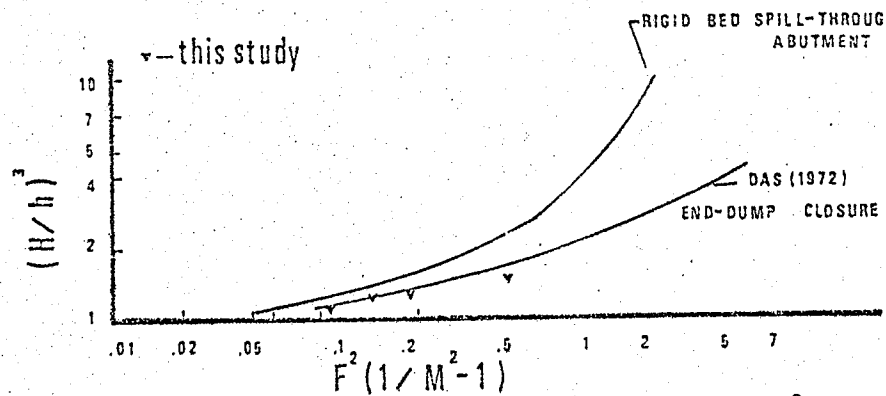


Fig. 5.9 COMPARISON OF RELATIONSHIP $(H/h)^3$ AND $F^2 (1/M^2 - 1)$ OBTAINED BY DAS (1972) AND LIU ET AL (1957) WITH THIS STUDY.

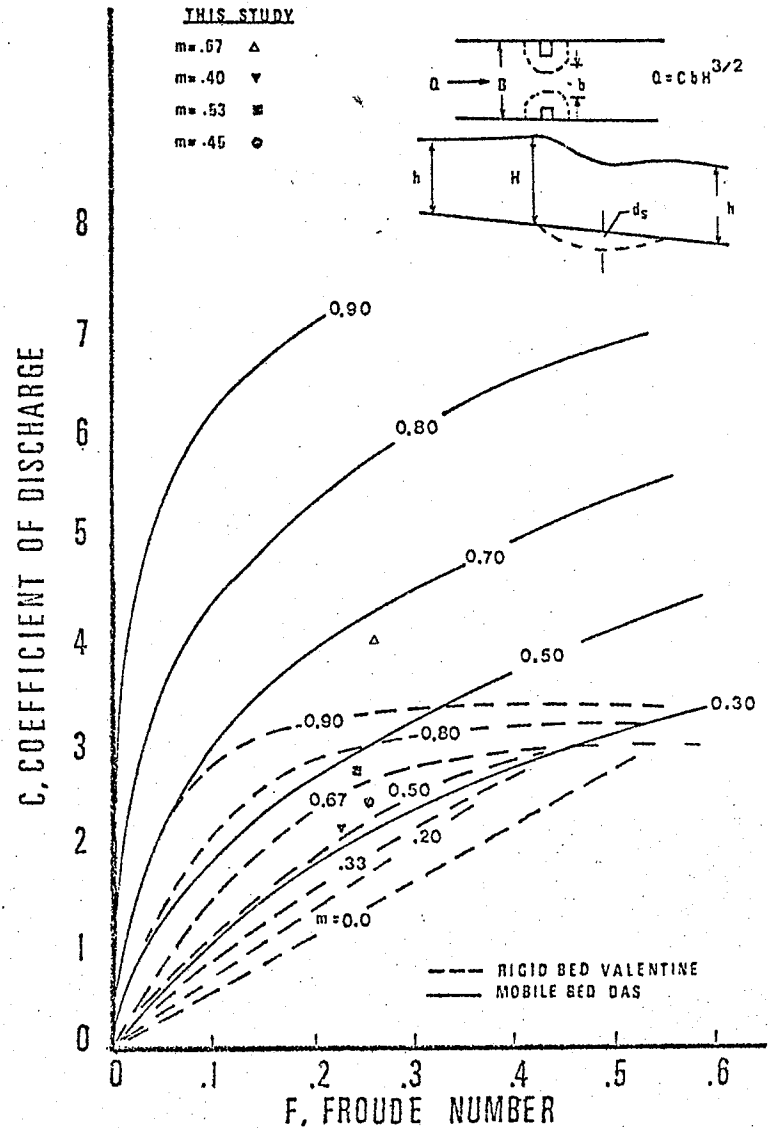


Fig. 5.10 RELATIONSHIP FOR MAXIMUM BACKWATER DEPTH ON MOBILE BEDS CORRELATING C , F , AND M .

The plotted points although similar to Das' Fig. 5.10 predicted a slightly lower discharge coefficient.

5.5. Analysis of Flow Patterns and Velocity Distribution

5.5.1. Maximum Contraction

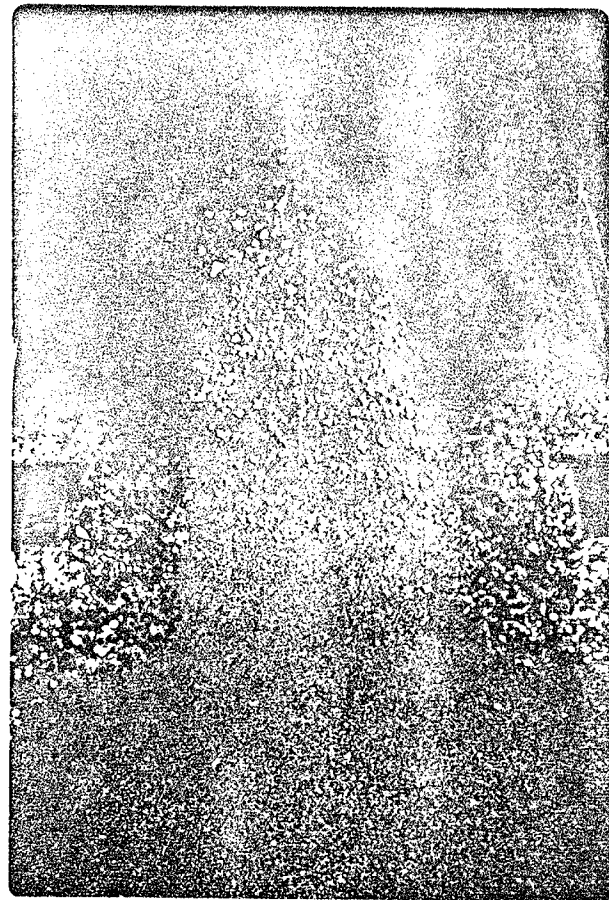
Das (1972) observed the maximum contraction further downstream of the constriction than this study seems to indicate. However, Das' end-dump constrictions advanced downstream with the flow and the resulting maximum contraction and scour were at the tip of the advancing face. From Fig. 5.11, the slightly higher constriction ratio and Froude number in photograph a) indicates the maximum contraction to be at the constriction while Fig. 5.11 b) shows it to be near the downstream toe of the constriction.

5.5.2. Flow Patterns

The live stream boundary in this test, unlike Das' (1972) did not expand equally on both sides of the channel. Lane (1920) also observed that although flow and channel properties were identical on both sides of the flume, flow usually picked a side. This resulted in scour to be more pronounced on one side of the flume, but as the scoured material built up downstream and the resistance increased, the flow would shift. Thus the resulting flow after scour had taken place and scour were symmetrical.



a) High Constriction ratio shows maximum contraction possible between abutments. Yellow dye upstream, blue dye downstream, green shows mixing.
RUN A-5 $F = .23$ $m = .53$



b) Low Constriction ratio shows maximum contraction at downstream toe of abutments. RUN A-6 $F = .24$ $m = .45$

FIG. 5.11 FLOW PATTERNS AT CONSTRICTIONS AS SHOWN BY DYE



FIG. 5.12 RUN A-5 $F = .23$ $m = .53$
FLOW EXPANDING UNIFORMLY AFTER SCOURING THE BED

5.5.3 Velocities

The average velocity distributions during testing were similar to those of Das (1972), however, due to the scale used in this study, velocity contours were not obtainable. Shown in Fig. 5.13 a) is a typical velocity distribution obtained by Das where $m = .65$, $h = .18$ and $V = 1.15$ fps. Shown in Fig. 5.13 b) is a typical live stream boundary from

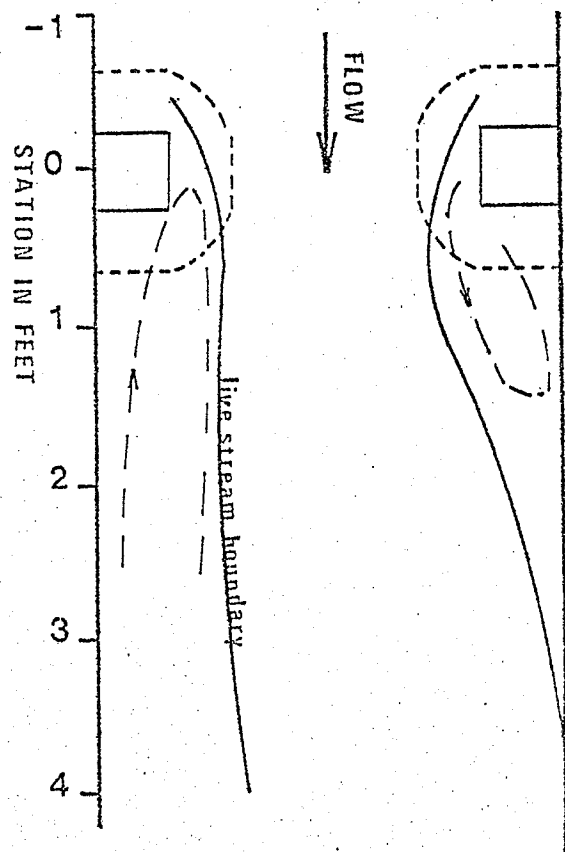


Fig. 5.13 b) TYPICAL LIVE STREAM BOUNDARY FOR THIS STUDY ON TESTS WITHOUT SCOUR.

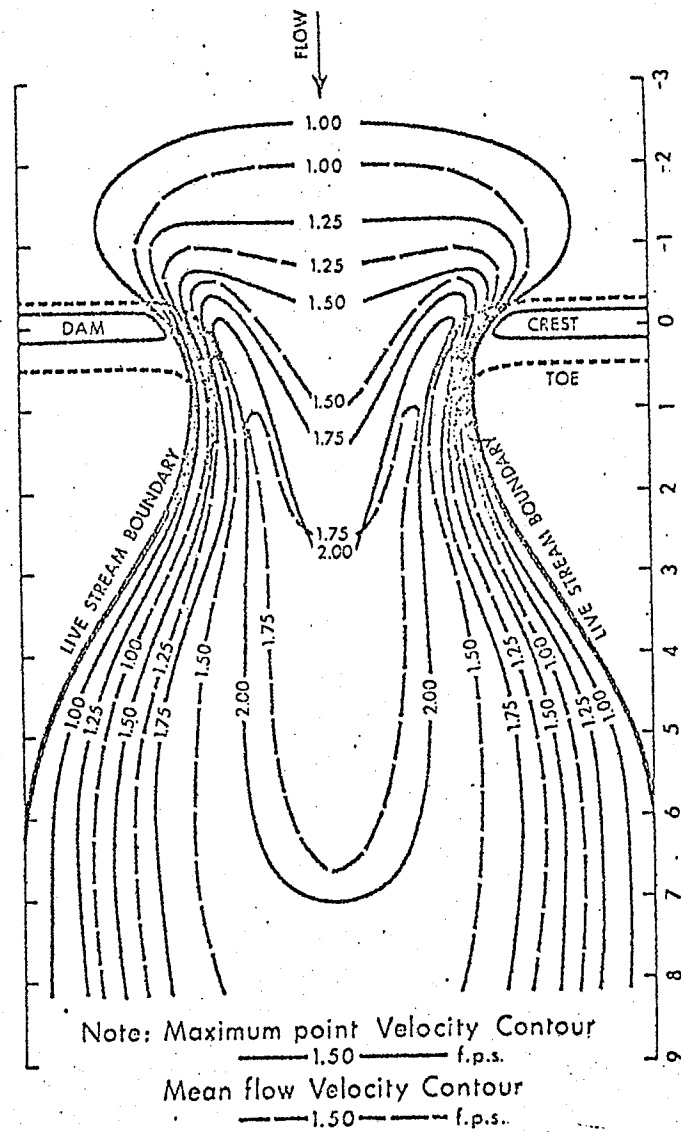


Fig. 5.13 a) VELOCITY DISTRIBUTION FOR END-DUMP CLOSURE DAS (1972)

this study. The left side did not fully expand until about station 14. This test did not experience scour and had a lower Froude number than Das (1972).

5.6 Conclusion

Backwater, flow patterns, scour depth and patterns agree with Das (1972) and other previous experimenters. When the constriction ratios were not unusually high, the maximum contraction and scour took place near the downstream toe of the abutments. Because of the agreement shown with existing design charts for open water conditions, the experimental apparatus appears to have a sound basis for testing with ice.

CHAPTER VI

ICE JAMMING STUDIES6.1 Description of Jamming6.1.1 Hanging Dam Formation

Consider a uniform channel with a constant width, flowing at a specific Froude number and depth where an ice cover is advancing upstream at a constant thickness. This ice cover advances into an area of expanding flow downstream of a constriction. Due to the fact that flow has not expanded fully, higher velocities prevail down the center of the channel and ice starts to turn under in this area. As the cover approaches the constriction, depth of jamming increases most notably down the center of the channel. Near the point of maximum contraction, the depth of jamming is most severe. The depth then reduces slightly as it advances into the constriction, ice floes will be swept under the cover and thicken the immediate edge of the arch. (The arch is the configuration and the term given to the upstream face of the hanging dam.) Depending upon the Froude number, thickening and travelling under the dam occur until the cover advances through the constriction at a single thickness or the dam becomes excessively deep and the

downstream cover fails, i.e. the particulate cover supporting the hanging dam begins turning under and the hanging dam moves downstream.

Hanging dams can achieve depths more than one-third the depth of flow because of the ability of a hanging dam to transfer the forces of a narrow flow width acting on a great depth to the downstream cover by means of an arch formation. Fig. 6.1 contains a sequence of photos of test HD-26 at a downstream Froude number of .07 and a constriction ratio of .47 exemplifying the formation of a hanging dam.

Appendix C-1 contains all hanging dams formed with detergent and a solid ice cover at 14 feet.

6.1.1 a) Effect of Solid Ice Cover on Hanging Dam Formation

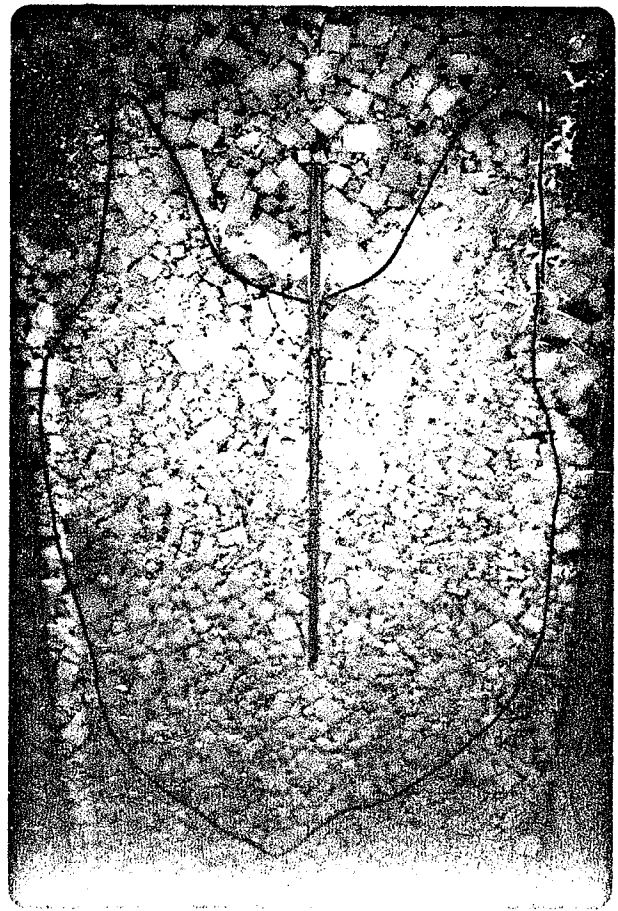
Charbonneau (1973), from model studies on closure of the Reviere des Roches, indicates that a solid ice cover downstream of a constriction will enable the jam to form to the bed where as a particulate cover which is susceptible to failure will not. This was also observed in the tests from this study. A hanging dam with no solid ice cover would not jam to the bed except in tests which lacked small blocks. One or two blocks might come in contact with the bed, but the average depth of thickening never approached the depth of flow.

At a Froude number at which the jam will become stable as a particulate cover, a solid ice cover will alter mainly at its leading edge. Fig. 6.2 a) and b) show that an increase in thickness of the hanging dam occurs mainly at the

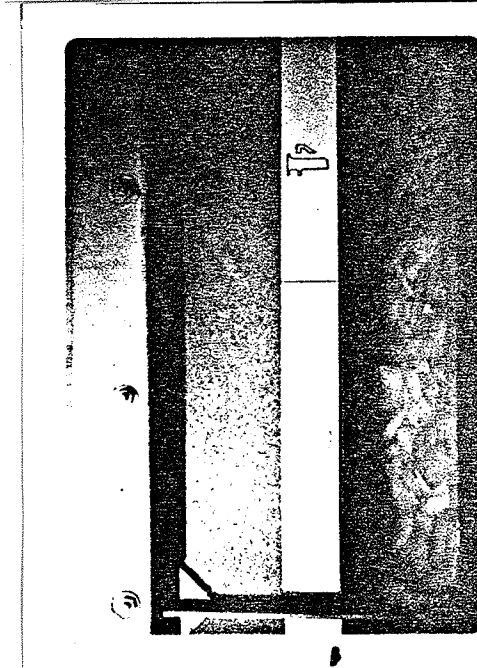
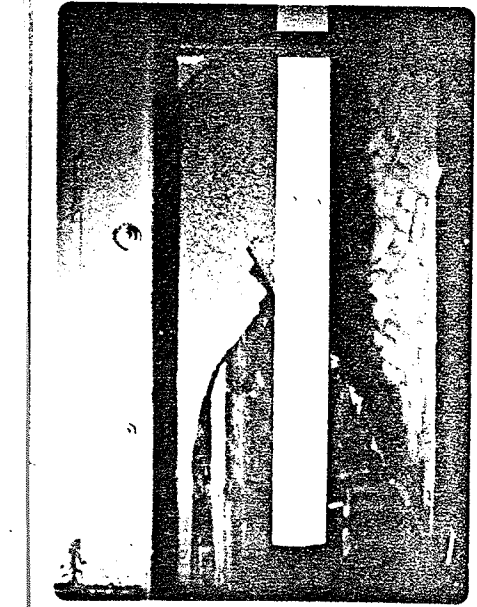
FIGURE 6.1

HANGING DAM FORMATION

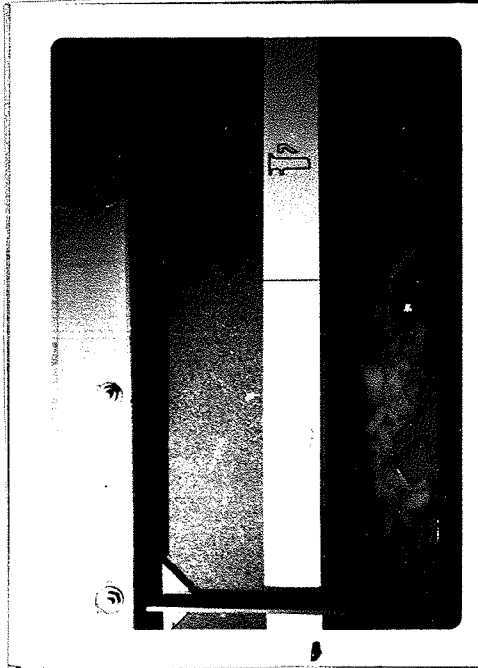
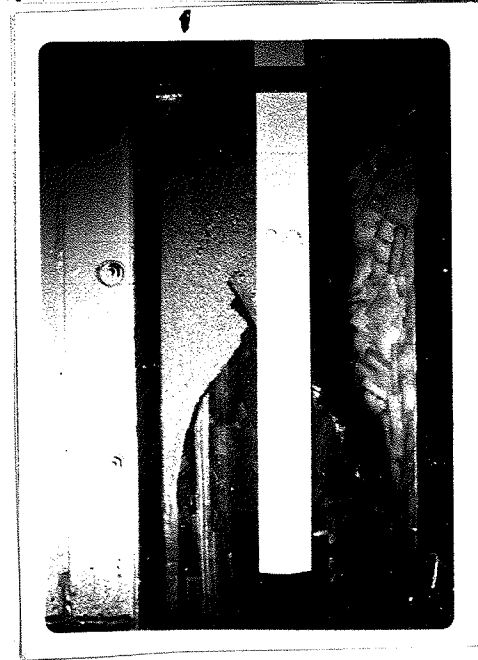
PLAN VIEW OF HANGING WALL (a)



(d) FINAL HANGING WALL AS ICE ADVANCES UPSTREAM THROUGH THE CONSTRICTION.

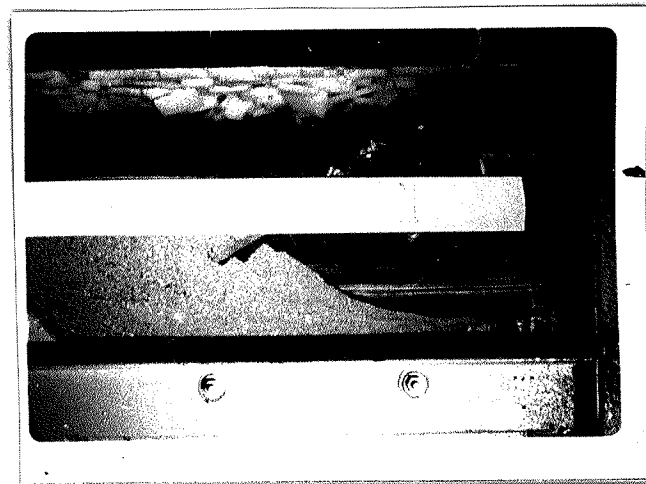


(c) CONTINUOUS THICKENING AND TRAVELLING POSTSTRIPING.

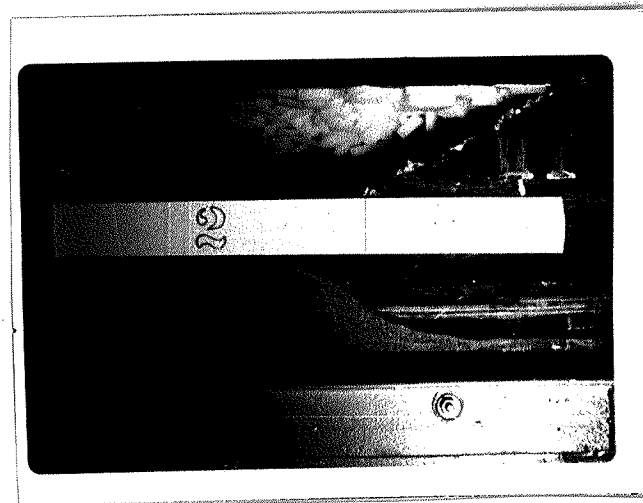


(b) START OF UNDERPINNING AT CONSTRICTION.





a) INITIAL ADVANCEMENT OF ICE TO
CONSTRICTION.



b) START OF UNDERTURNING AT
CONSTRICTION.

leading edge of the solid cover.

Fig. 6.2 c) shows HD-14 jammed to the bed at the upstream edge of the solid cover where as it did not without the cover.

6.1.2 Dry Ice Jams

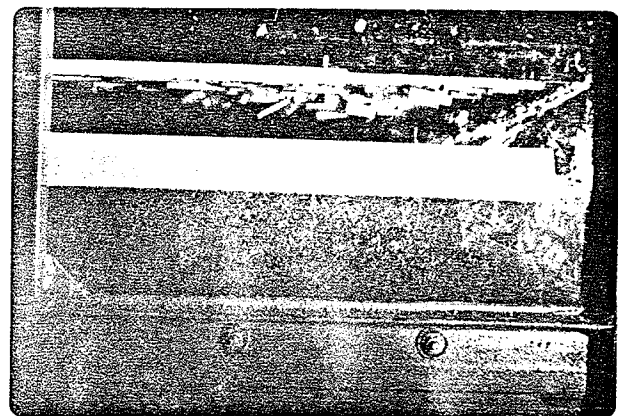
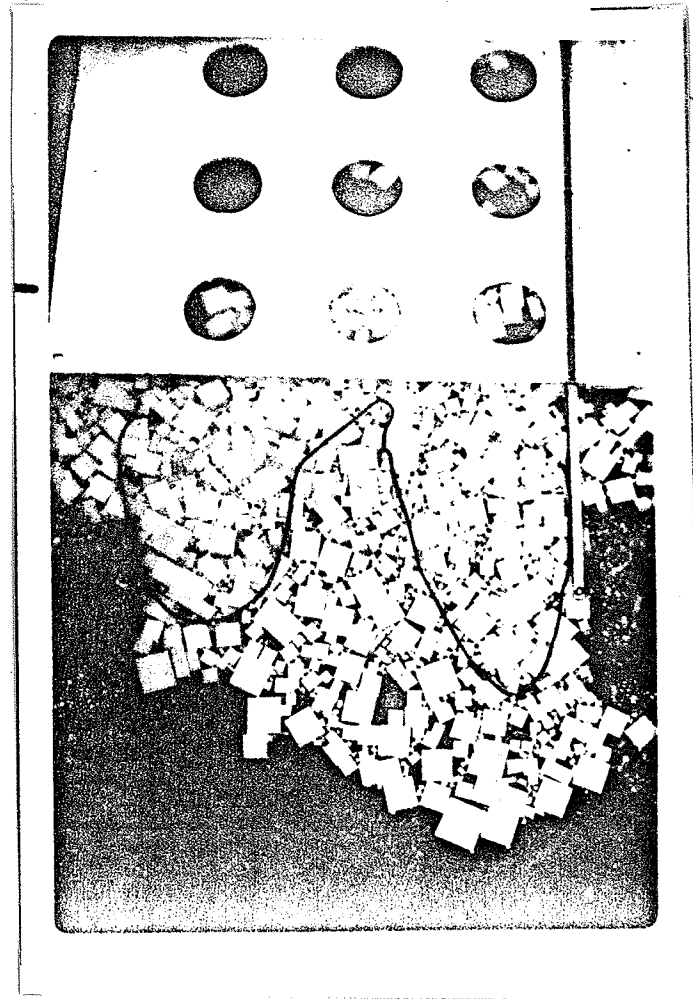
In all of the reported tests, the ice cover situation ranged from Station 14 to zero. On each occasion when the ice cover failed, a dry jam would form against the downstream ice cover. Having the solid ice cover within approximately one foot of the constriction prevented this typical dry jam since a dry jam would not form into the constriction. In the main set of tests, the solid ice cover was at Station 14. On failure of a hanging dam, a triangular dry jam would form against the downstream cover. A typical jam is shown by Fig. 6.3.

6.1.3 Location and Stability of Hanging Dam

The hanging dam in all tests, was located downstream of the maximum contraction with single thickening in the vicinity of the maximum contraction and through the constriction. The maximum contraction can not be explained fully by the Froude number of flow and constriction ratio, therefore the location of the hanging dam also cannot be described with these parameters.

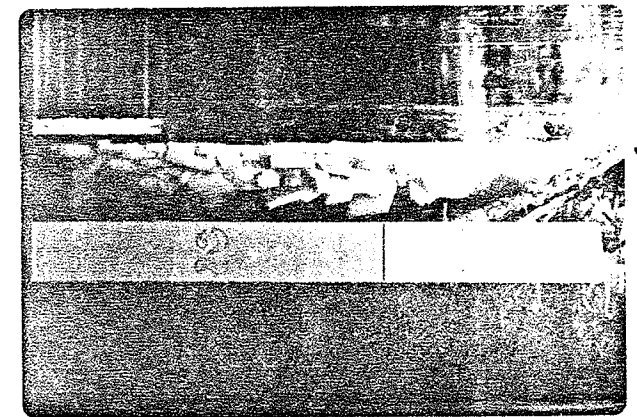
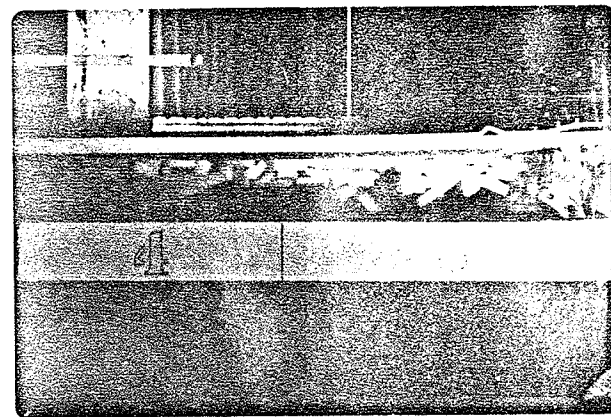
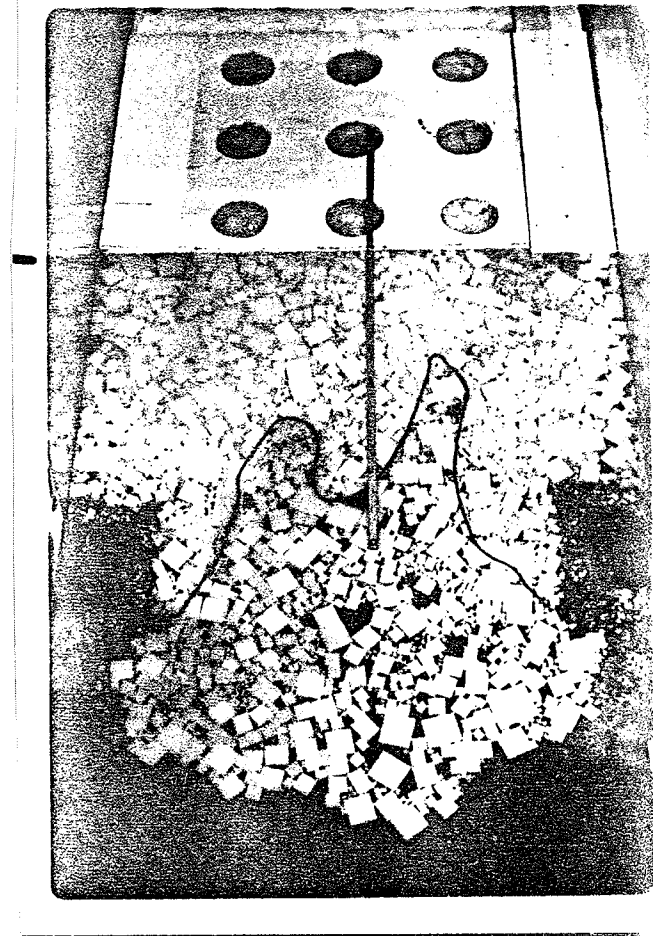
From the general behavior of the hanging dam, a

FIGURE 6.2
EFFECT OF SOLID ICE COVER NEAR
CONSTRICTION ON HANGING DAM FORMATION



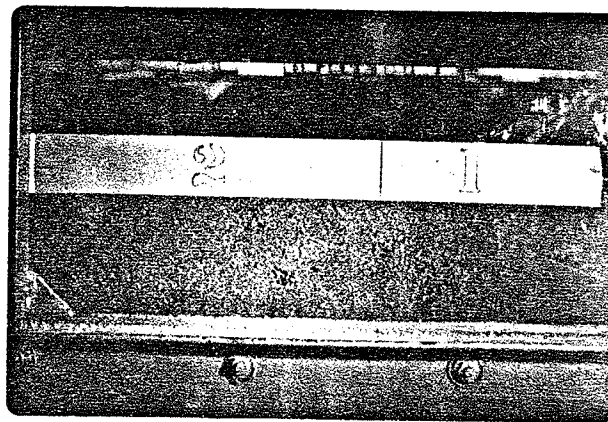
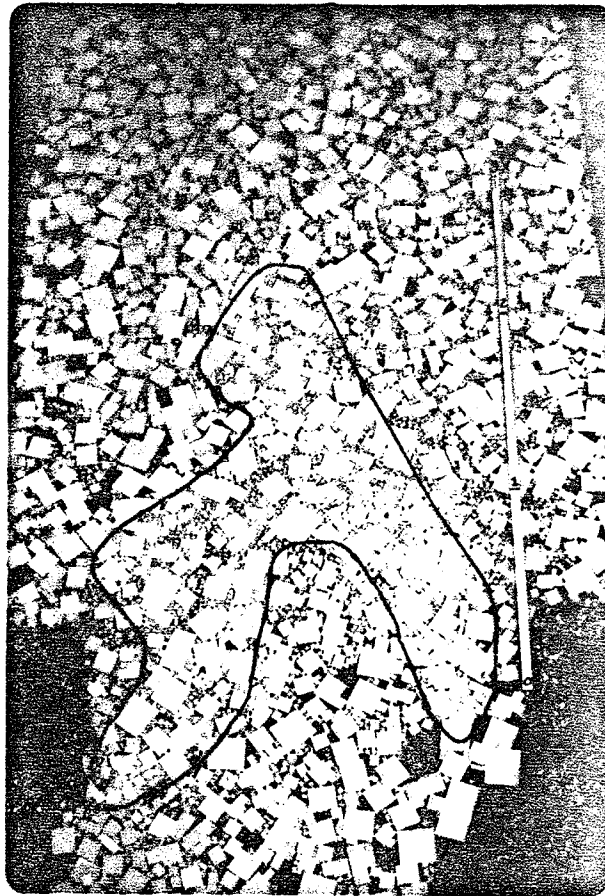
b) RUN HD-13 $F = .07$ $d = .2$

HANGING DAM FORMED AT LOW FROUDE NO. WITH SOLID ICE COVER AT STATION 1. ICE COVER AFFECTS THICKENING AT EDGE.



c) RUN HD-14 $F = .089$ $d = .2$
SOLID ICE COVER AT STATION 2

AT HIGHER FROUDE NUMBER, ICE COVER ENABLES ICE TO JAM TO BED WHERE AS IT WOULD NOT WITHOUT THE COVER.



a) RUN HD-13 $F = .07$ $d = .2$

HANGING DAM FORMED AT LOW FROUDE NO.

few general conclusions can be made on the pattern.

- hanging dam appeared to build up to the constriction with increasing constriction ratio.
- at a particular constriction ratio distance to the hanging dam was proportional to the Froude number.
- increasing Froude number and depth increased the length of the dam.

In all the tests, maximum thickening of the hanging dam was observed from one foot to two and one-half feet downstream of the constriction.

6.2 Flow Patterns and Scour Under Ice Conditions

6.2.1 Flow Patterns

a) Particulate Cover.

As the particulate cover advances upstream from the solid ice cover, maximum thickening takes place in the area of highest velocity thus constricting the flow area. This in itself tends to shift the flow to the sides of the channel, an area of less resistance.

b) Dry Jam.

Greatest accumulation and grounding takes place down the centre of the channel. The resulting flow is usually deflected to both walls.

c) Hanging Dam

The initial high velocities at the centre of the channel create the arch shaped hanging dam. The rate at which the flow will expand and shift to the walls will depend upon the thickening of the hanging dam. Fig. 6.5 exemplifies the expanding flow.

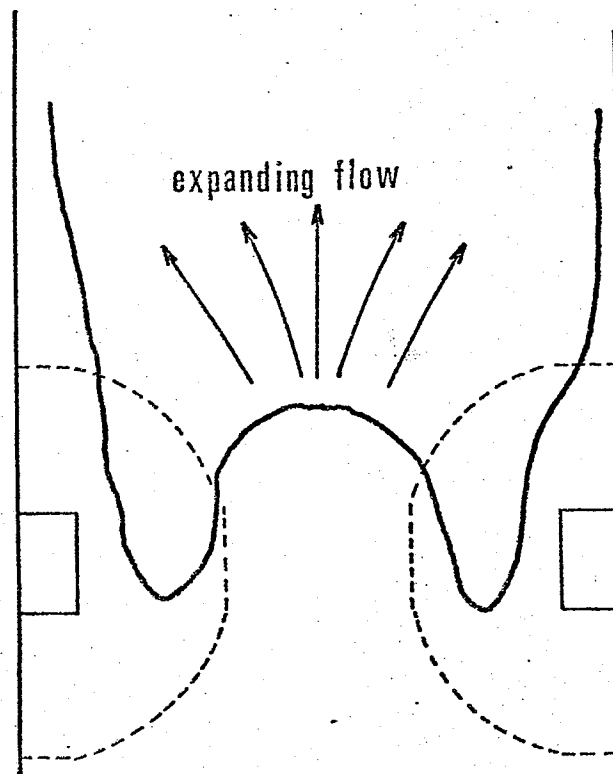


Fig. 6.5 EXPANDING FLOW BENEATH HANGING DAM

d) Other Flow Patterns

In some of the runs with and without a solid ice

cover downstream of the constriction, blocks were gently nudged at the constriction after the particulate cover had advanced through it. Small channels broke through the hanging dam formation running approximately 45° to either wall and often angling from one wall to the other. As these channels filled with ice blocks, high velocities would usually take place on the opposite side of the flume and the channel would erode a new path to the opposite side. Fig. 6.6. demonstrates typical paths. Because the same type of channels formed in every attempt, it was considered to be more than a coincidence. A situation such as this could arise during artificial breakup of a jam.

6.2.2 Scour Due to Ice

In the performed tests with constriction ratios of .46, .4 and .36, a particulate ice cover can not be stable through the constriction at downstream Froude numbers higher than .1 at a depth of approximately .2 feet. With a solid ice cover slightly higher Froude numbers are possible, but it is not known when the ice cover will fail for this depends on its thickness and strength. For gravel bed rivers, there will be absolutely no scour due to the constriction in this Froude number range.

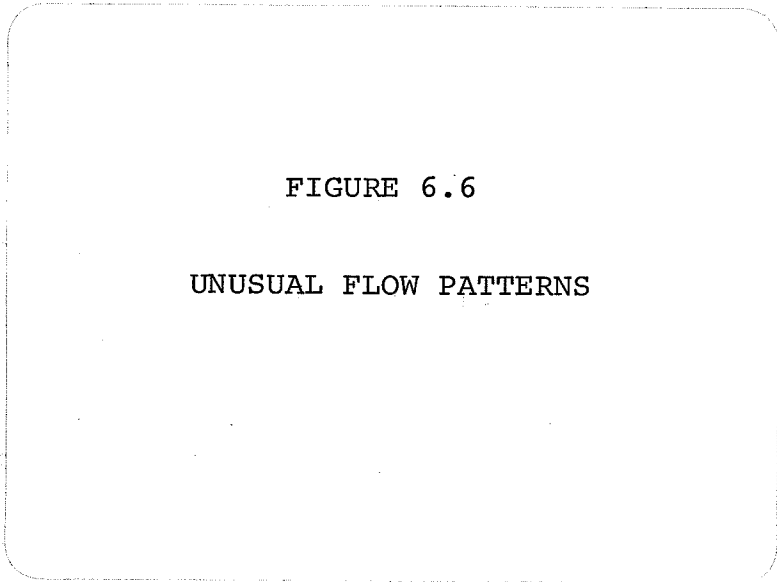
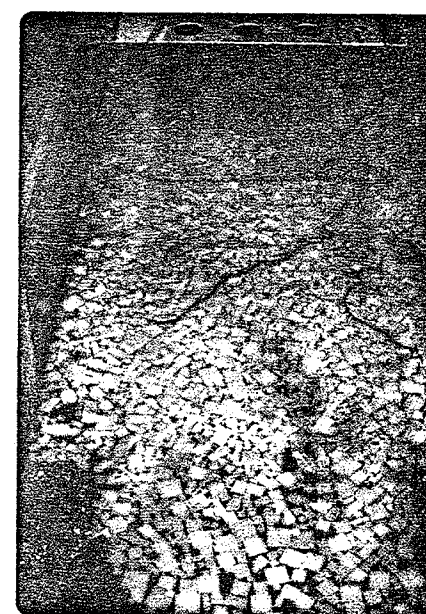
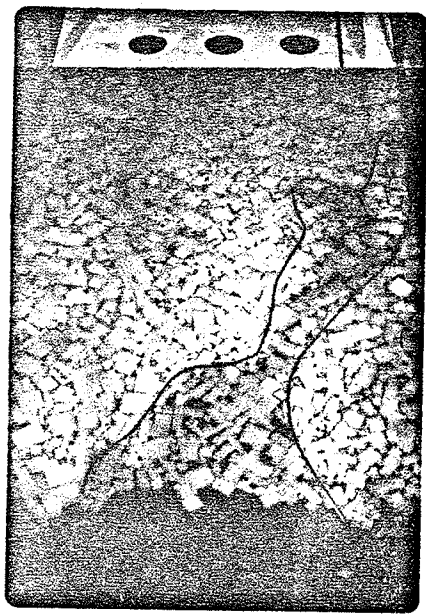


FIGURE 6.6

UNUSUAL FLOW PATTERNS



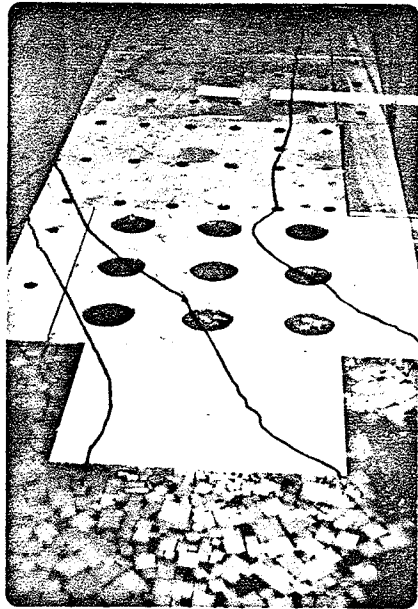
b) HD-6 $F = .09$ $d = .2$ $m = .46$

STABLE HANGING DAM DEVELOPS CHANNELS AS ICE IS HELPED UNDER.

c) HD-5 $F = .08$ $d = .2$ $m = .46$ d) HD-7 $F = .1$ $d = .2$ $m = .46$

ARROW SHOWING FLOW PATH

HIGH VELOCITY OF FLOW DOWN ONE OF THESE CHANNELS RESULTING IN EROSION OF PARTICULATE COVER AND FAILURE OF HANGING DAM.



a) HD-6 SOLID ICE COVER AT 0 F = .09 d = .2 m = .46

AS ICE FLOES ARE HELPED UNDER, CHANNELS DEVELOP UNDER
THE ICE COVER.

6.2.2 a) Scour Due to Hanging Dam

If the scour does occur due to the hanging dam, it usually takes place in the area of the hanging arch shape downstream of the constriction and extends across the bed approximately the width of the constricted opening, see Fig. 6.7. The scour observed was random pothole scour.

The two tests which experienced scour were at a constriction ratio of .46. The tests at this constriction ratio were lacking in small ice material, i.e., 1' x 1' x 1' floes. This resulted in the porosity of the accumulation being higher than that of the remaining tests and led to a larger depth of accumulation without raising the backwater level significantly and the resulting pressures on the dam. With larger material and lack of small blocks to decrease the porosity, a deeper jam can form and still remain stable. This can result in floes at or near the bed causing scour.

The remainder of the tests run at similar or higher Froude numbers at constriction ratios of .4 and .36 experienced no scour. These tests had large amounts of small ice material which decreased the overall porosity. The tendency was to keep the hanging dam well away from the bed and although larger material was not removed, it did not jam to the bed beneath the hanging dam.

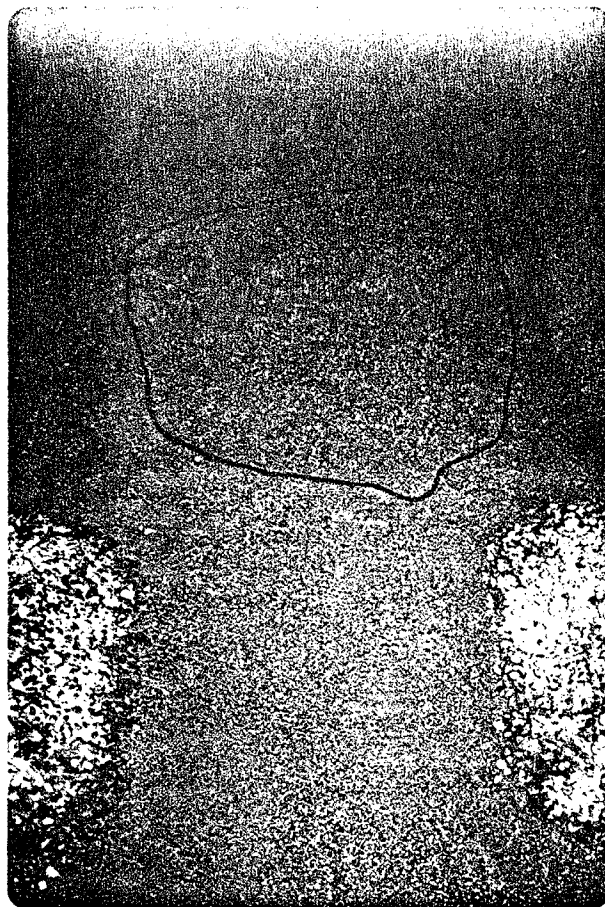


FIGURE 6.7 HD-11 SCOUR BELOW MAXIMUM ICE ACCUMULATION
FOR RUNS PARTIALLY LACKING IN 1' x 1' x 1'
BLOCKS. $F = .08$ $d = .2$ $m = .46$

TEST WITH RANDOM SCOUR HOLES BELOW HANGING DAM.

The above tests seem to indicate that scour, if it takes place, will be downstream of the constriction below the dam whereas scour at high Froude numbers without ice will take place at the downstream corners of the constrictions.

c) Effect of Ice Cover on Scour

An ice cover can have an influence on scour by

i) holding a hanging dam in place beneath the cover when without the cover it would have failed, and ii) stoppage of a failed hanging dam and the formation of a dry jam.

i) Retention of Hanging Dam

A hanging dam formed beneath a cover can attain a greater depth and length. The scour caused is mainly below the arch formation. Scour in other places had been noticed especially with the formation of a permeable dam. At higher Froude numbers, the complete channel fills with ice and the formation bears no resemblance to a hanging dam. All that remains is the arch. Scour below the hanging dam at a solid cover is shown in Fig. 6.8. Note that scouring is more severe than that observed in tests without a solid downstream cover.

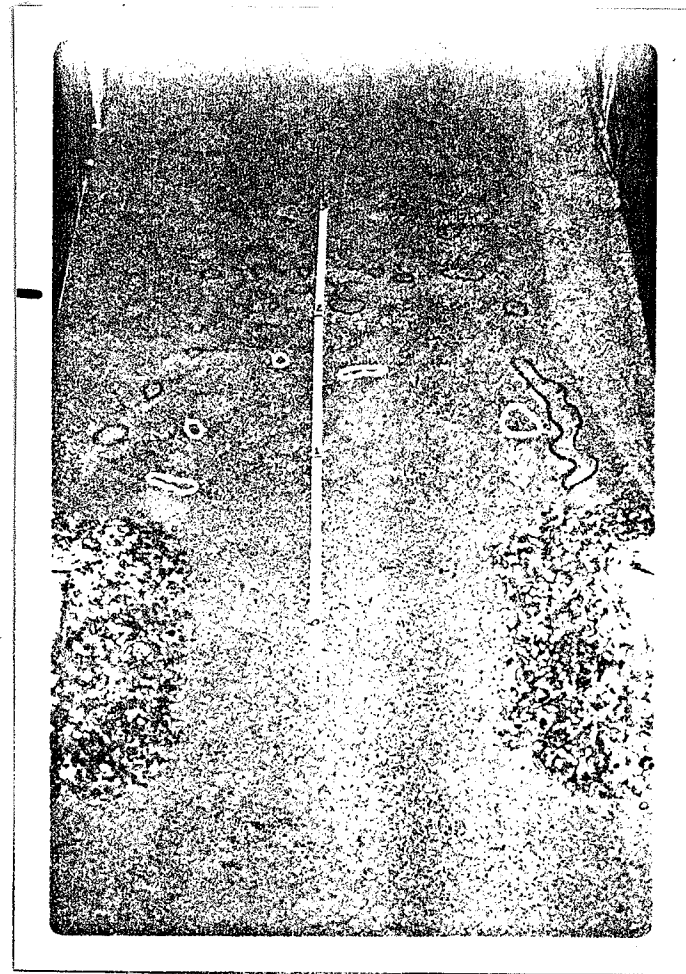
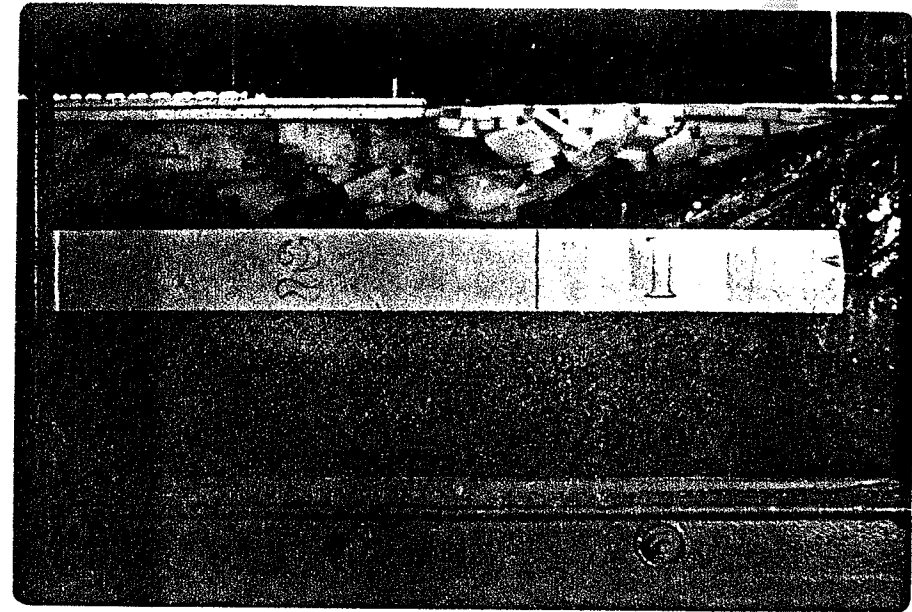
Scour also occurred in tests in which floes were being helped under and which contained a solid ice cover near the constriction. Scour occurred in the hanging dam area and downstream of the hanging dam along both sides of the channel. Bed movement took place while floes were moving down these channels and while new channels were being formed. These tests always consumed all the ice material available thus when material ran out, scour stopped shortly after.

ii) Dry Jam

In the main set of runs the cover was 14 feet downstream of the constriction. Upon failure of a hanging

FIGURE 6.8

SOLID ICE COVER EFFECT ON
SCOUR AT CONSTRICTIONS



c) HD-15 $F = .1$ $d = .2$ WHITE THREAD SHOWING SCOUR HOLES UNDER HANGING DAM. ICE COVER AT 2 FEET. DETERGENT AND SOME SMALL BLOCKS USED.

USUAL POT HOLE SCOUR WITH HANGING DAM HELD IN PLACE BY SOLID DOWNSTREAM ICE COVER.



d) HD-14 $F = .089$ $d = .2$ ICE COVER AT 2 FEET. DETERGENT AND SOME SMALL BLOCKS USED.

USUAL POT HOLE SCOUR WITH HANGING DAM HELD IN PLACE BY SOLID DOWNSTREAM ICE COVER.

dam, a wedge formed with flow taking place mainly on both sides of the wedge. Scour holes in the order of .1' occurred instantaneously along both walls and slightly below the jam. Fig. 6.9 shows scour occurring. If the cover is too near the constriction, flow will not have reached the walls and scour will occur in the centre of the channel.

It is questionable what effect the smooth glass walls have on failure of hanging dams. Naturally rough walls would tend to support the hanging dam in place under higher forces. When observing the mode of failure, together with sliding along the walls which takes place, the increased velocity along the walls turn floes under causing voids and thus room for slippage. It is foreseeable that a rough wall might cause more headloss and result in lower velocities.

d) Gouging of Bed

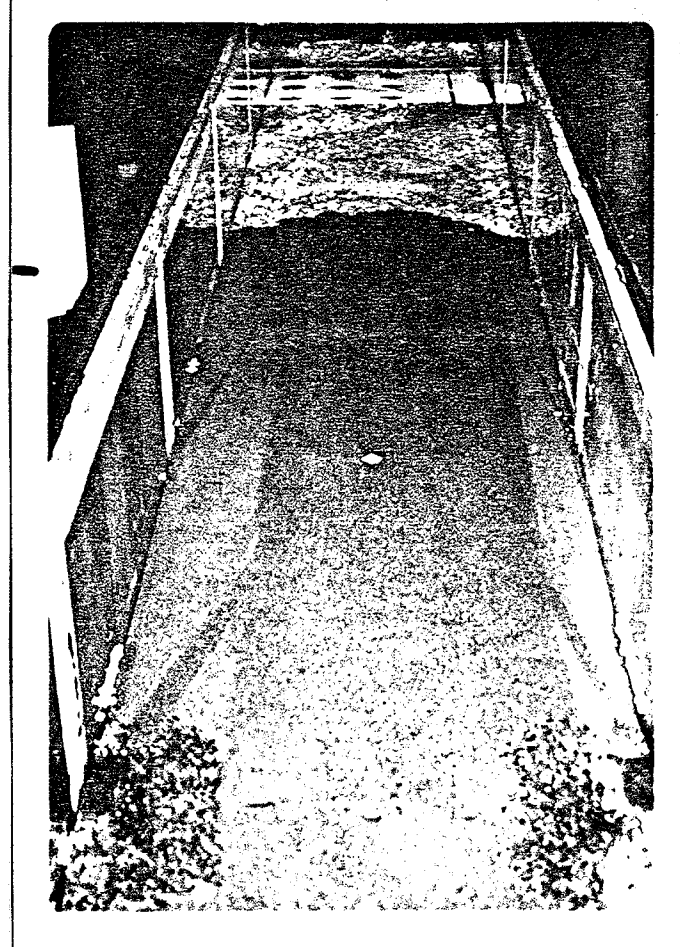
As one of the hanging dams became unstable and moved downstream, scratch marks the width of the dam were observed from the constriction to the downstream solid cover. This is due to the blocks actually scraping the bed or because the jam is moving downstream at a lower velocity than the flow beneath the jam, scour takes place from the increased thickening and velocity.

e) Scour Within Constrictions

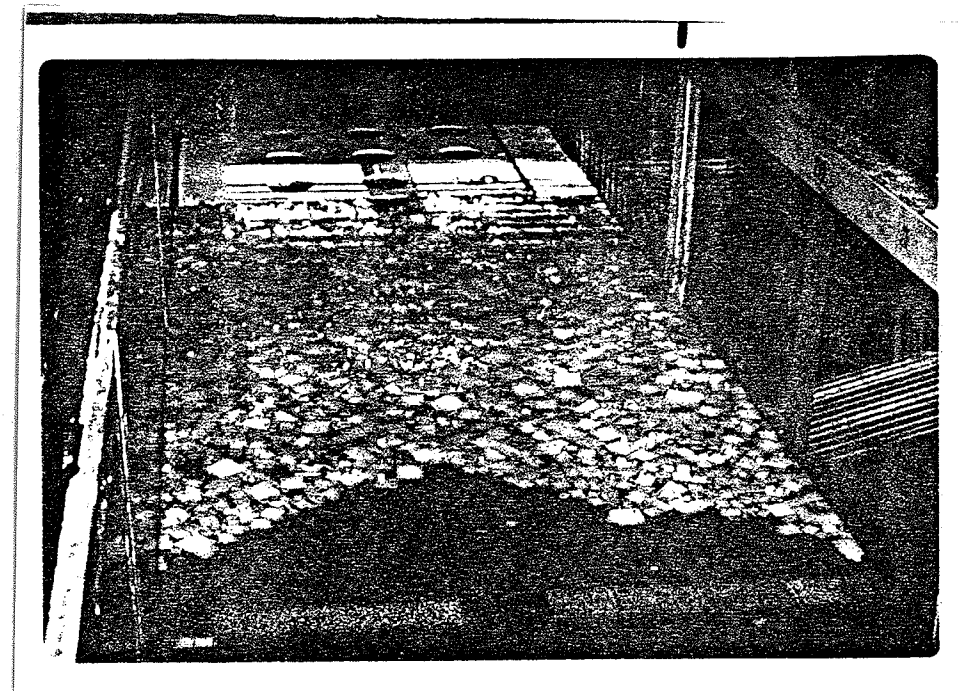
When the ice cover was continued right into the constriction for flow depth = .2 feet, blocks would jam on

FIGURE 6.9

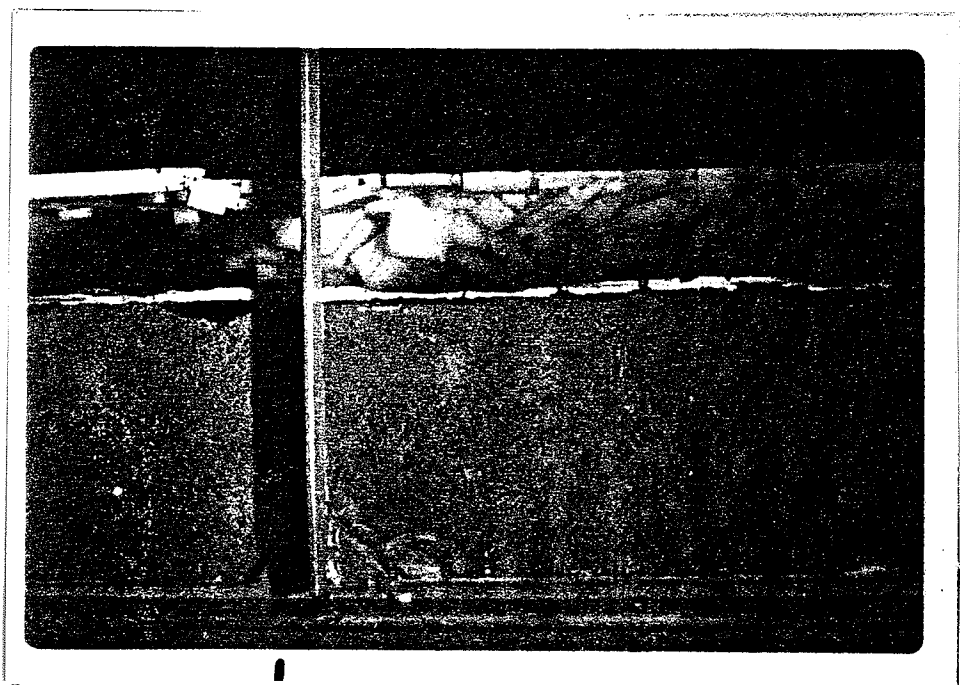
DRY ICE JAMS



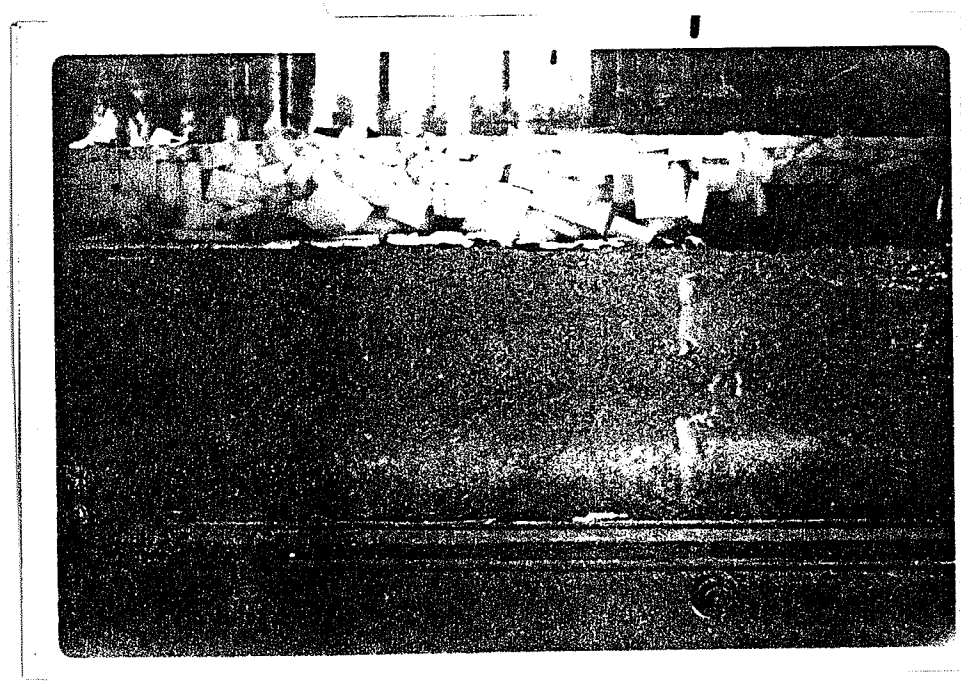
HD - 17 DRY JAM RESULTING FROM FAILED
 HANCOCK DAM $F = .11$ $d = .2$ $m = .36$



HD - 16 DRY JAM RESULTING FROM FAILED
 HANCOCK DAM $F = .089$ $d = .12$ $m = .14$



HD - 18 DRY JAM AT DOWNSTREAM ICE
 COVER. SEVERE SCOUR AT SIDES

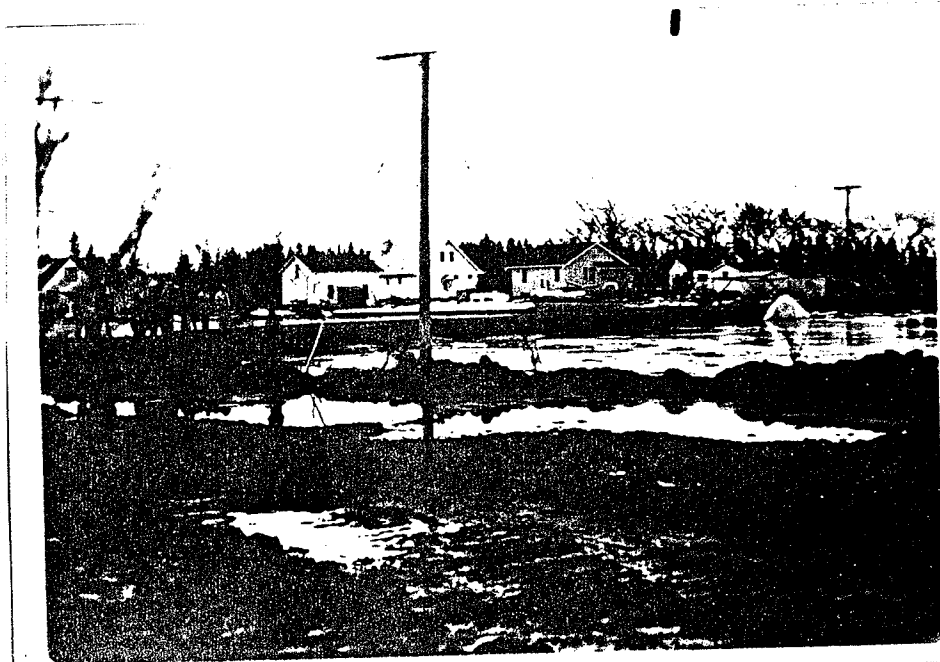


HD - 19 DRY JAM AT DOWNSTREAM
 ICE COVER. SEVERE SCOUR AT SIDES

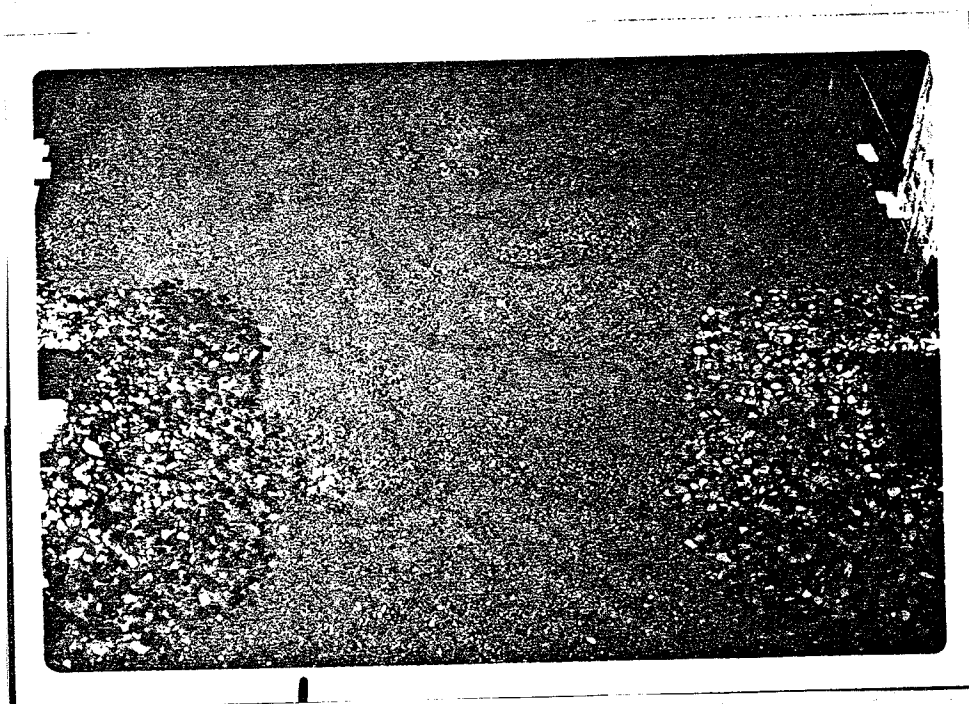
edge between the abutment and the ice cover. The block acted as a sharp edged constriction. Scour was caused at both abutments below the front edge of the cover. Shown in Fig. 6.10 b) are observed scour holes. It is, however, questionable whether an ice cover would remain in a constricted area. A submerged bridge structure can act in the same manner as the ice cover. Fig. 6.10 a) is an example of such an occurrence. It does seem possible that wherever block sizes approach the depth of the flow, this type of scour could take place and depth would be dependent upon the velocity. Block size would be limited to ones which submerged by rotation.

6.2.3 Time of Scour

Time available for scour below hanging dams was between one half hour and one hour. Scour usually took place as floes were going under the dam or immediately after floes went under. Since continuing scour was not occurring these tests were stopped. Test J-9-2 with severe scour was run four hours since scour was taking place. Dry jams had almost immediate scour. After formation of the dry jam, water levels rose and scour ceased. These tests were stopped within one half hour also.



a) PHOTO OF BLOCK JAMMED AGAINST C.P.R. BRIDGE
AT RIVERTON, MANITOBA, 1974.



b) PHOTO OF SCOUR WITHIN CONSTRICTION CAUSED BY BLOCKS
JAMMED BETWEEN ICE COVER AND ABUTMENTS.
(Downstream scour caused by helping blocks under
cover has no relation to constriction scour.)

FIG. 6.10 SCOUR WITHIN CONSTRICTIONS

6.3. Comparison With Other Experimenters

6.3.1. Limits of Hanging Dam Stability

According to Estiveef (1958), a velocity of 2.3 to 2.6 ft./sec. is the limiting velocity at which ice may move upstream. Shown in Table III are average velocities in the constriction from this study.

Michel (1966) states that the Froude number at which ice may proceed upstream is equal to $F = .154/\sqrt{1-e}$ when thickening is equal to .33 the depth of flow. However, at the constriction, ice is always one layer in thickness.

TABLE III

MAXIMUM FROUDE NUMBER AND VELOCITY AT THE CONSTRICTION

Test	V Average Prototype At Constriction ft./sec.	V Estiveef (1958) ft./sec.	F at Constriction	F Michel
HD11	2.4	2.3 - 2.6	.146	.154
HD14	2.7	2.3 - 2.6	.157	.154
HD16	2.5	2.3 - 2.6	.147	.154
HD20	2.5	2.3 - 2.6	.149	.154
HD25	2.3	2.3 - 2.6	.148	.154
HD26	2.8	2.3 - 2.6	.144	.154

Although Estiveef does not mention the effect of flow depth, a limiting velocity of 2.6 ft./sec. has some merit.

It seems that the predicting limit of a stable hanging dam is a Froude number of .154. Tests at higher Froude numbers failed and ones at lower Froude numbers proceeded upstream.

Froude numbers upstream and downstream do not take into account the constriction ratio and cannot be used as a criterion for upstream progression.

6.3.2. Comparison With Kivisild

For the three constriction ratios tested, the test with the highest Froude number at which the hanging dam was stable was plotted on Kivisild's (1959) chart (discharge per foot width at maximum deposits in hanging dam vs. depth from jam to bed). These tests corresponded roughly to the Froude number which the channel must attain to proceed upstream and therefore the maximum thickening at each constriction ratio. The above plots demonstrate that ice floes can achieve greater thickening than can frazil ice.

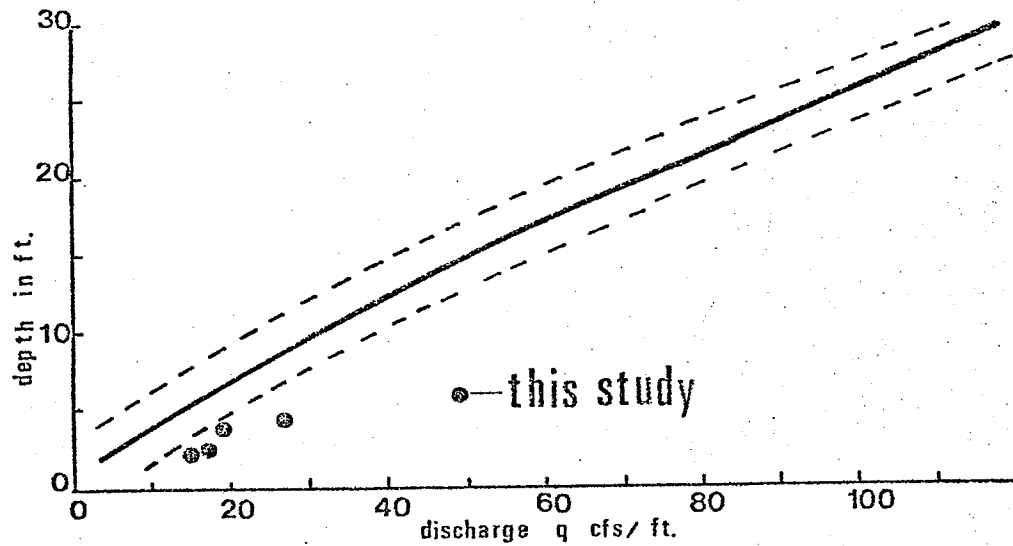
From Michel

$$F = .154\sqrt{1-e}$$

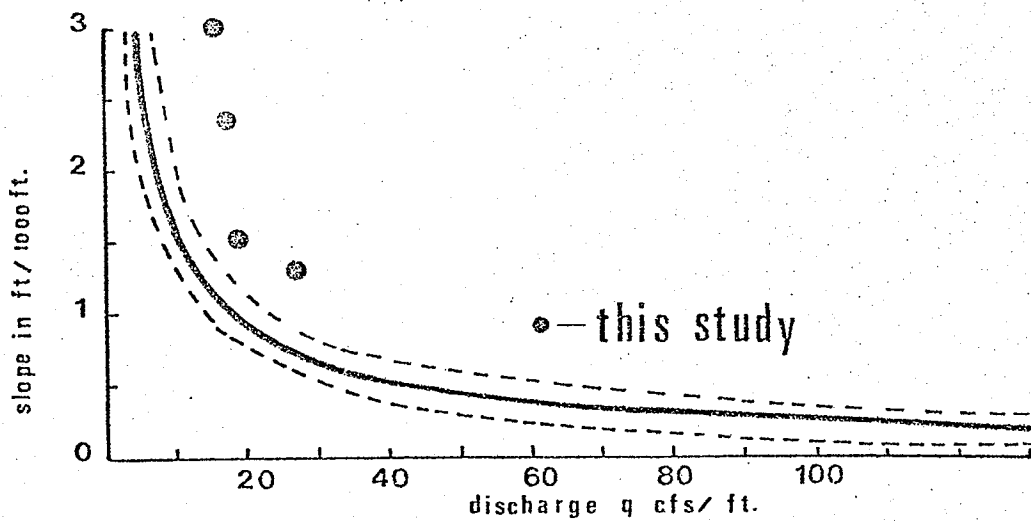
for floes $e = 0$. As seen from the above experiments the Froude number at the constriction approaches .154.

Kivisild's average porosity being .73 results in the maximum Froude number in the constriction being .08. At a constriction Froude number of .08 overturning does not take place in this study. Thus, Kivisild's charts are not useful in predicting depth of jamming with ice floes.

In Fig. 6.11 b), Kivisild proposes a relationship between discharge per foot and slope in feet per thousand.



- a) CURVE SHOWING THE AVERAGE DEPTH FROM UNDERSIDE OF ICE COVER TO RIVER BED AS A FUNCTION OF FLOW PER UNIT WIDTH AT MAXIMUM ICE DEPOSITS IN HANGING DAMS.



- b) CURVE SHOWS THE GRADIENT OF ENERGY HEAD AS A FUNCTION OF FLOW PER UNIT WIDTH UNDER AN ICE COVER AT MAXIMUM POSSIBLE ICE DEPOSITS IN HANGING DAM.

Fig. 6.11 FROM KIVISILD (1959)

The tests performed in this experiment also show larger slopes than those predicted by Kivisild.

6.4. Preliminary Tests

6.4.1. Effect of Detergent

Run C1 to C4 were used to study the mode of underturning. It was observed that floes were sinking vertically and not turning under about their downstream corner as described by Uzuner (1971) for t/L values of .1 to .8.

Since floes tested were in this range, it was believed that surface tension was effecting the mode of submergence and Froude number at which submergence took place.

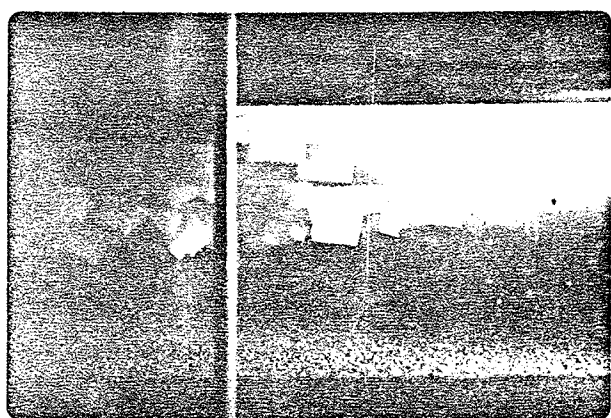
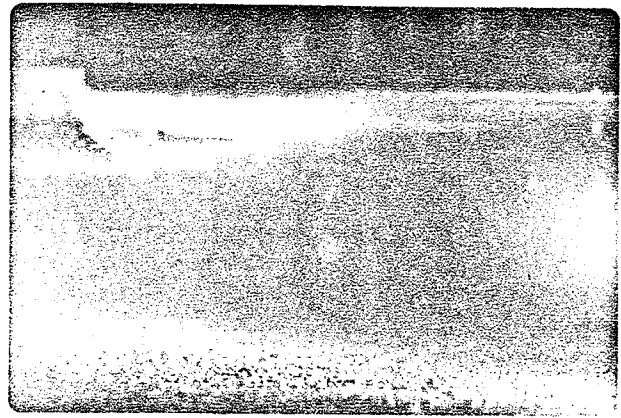
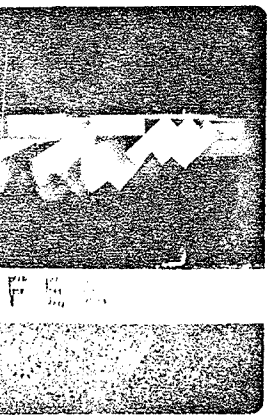
Kennedy (1958) states that a scale of 1:20 was chosen in his pulpwood tests because it was believed to be the smallest scale at which surface tension did not effect the behavior of model logs. The scale used in this model was 1:50. A thorough look at previous ice tests at smaller scales did not reveal any discussion on addition of detergent or the effect of surface tension.

Appendix A shows the results of tests run with and without detergent.

A general conclusion of tests C1 to C4 show that

FIGURE 6.12

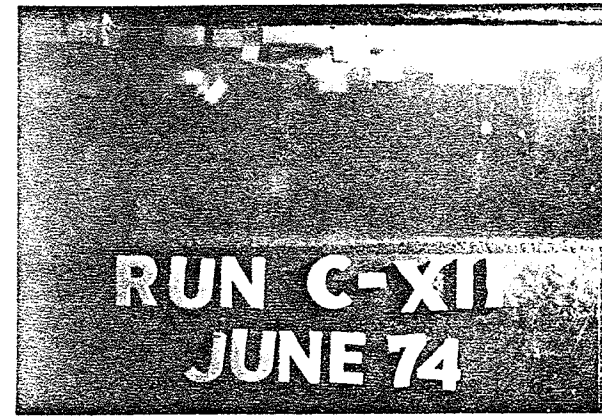
USE OF DETERGENTS TO REDUCE
SURFACE TENSION



e) WITHOUT DETERGENT

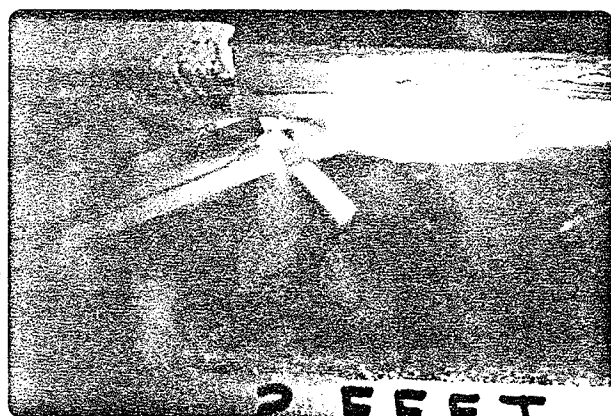
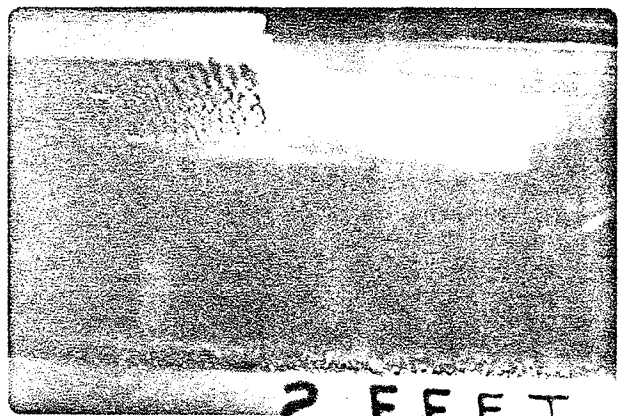
f) WITH DETERGENT

RUN C-6 F = .12 D = .31 3' x 3' x 1' BLOCKS



i) WITH DETERGENT

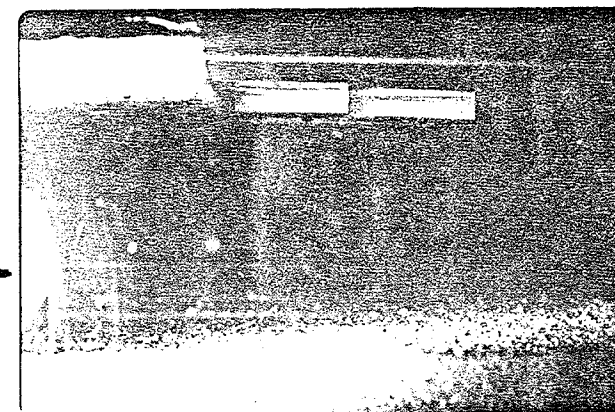
RUN C-12 F = .08 D = .31 2' x 2' x 1' BLOCKS



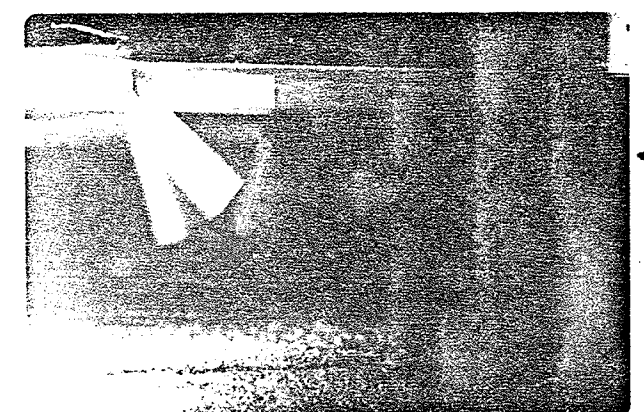
g) WITHOUT DETERGENT

h) WITH DETERGENT

RUN C-7 F = .14 D = .31 7' x 7' x 1' - 9' x 9' x 1' BLOCKS



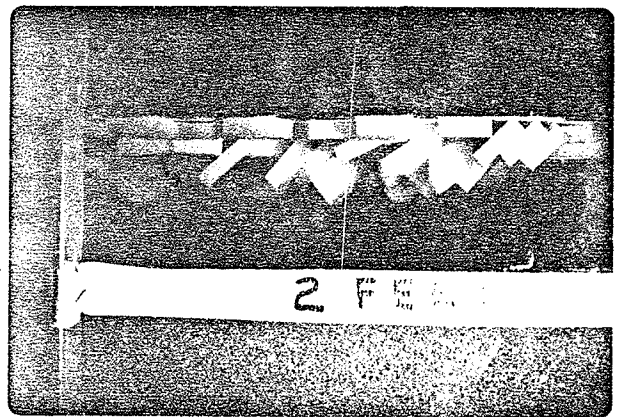
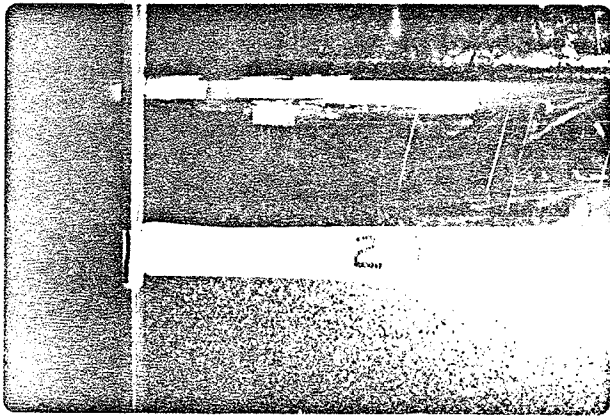
j) WITHOUT DETERGENT



k) WITH DETERGENT

CORRECT MODE OF UNDERTURNING

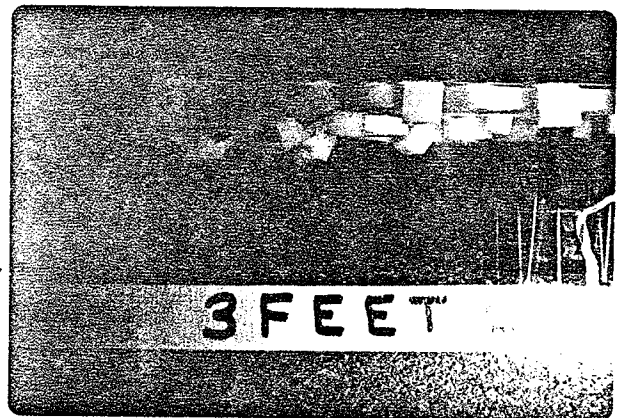
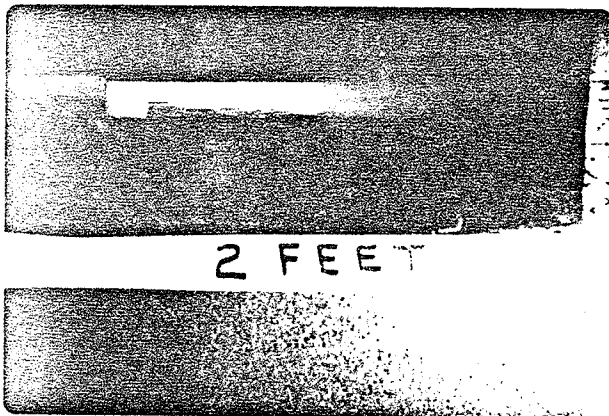
RUN C-10 F = .1 D = .31 7' x 7' x 1' BLOCKS



a) WITHOUT DETERGENT

b) WITH DETERGENT

RUN C-5 $F = .12$, $D = .2$, 3' x 3' x 1' BLOCKS



c) WITHOUT DETERGENT

d) WITH DETERGENT

RUN C-5 $F = .12$, $D = .2$, 2' x 2' x 1' BLOCKS

at a depth of .31 feet and Froude number of .08, very few floes turn under and at a Froude number of .12, all floes turn under with detergent. Without detergent, floes begin turning under at a Froude number of .16 to .18.

Table IV compares the results from runs with detergent to thickening predicted by Pariset et al (1966) and Uzuner (1971).

Since a cover of any length was not formed, t/h values are very approximate, however, there seems to be considerable agreement with Uzuner's plot of $C_m = .3$. Thus, detergent seems to have eliminated the surface tension effect.

Surface tension also affects the formation of hanging dams. In the performed tests without detergent, ice advances to the constriction with no underturning. As the hanging dam develops, the single layer downstream usually too thin to support the pressure from the hanging dam fails in compression.

Charbonneau (1973) in tests run without detergent describes the solid ice cover advancing into the constriction at one thickness. He also reports that the cover failed a number of times before it finally advanced through the constriction to stay.

6.4.2. Affect of t/L Ratio

Various sizes of floes were used since it was

TABLE IV

COMPARISON OF F_2 AND THICKNESS OF ICE WITH PARISET AND UZUNER

Test	h	F	F_2	Uzuner t/h	Pariset t/h	This study t/h
C - 6	.31	.12	.085	.26	.105	.3
C - 7	.31	.14	.099	unstable	.17	unstable
C - 8	.2	.14	.099	unstable	.17	unstable
C - 10	.2	.10	.07	.31	.07	.2
C - 12	.31	.08	.057	.1	.05	.1
C - 13	.31	.09	.064	.13	.06	.1
C - 14	.2	.12	.085	.28	.11	.25

believed that if the overturning moment varies with the t/L ratio, floe size would affect the Froude number at which it overturns. Appendix A shows that this effect seems negligible.

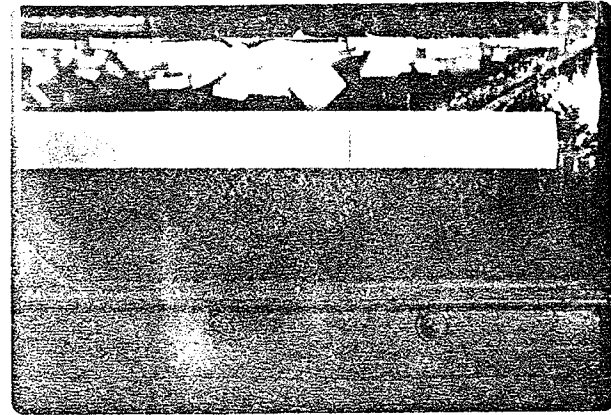
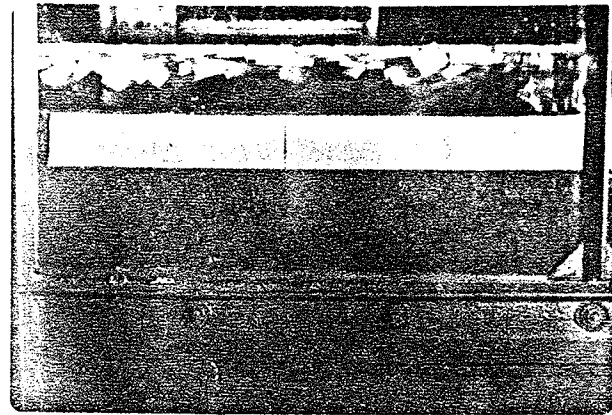
Uzuner (1971) also states that the t/L ratio is important, but the effect is only noticeable for t/L values very small and very large.

It then appears that, at a given Froude number, and block size being in the range of $t/L = .1$ to $.8$, block size will not effect the Froude number of submergence nor the depth of jamming. The only noticeable affect will be the roughness of the underside of the ice cover which will have a considerable importance in shallow rivers.

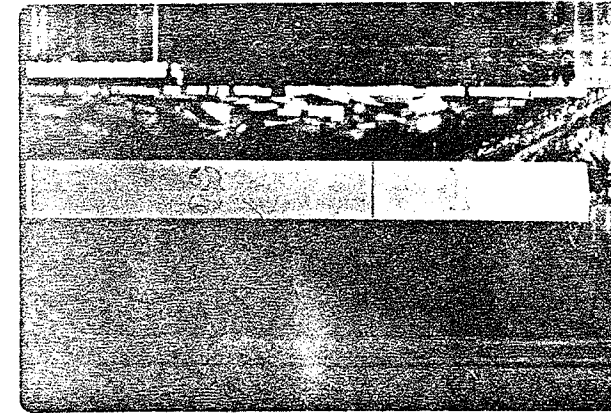
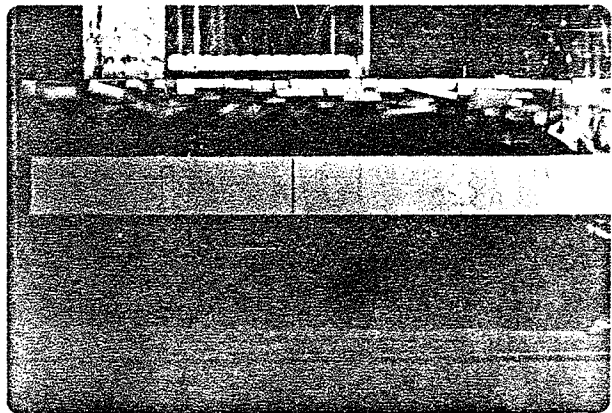
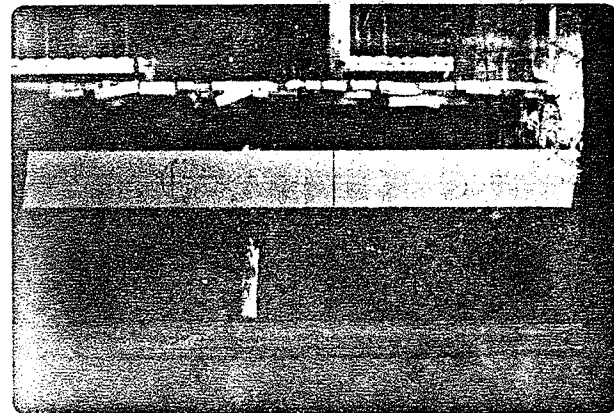
6.4.3. Rate of Feeding

The opinion was held that at a very slow rate of feeding, transport under the cover is not effected by incoming floes. A hanging dam will develop with negligible or no shoving. At higher rates of feeding, i.e. when some overturning is prevented, the desired thickness of the cover and dam are not achieved and shoving after the dam has reached a considerable thickness will occur resulting in a hanging dam situated further downstream. This is possibly the extreme case. The hanging dam formed with shoving is usually larger and more unpredictable, but is downstream of a jam formed without shoving, thereby increasing the water level through the dam and approaching the constriction at a lower Froude number.

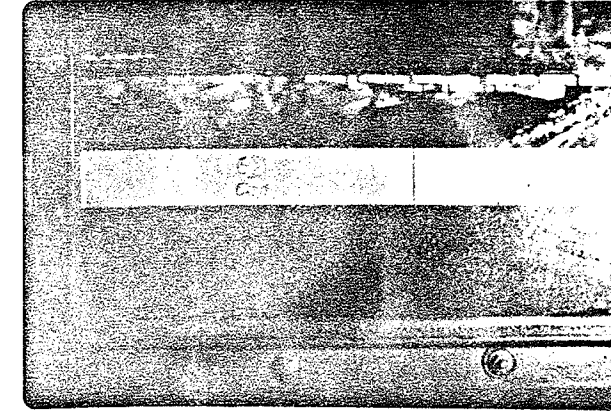
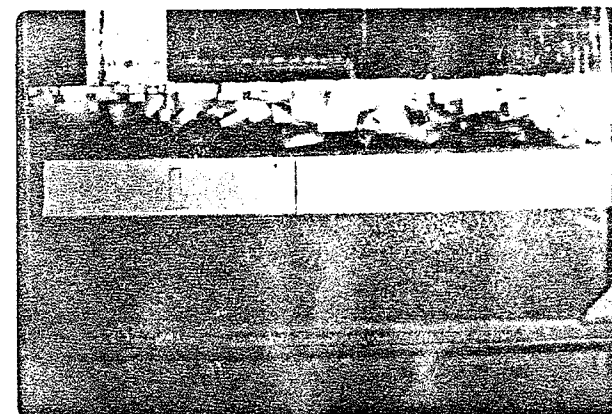
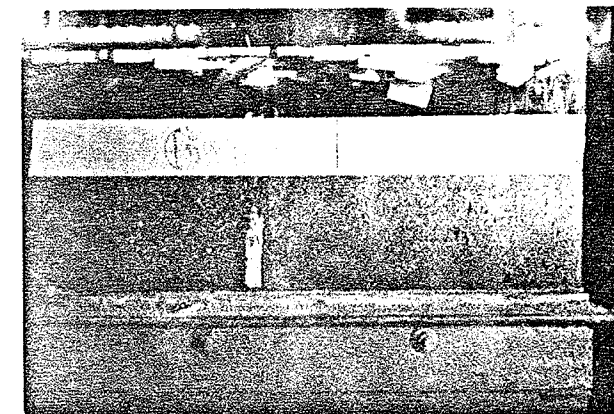
FIGURE 6.13
RATE OF FEEDING EFFECT ON
HANGING DAM FORMATION
RUN HD-14



WITH SLOW PLED HANGING DAM FORM



WITH FAST COLLAPSE SMALLER HANGING DAM FORMS

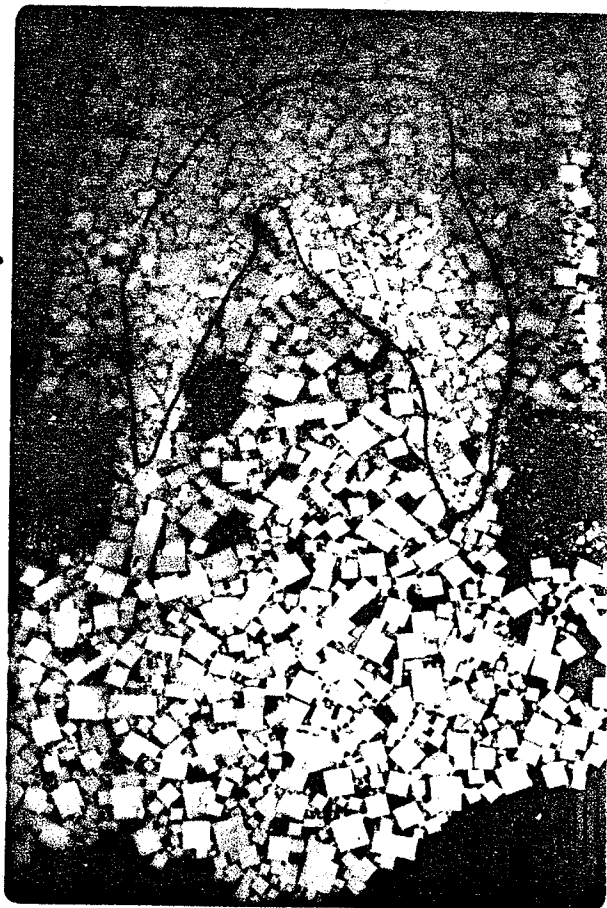


THE UNSTABLE HANGING DAM RESULTS IN A LARGER HANGING DAM FORMED FURTHER DOWNSTREAM OF THE CONSTRUCTION

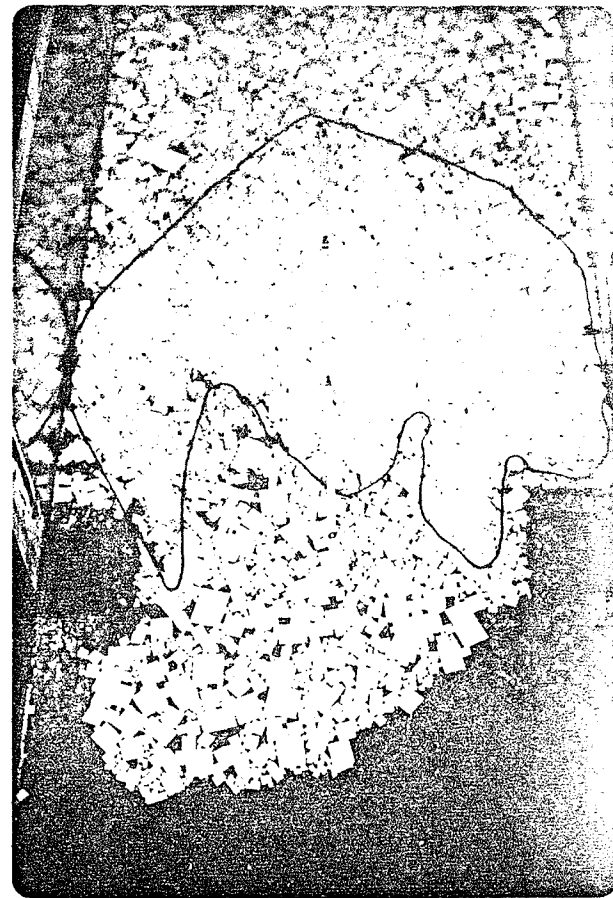
c) FAILURE OF INITIAL HANGING DAM RESULTING IN FINAL HANGING DAM FURTHER DOWN-STREAM.



b) INITIAL HANGING DAM FORMED WITH FAST FEEDING.



a) HANGING DAM FORMED WITH SLOW FEEDING.



6.4.4. Fast Ice Feed Affect on Scour

The affect of fast feeding would be more noticeable on shallow rivers where some ice floes approach or better the depth. Contrary to the orderly overturning and progression of the cover at slow feeding rates, fast feeding leads to multiple floes turning under at one time. Test HD-14, Fig. 6.13 was run over again with a very high rate of feeding, i.e. the upstream 18 feet of the channel was completely filled with ice and then sent downstream. Ice was turning under in all parts of the channel, but most noticeably in the constriction and maximum contraction area. More severe scour was recorded in this case. The resulting hanging dam formed is usually downstream of the dam formed with slow feeding. Thus, any scour which will develop below it will be further from the constriction.

6.4.5. Porosity

Pariset et al (1966) and Uzuner (1971) both considered porosity equal to zero in the criterion for the progression of an ice cover. Naturally ice floes at breakup will have a porosity of zero, but the accumulation porosity is not as dependent on the size of ice flow as it is on the shape and assortment of sizes. By adding small floes, it was discovered that the depth of the hanging dam formed, decreased.

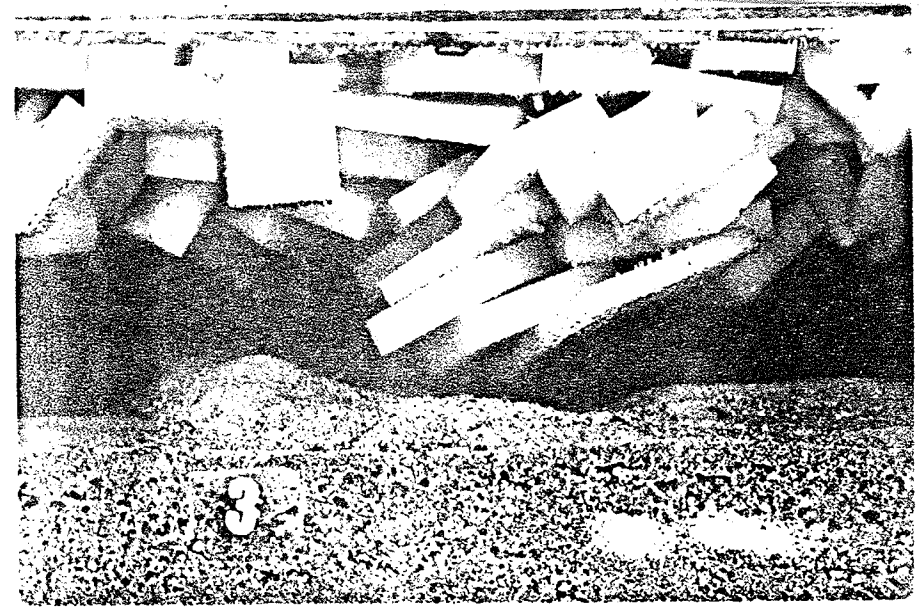
Test J-9-2 had a solid ice cover at two feet. Only

FIGURE 6.14

UNUSUAL SCOUR OBSERVED
BELOW HANGING DAM
SUPPORTED BY DOWNSTREAM
ICE COVER AND LACKING
IN SMALL ICE FLOES



a) J-9-0 F = .08 d = .3 RUN WITHOUT DETERGENT OR SMALL BLOCKS. ICE COVER AT 0. RED THREAD SHOWS SCOUR HOLE.



b) J-9-2 F = .08 d = .3 WITH RED THREAD SHOWING SCOUR RUN WITHOUT DETERGENT OR SMALL BLOCKS. ICE COVER AT 2 FEET.

SCOUR OBSERVED HERE COULD NOT BE DUPLICATED WHEN SMALL BLOCKS AND DETERGENT WERE ADDED.

large floes were used $F = .08$ $d = .31$ and the detergent was omitted. More than .2 feet of scour occurred at the downstream toe of the abutment, Fig. 6.14 a. On moving the cover to 0, test J-9-0, only slight scour was observed downstream of the constriction, Fig. 6.14 b. The remainder of the tests contained a good percentage of small floes and scour of this type could not be duplicated. The exact cause of this unusual scour hole is not known.

6.5. Bed Material Affect On Scour And Hanging Dam Formation

One test was run with Walnut Shells as the bed material in order to observe the effect bed material has on scour and hanging dam formation. Using a constriction ratio of .36, and an average downstream Froude number of approximately .08, the test was run for three hours before ice addition, without any scour taking place. As ice jamming approached the constriction, overturning caused scour which in turn effected depth and stability of the hanging dam. As ice began turning under near the constriction, scour began, thus constricting the opening causing greater pressure on the ice formation. This is shown in Fig. 6.15. A prior run with an average downstream Froude number slightly larger than .08 failed. Tests run with the sand bed in the model experienced less bed material movement and at equivalent constriction ratios and Froude numbers were stable at a Froude number of .098.

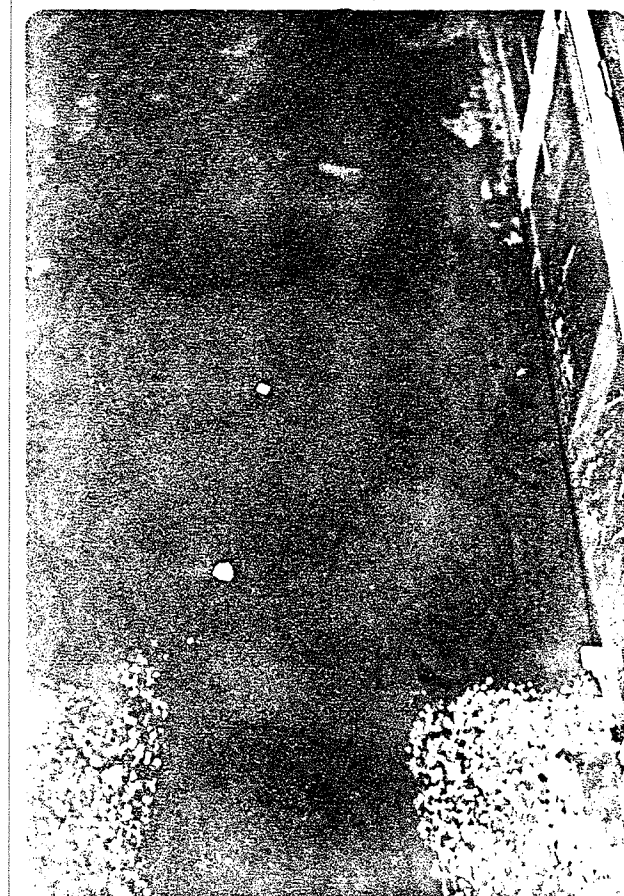
FIGURE 6.15

TEST RUN WITH WALNUT SHELLS

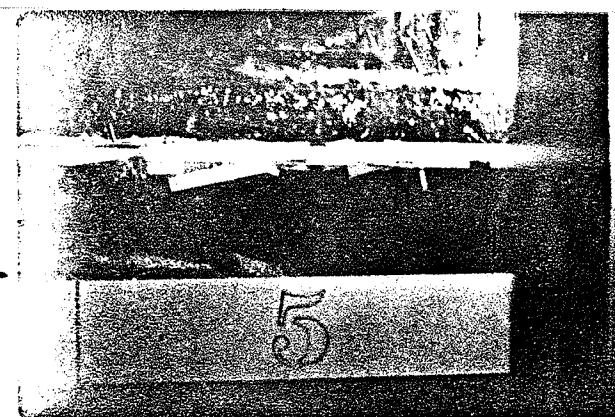
AS BED MATERIAL



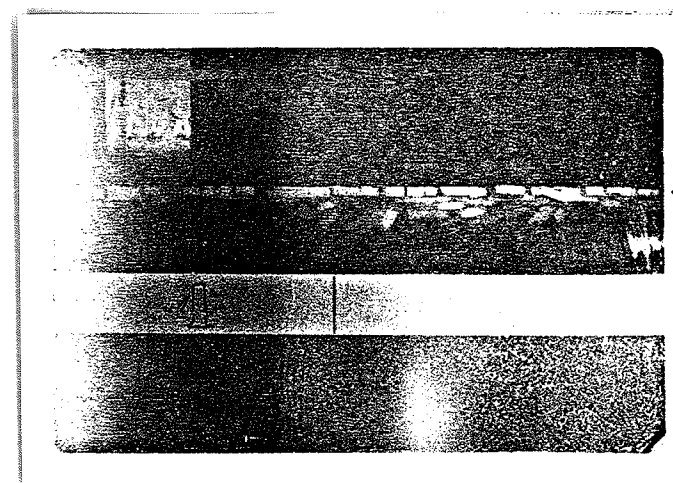
a) HANGING DAM FORMATION



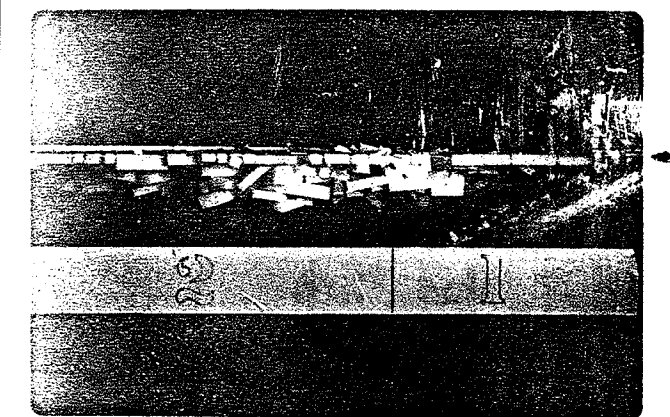
b) SCOUR AT DOWNSTREAM TOE OF THE
ATUMENTS AND BELOW HANGING DAM



c) TEMPORARY POTHOLE SCOUR ALONG
FLUME WALL



d) SIDE VIEW OF HANGING DAM FORMATION



i) DUNE FORMATION

ii) BED MATERIAL BUILT UP TO
HANGING DAM

With walnut shells the bed was less stable and it is therefore harder to predict the Froude number of stability due to interference of the bed material in the overturning process. The resulting scour holes at the downstream toe of the abutments were approximately .21 feet in depth.

6.6. Conjectures

6.6.1. Conjecture on Froude Number of Upstream Progression

Several investigators have noted that ice jams occur at nearly the same value of the Froude number, either F or F_2 (F ranging from .06 to .15). Uzuner (1971) explains this in the following manner: Stability will be reached when t/H increases to the point where the F on the stability curve is equal to F of the river, this will generally be the maximum value of F on the stability curve. When the stability is reached, the ice cover will propagate upstream and ice blocks will no longer be swept under the cover.

An explanation as to one cause of this Froude number range could be that irregularities in the channel control the Froude number at which progression takes place. For example, downstream of the constriction in a particular run, an average downstream Froude number of .08 allowed progression upstream whereas without the constriction a Froude number of .11 allowed progression upstream. The

resulting Froude number at the constriction was about .15 and that upstream was less than .08. The argument is that irregularities in the channel control upstream progression and unless one is examining a perfectly straight channel with uniform flow, there will be deviations in the Froude number for upstream progression of an ice cover.

6.6.2. Conjecture on Overbank Flow Affect On Hanging Dam Formation and Scour

With overbank flow, the water surface elevation will be greater on the upstream side of the embankment than normal (in the absence of the crossing) partly because of the backwater due to the valley crossing and partly because a gradient is required for the flow to move latterly across the flood plain to the main channel. On the downstream side of the embankments the water surface elevation will tend to be lower than normal because the water is slack for some distance, until the flow in the flood plain is re-established. This will cause jamming and instability to result at a lower average upstream or downstream Froude number. The major change would be a hanging dam possibly nearer to the constriction. With the hanging dam, flow would be re-established on the flood plain sooner than it would have without the hanging dam, possibly causing flood plain scour. High velocities on the flood plain are also possible immediately downstream of the hanging dam.

6.6.3 Conjecture on a Quick Check for Detecting Possible Scour Due to Ice at Constrictions.

Scour at constrictions may not be accounted for entirely by existing scour depth equations if the following conditions exist:

- 1) The river has some history of ice jamming.
- 2) At some time during breakup an average Froude number less than .1 takes place.
3. The new constriction ratio is larger than one that occurs naturally just downstream of the site under consideration.
- 4) The bed material is finer than gravel.

6.7 Conclusions

The results of the model study indicate:

- a) Hanging dam formation occurs downstream of the constriction. Single thickening is observed at, and upstream of, the constriction. The Froude numbers in the model were within the Froude number range observed by previous experimenters. The largest average downstream Froude number at which an ice jam would be stable ranged from .08 to .1. This varied with the contraction ratio, depth, porosity, and also bed material.
- b) Scour observed below the hanging dam in tests run with a sand bed appeared as pothole scour in the vicinity of the hanging dam. Scour observed from tests run with walnut shells as the bed material was more severe and occurred at the toe of the constrictions. The scour holes observed below the hanging dam never

approached the depth of flow, whereas scour in the walnut shell bed equalled or bettered the depth of flow.

c) Interference of a solid ice cover near the constriction increased scour.

d) Froude number at constriction approached .154 as ice proceeded upstream.

e) Kivisild's charts predicted greater distances from bottom of hanging dam to the bed and a smaller slope of the hanging dam.

f) Detergent was necessary to reduce surface tension.

CHAPTER VII

CONCLUSIONS AND RECOMMENDATIONS

7.1. Introduction

The purpose of this investigation was to determine if ice jams cause scour at constrictions. Spill-through abutments placed in a sand bed flume were used to assess scour hole depth and shape, and backwater effects. These were compared with previous experimenters to determine the soundness of the model and to assess which design curves best describe scour at spill-through abutments on small rivers.

Upon affirmation of the model, polyethylene blocks representing ice were added. The initial tests with ice and uniform flow in a straight channel were run for comparison of Froude number of submergence with Pariset et al (1966) and Uzuner (1971). Here it was determined that surface tension was effecting submergence and detergent was necessary for this scale of model. Constrictions were then placed back in the flume and tests were run in order to observe at what Froude numbers ice jams occurred, their location and depth, and also any scour which resulted. Location of a solid ice

cover was also varied to observe the effect it has on hanging dam formation and scour. Finally walnut shells were used as the bed material to determine if the scour patterns observed for gravel bed rivers are typical of all bed types.

7.2. Conclusion

Added magnitude of scour due to ice jamming:

- a) For gravel bed rivers (prototype), without downstream ice cover near constriction, scour only occurs beneath hanging dam and is only random pothole scour. It only occurred with high porosity accumulations.
- b) Scour in sand bed rivers (prototype) can occur near the downstream toe of the abutment, similar to scour without ice.
- c) Porosity of accumulation effects depth of thickening and random scour hole depth.
- d) A solid downstream ice cover can increase scour and thickness of jam. Limits are dependent on strength of solid cover.
- e) Bed scour effected hanging dam stability in tests run with walnut shells.

Hanging dam prediction:

- a) Kivisild's charts do not apply to ice floes.
- b) Froude number at constriction appears to be the only consistent variable at maximum ice thickening.

Uniform flow in straight channels:

a) Uzuner's (1971) equation best predicted thickening for straight channels and uniform flow.

Without ice conditions:

a) Das (1972) equations for scour depth and backwater for end-dump closure constrictions apply to spill-through abutments on small rivers.

b) Other scour depth equations were developed for larger rivers, i.e. constriction not as streamlined.

7.3. Recommendations

Various scour holes have been observed below ice in the model studies. It is therefore felt that further research is warranted.

The model study indicates:

- more field work is needed in determining ice jam depths, corresponding Froude number of flow and bed soundings for scour depth.
- model studies on scour due to ice jams on a larger scale. This would enable tests to be run without detergent using finer bed material without the use of walnut shells, which usually are subject to large dune formation.
- further tests to develop a mathematical model which would explain thickening in terms of average Froude number and

constriction ratio.

- studies on jamming and scour at river bends.
- model studies on scour due to frazil ice accumulations.

(Scour below frazil ice accumulations will not be as severe as that below chunk ice accumulations. However, frazil ice accumulations may be the dominant type of formation on some northern rivers.)

LIST OF REFERENCES

- Ahmad, M., 1953 - "Experiments on Design and Behaviour of Spur-Dikes", Proceedings, 5th I.A.H.R. Congress at Minneapolis, Minnesota, pp. 145-159.
- Awazu, S., 1967 - "On Scour Around Spur-Dike", Proceedings 12th I.A.H.R. Congress at Fort Collins, Colorado, Vol. 3, pp. 97-104.
- Biery, P.F. and Delleur, J.W., 1962 - "Hydraulics of Single Span Arch Bridge Constrictions", Journal of the Hydraulics Division, ASCE Vol. 88, No. HY2, Proc. Paper 3076, pp. 75-108.
- Bolsenga, S.J., 1968 - "A Literature Review of River Ice Jams", U.S. Lake Survey, Research Report 5-5.
- Breusers, H.N.C., 1967 - "Time Scale of Two-Dimensional Local Scour", Proceedings 12th I.A.H.R. Congress at Fort Collins, Colorado, Vol. 3, pp. 275-282.
- Carstens, M.R., 1966 - "Similarity Laws for Localised Scour", Journal of the Hydraulics Divisions, ASCE Vol. 92, No. HY3, Proc. Paper 4818, pp. 13-36.
- Chang, Y.U., 1939 - "Laboratory Investigations of Flume Traction and Transportation", Transactions ASCE Vol. 65, No. 8, Pt. 2, pp. 1246-1313.

- Charbonneau, A., 1973 - "Preliminary Report on Hydraulic Model Tests Proposed Riviere des Rochers Ice Dam", Edmonton, Alberta.
- Chow, V. T., 1959 - "Open Channel Hydraulics", McGraw-Hill, New York.
- Cousineau, E., 1959 - "Some Aspects of Ice Problems Connected With Hydro-Electric Developments", Engineering Journal, Vol. 42-3, pp. 48-54.
- Das Bishnu Presad, 1972 - "Hydraulics of End-Dump Closure of Alluvial Channels", Department of Civil Engineering, Edmonton, Alberta.
- Doddiah, D., Albertson, M.L., and Thomas, R., 1953 - "Scour from Jets", Proceedings, 5th I.A.H.R. Congress at Minneapolis, Minnesota, pp. 161-169.
- Garde, R.J., Subramanya, K., and Nambudripad, K.D., 1961 - "Study of Scour Around Spur-Dikes", Journal of the Hydraulic Division, ASCE, Vol. 87, No. HY6, Proc. Paper 2978, pp.23-37.
- Garde, R.J., Subramanya, K. and Nambudripad, K.D., 1963 - Closure of "Study of Scour Around Spur-Dikes", by R.J. Garde et al, Journal of the Hydraulics Division, ASCE, Vol. 89, No. HY1, Proc. Paper 3405, pp. 167-175.

- Groat, B.F., 1918 - "Ice Diversion, Hydraulic Models and Hydraulic Similarity", Transactions of the American Society of Civil Engineers, Vol. 82, pp. 1138.
- Highway Research Board, National Cooperative Highway Research Programme, Synthesis of Hwy. Practice 5, 1970 - "Scour at Bridge Waterways".
- Izbash, S.V. and Lebedev, I.V., 1961 - "Change of Natural Streams During Construction of Hydraulic Structures", Proc. 9th I.A.H.R. Congress at Dubrovnik, pp. 1114 - 1121.
- Izzard, C.F., and Bradley, J.N., 1957 - "Field Verification of Model Tests on Flow Through Highway Bridges and Culverts", Proceedings, 7th Hydraulics Conference, Iowa.
- Keulegan, G. H., 1938 - "Laws of Turbulent Flow in Open Channels", Journal of Research of the National Bureau of Standards, Vol. 21, pp. 707 - 741.
- Kennedy, R.J., 1958 - "Forces Involved in Pulpwood Holding Grounds", Engineering Journal (Canada), pp. 58-68.
- Kindsvater, C.E., and Carter, R.W., 1953 - "Transquil Flow Through Open Channel Constrictions", Transactions ASCE, Vol. 120, pp. 955-930.

- Kivisild, H.R., 1959 - "Hanging Ice Dams", Proceedings of the 8th Congress of the International Association for Hydraulic Research, Vol. 3, pp. 1-1.
- Komura, S., 1966 - "Equilibrium Depth of Scour in Long Constrictions", Journal of the Hydraulics Division, ASCE Vol. 92, No. HY5, Proc. Paper 4898, pp. 17-37.
- Lane, E.W., 1919-20 - "Experiments on the Flow of Water Through Contractions in an Open Channel", Transactions ASCE Vol. 83, pp. 1149-1219.
- Laursen, E.M., and Toch, A., 1953 - "A Generalized Model Study of Scour Around Bridge Piers and Abutments", Proceedings 5th I.A.H.R. Congress at Minneapolis, Minnesota, pp. 123-131.
- Laursen, E.M., 1962 - "Scour at Bridge Crossings", Transactions, ASCE, Vol. 127, Part I, pp. 166.
- Laursen, E.M., 1963 - "An Analysis of Relief Bridge Scour", Journal of the Hydraulics Division, ASCE, Vol. 89, No. HY3, Proc. Paper 3516, pp. 93-118.
- Leliavsky, S., 1955 - "An Introduction to Fluvial Hydraulics", Constable, London.
- Liu, H.K., Chang, F.M., and Skinner, M.M., 1961 - "Effect of Bridge Constrictions on Scour and Backwater", Colorado State University, Civil Engineering Section Report CER60HKL22.

- Liu, H.K., Chang, F.M., and Plate, E.J., 1957 - "Backwater Effects of Piers and Abutments", Colorado State University, Civil Engineering Section, Report CER57HKL10.
- Melin, R., 1954 - "Stream Erosion and Sedimentation at Low Water in Winter", Union Geodesique et Geophysique Internationale, Association Internationale d'Hydrologie Scientifique, Assemblee generale de Rome. Tome III, Comptes Rendus et Rapport de la Commission des Eaux de Surface.
- Michel, Bernard, 1971 - "Winter Regime of Rivers and Lakes", U.S. Army Corps of Engineers, Cold Regions Research and Engineering Laboratory, New Hampshire.
- Morton, R.I., 1963 - "Criteria for Stability of Ice Covers on Rivers", Proceedings 20th Annual Meeting, Eastern Snow Conference, Quebec, pp. 130 - 148.
- Neill, C.R., 1962 - Discussion of "Study of Scour Around Spur-Dikes", by R.J. Garde et al, Journal of the Hydraulics Division, ASCE, Vol. 88, No. HY2, Proc. Paper 3087, pp. 191 - 192.
- Neill, C.R., 1964 - "River Bed Scour, A Review for Bridge Engineers", Canadian Good Roads Association, Publication No. 23.
- Newbury, Robert - "The Nelson River", A Study of Subarctic River Processes. 1968 PhD thesis, Johns Hopkins University, Baltimore.

- Pariset, E., Hausser, R., and Gagnon, R., 1966 - "Formation of Ice Cover and Ice Jams in Rivers", Journal of the Hydraulics Division No. HY6, Proc. Paper 4965, pp. 24.
- Pariset, E. and Hausser, R., 1963 - "Criteria for Stability of Ice Covers on Rivers", Proceedings, 20th Annual Meeting, Eastern Snow Conference, Quebec, pp. 123-129.
- Pariset, E. and Hausser, R., 1963 - "Formation and Evolution of Ice Covers on Rivers", Trans. of the Engineering Inst. of Canada, Vol. 5, No. 1, pp. 41-49.
- Pariset, E. and Hausser, R., 1959 - "Evolution of Ice Covers On Rivers", Proceedings, 8th Congress, International Association for Hydraulics, Montreal, Paper No. 476, Sem. I, pp. 4-SI-1/4.
- Pariset, E. and Hausser, R., 1959 - "Formation of Ice Covers On Rivers", Proceedings, 8th Congress, International Association for Hydraulics, Montreal, Paper No. 477, Sem. I, pp. 3-SI-1/5.
- Sandover, J. A., 1969 - "Discharge Coefficients of Constrictions in Open Channels", Water Power, London, pp. 256-261.
- Sandover, J. A., 1970 - "Backwater Effects Due to Channel Constrictions", Water Power, London.

Task Committee on Preparation of Sedimentation Manual,
Committee on Sedimentation, 1962 - "Sediment
Transportation Mechanics: Introduction and
Properties of Sediment", Journal of the
Hydraulics Division, ASCE, Vol. 88, No. HY4,
Proc. Paper 3194, pp. 77-107.

Task Committee Preparation of Sedimentation Manual,
Committee on Sedimentation, 1962 - "Sediment
Transportation Mechanics: Erosion of Sediment",
Journal of the Hydraulics Division, ASCE, Vol. 88
No. HY4, Proc. Paper 3195, pp. 109-127.

Task Committee on Preparation of Sedimentation Manual, Committee
on Sedimentation, 1966 - "Sediment Transportation
Mechanics: Initiation of Motion", Journal of the
Hydraulics Division, ASCE, Vol. 92, No. HY2, Proc.
Paper 4738, pp. 291-314.

Tietze, Wolf, 1961 - "On Erosion of Water Flowing Under Ice",
Translation of Section 1 by Rolf Kellerhals,
Dept. of Civil Engineering, University of Alberta,
Edmonton.

Tracy, H.J., and Carter, R.W., 1955 - "Backwater Effects of
Open Channel Constrictions", Transactions, ASCE,
Vol. 120, pp. 993 - 1006.

Uzuner, Mehmet, Secil, 1971 - "Stability of Floating Ice Blocks", A Thesis Submitted in Partial Fulfillment of the Requirements for the Degree of Master of Science in the Dept. of Mechanics and Hydraulics in the Graduate College of the University of Iowa,

Vinje, J. J., 1967 - "On the Flow Characteristics of Vortices in Three-Dimensional Local Scour", Proceedings 12th I.A.H.R. Congress at Fort Collins, Colorado, Vol. 3, pp. 207-217.

Wentworth, C. K., 1932 - "The Geologic Work of Ice Jams in Subarctic Rivers", Washington University Studies, New Series, Science and Technology, No. 7.

APPENDIX A

EXPERIMENTAL DATA ON TESTS WITHOUT ICE

A.1 SCOUR AT SPILL-THROUGH ABUTMENTS

Run No.	Wave downstream	Constriction Ratio m	Flow depth downstream of const.	Maximum depth of scour ft.	Froude No. downstream
A - 2	.61	.667	.19	.26	.25
A - 4	.573	.4	.21	.06	.22
A - 5	.581	.53	.2	.2	.23
A - 6	.604	.45	.2	.14	.25
B - 6	.62	.45	.2	.25	.25
A - 7	.32	.46	.33	0	.1

A - 1

APPENDIX B

EXPERIMENTAL DATA ON ICE JAMMING TESTS

B.1 HANGING DAM

Run No.	HD-11	HD-12	HD-13	HD-14	HD-15	HD-16	HD-17	HD-18	HD-19	HD-20	HD-21	HD-22	HD-23	HD-24	HD-25	HD-26	HD-27
V ave. at 10'	.20	.15	.18	.22	.25	.24	.22	.28	.21	.25	.17	.14	.19	.23	.21	.23	.19
Q Discharge	.11	.09	.11	.13	.15	.15	.13	.17	.12	.15	.11	.09	.12	.13	.13	.23	.19
M Const. Ratio	.46	.46	.46	.45	.45	.36	.37	.36	.36	.36	.40	.40	.40	.40	.40	.45	.45
F ave. at 10'	.08	.06	.07	.09	.098	.093	.084	.11	.082	.098	.067	.055	.074	.089	.08	.07	.057
H ft	.203	.205	.206	.208	.209	.209	.207	.21	.21	.207	.21	.208	.21	.206	.205	.336	.338
h at 10' ft.	.198	.2	.2	.202	.2	.202	.202	.204	.206	.202	.205	.203	.204	.201	.2	.330	.332
H/h	1.025	1.025	1.03	1.03	1.045	1.035	1.025	1.029	1.019	1.025	1.022	1.025	1.029	1.025	1.025	1.015	1.03
H	.213	.202	.208	.221	.24	.225	.215		.205	.227	.216	.214	.218	.216	.228	.346	.347
h at 10' ft	.194	.194	.197	.199	.211	.205	.203		.195	.204	.205	.208	.198	.2	.204	.333	.337
H/h	1.098	1.041	1.056	1.111	1.137	1.098	1.059		1.05	1.113	1.054	1.029	1.098	1.08	1.118	1.039	1.02

Run No	HD-11	HD-12	HD-13	HD-14	HD-15	HD-16	HD-17	HD-18	HD-19	HD-20	HD-21	HD-22	HD-23	HD-24	HD-25	HD-26	HD-27
n_2 at constriction	.208	.197	.202	.215	.216	.218	.209	.228	.201	.221	.211	.211	.211	.213	.215	.342	.342
V ave. at constriction	.34	.28	.32	.38	.42	.35	.33	.38	.31	.36	.28	.23	.32	.35	.33	.40	.34
F in constriction	.146	.123	.139	.157		.147	.141		.13	.149	.119		.133		.148	.144	
Stability					failed			failed						failed			
V max. down-stream of const. current meter.	.40	.35	.42	.57	.57	.52	.45	.54	.39		.39	.35	.47	.52	.47	.54	.47
Location of max. thickening	2'	3/4'	1'	2'		2'	2'		1/4'		1/4'				2'	3'	1'
Dist. dam to bed at max. thickening ft.	.083	.16	.119	.045		.07	.12	.14	.14	.07	.125		.1		.04	.08	.104
Station at which flow fully expands	4'	flow two lanes 12' left+right			1 1/2'						3'				3'		
Q/foot of hanging dam	13.48	10.42	12.33	15.62	17.50	17.15	15.27		14.06	17.96	12.44	10.28	13.95	15.74	14.80	26.40	22.13
Depth of isolated scour holes	.02 at 1-2 1/2'				.02 at 1-2 1/2'												

B.2 EFFECT OF DETERGENT

Test	Depth	Froude	Without Detergent								With Detergent							
			Ice 1 foot thick t/L				Ice 1½ feet thick t/L				Ice 1 foot thick t/L				Ice 1½ foot thick t/L			
			t/h	.125	.2	.33	.5	t/h	.188	.3	t/h	.125	.2	.33	.5	t/h	.188	.3
C-1	.2	.12	.1	stay	stay	stay	stay	.15										
C-2	.2	.16	.1	turn under	stay	stay	stay	.15	turn under	stay								
C-3	.2	.18	.1	turn under	stay	stay	stay	.15	turn under	stay								
C-4	.2	.18									.1	turn under	turn under	turn under	turn under	.15	turn under	turn under
C-5	.2	.12	.06	stay	stay	stay	stay	.1	stay	stay	.06	turn under	turn under	turn under	turn under	.1	turn under	turn under
C-6	.31	.12	.06	stay	stay	stay	stay	.1	stay	stay	.06	turn under	turn under	turn under	turn under	.1	turn under	turn under
C-7	.31	.14	.06	stay	stay	stay	stay	.1	stay	stay	.06	turn under	turn under	turn under	turn under	.1	turn under	turn under
C-8	.2	.14	.1	stay	stay	stay	stay	.15	stay	stay	.1	turn under	turn under	turn under	turn under	.15	turn under	turn under
C-10		.10	.1	stay	stay	stay	stay	.15	stay	stay	.1	turn under	turn under	turn under	turn under		turn under	turn under
C-12	.31	.08	.1	stay	stay	stay	stay	.15	stay	stay	.1	stay	stay	stay	stay		stay	stay
C-13	.31	.085	.1	stay	stay	stay	stay	.15	stay	stay	.1	stay	stay	stay	stay		stay	stay
C-14	.2	.12	.1	stay	stay	stay	stay	.15	stay	stay	.1	turn under	turn under	turn under	turn under	.15	turn under	turn under

APPENDIX C

HANGING DAM ILLUSTRATIONS

APPENDIX C

HANGING DAM ILLUSTRATIONS

Photograph of Constriction - Hanging dam outlined tries to show extent of severe thickening.

Side Photographs - Show depth of hanging dam.

Plan View - Station -1 to station 10. Amount of ice consumed plus outline of severe thickening.

Water Surface Profile - Change in water elevation due to ice. Upstream of constriction water surface profile altered negligably and is therefore not shown.

Cross-sections - Show thickening of hanging dam.

C1 - C4 m = .46

d = .2 ft.

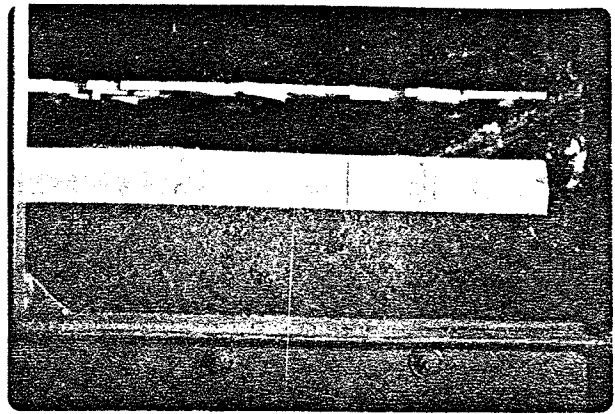
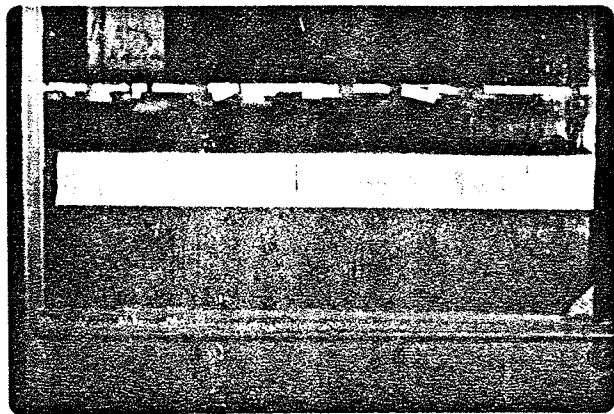
C1

m = .46

AVERAGE DOWNSTREAM F = .06

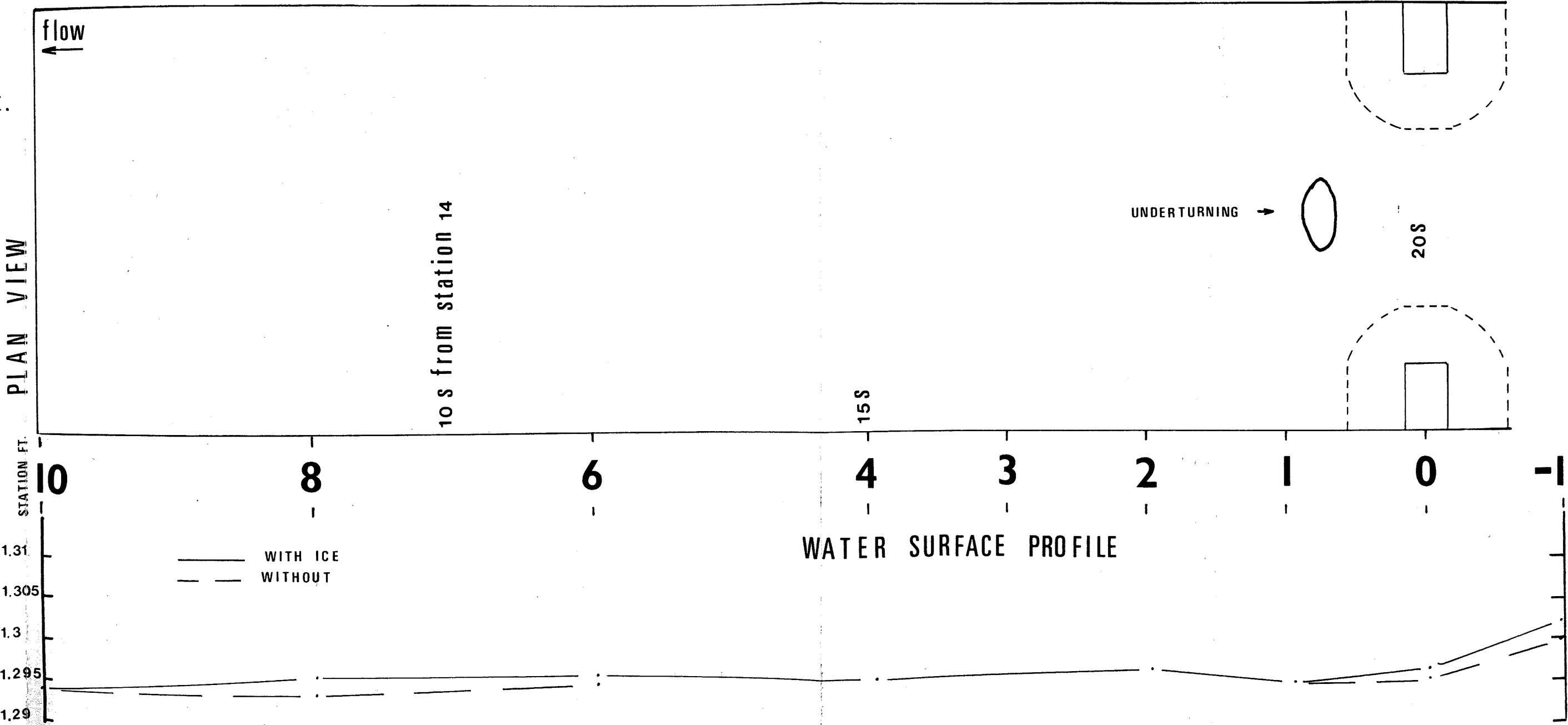
d = .2 ft.

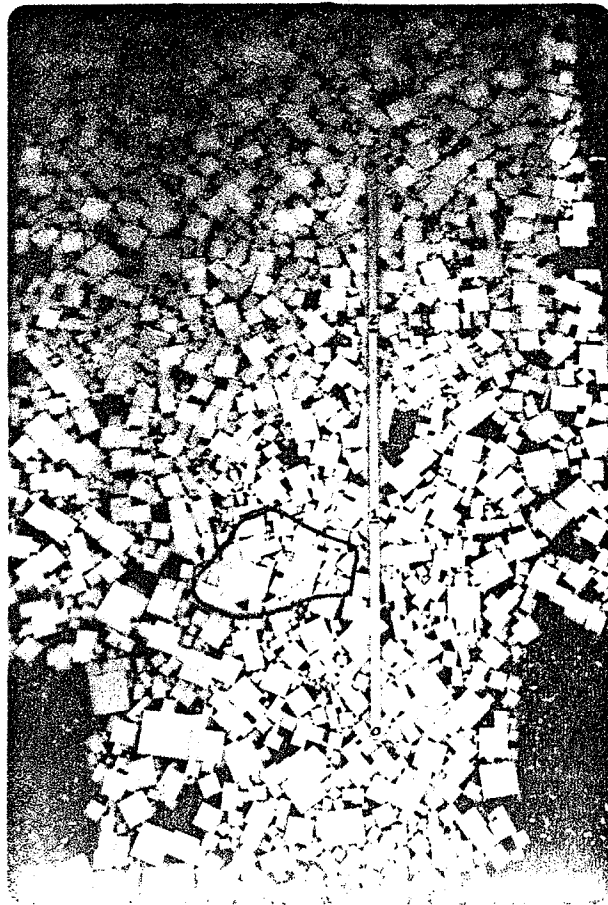
RUN HD - 12.



SIDE PHOTOGRAPHS

S = .08 CU. ft.
of ice





S = .08 CU. ft.
of ice

PHOTOGRAPH OF CONSTRICTION

ELEVATION
STATION FT.
1.31
1.305
1.3
1.295
1.29

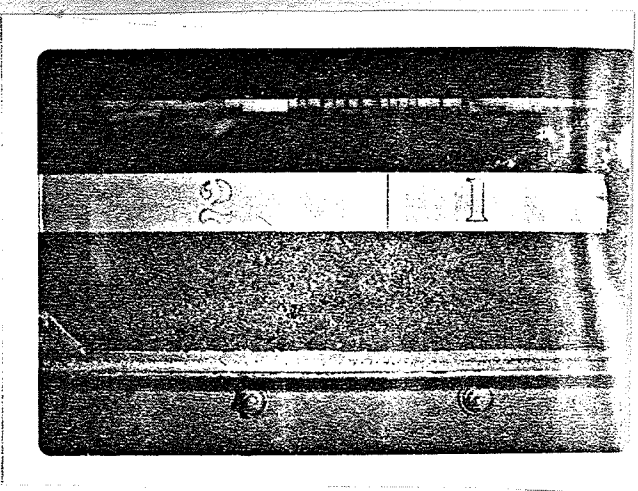
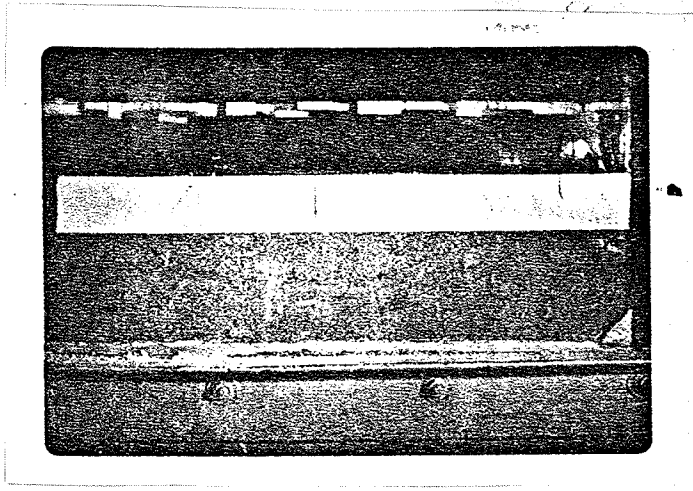
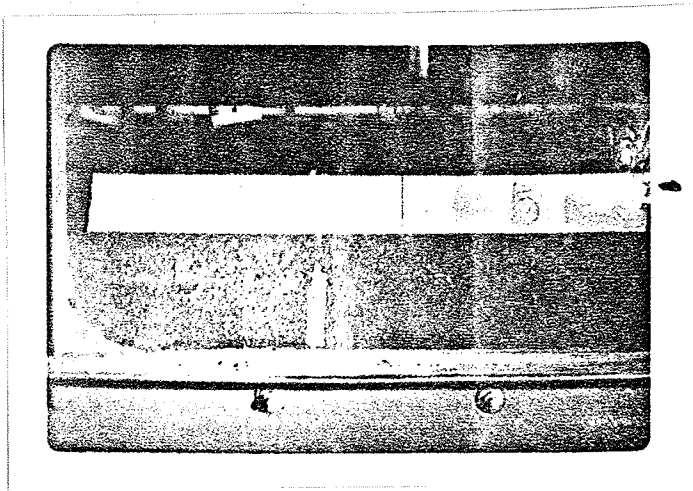
C2

m = .46

AVERAGE DOWNSTREAM F = .07

d = .2 ft.

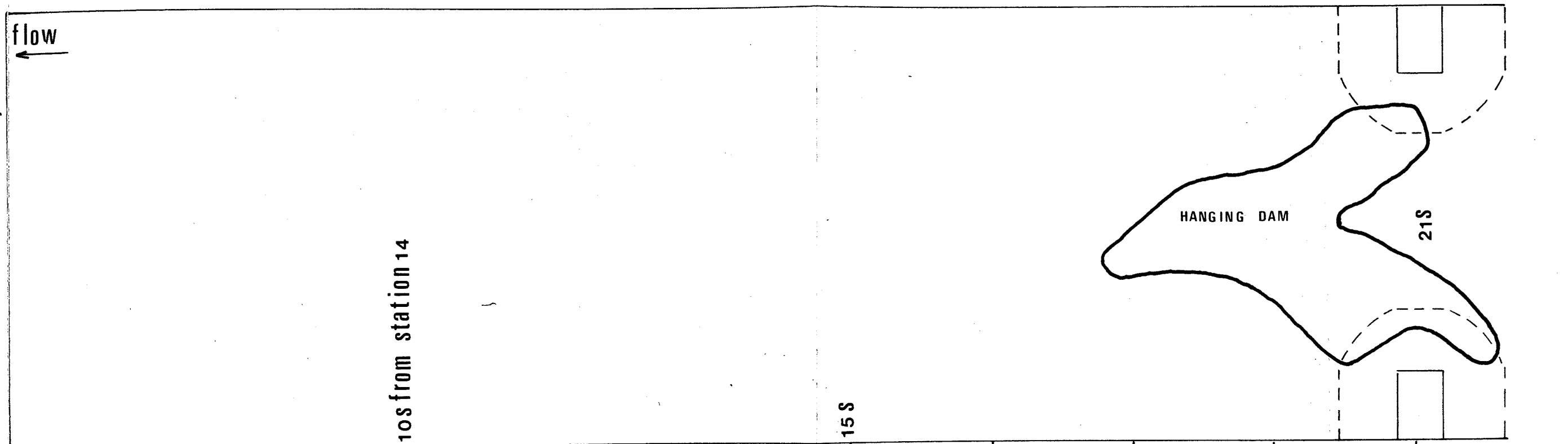
RUN HD - 13.



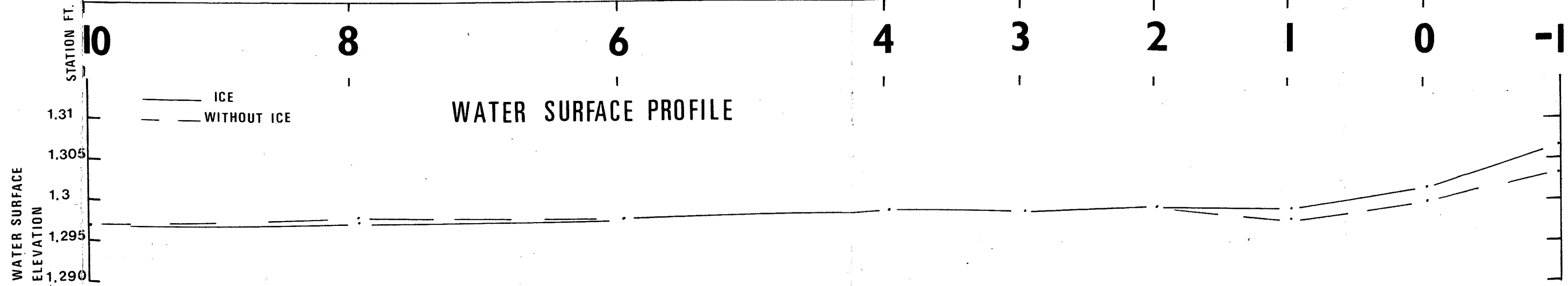
SIDE PHOTOGRAPHS

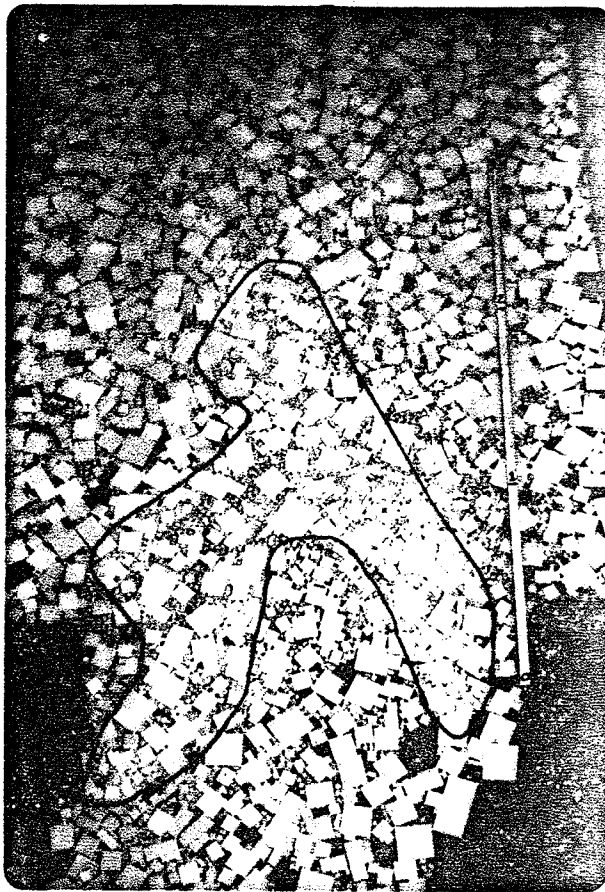
$s = .08$ cu. ft.
of ice

PLAN VIEW



WATER SURFACE PROFILE

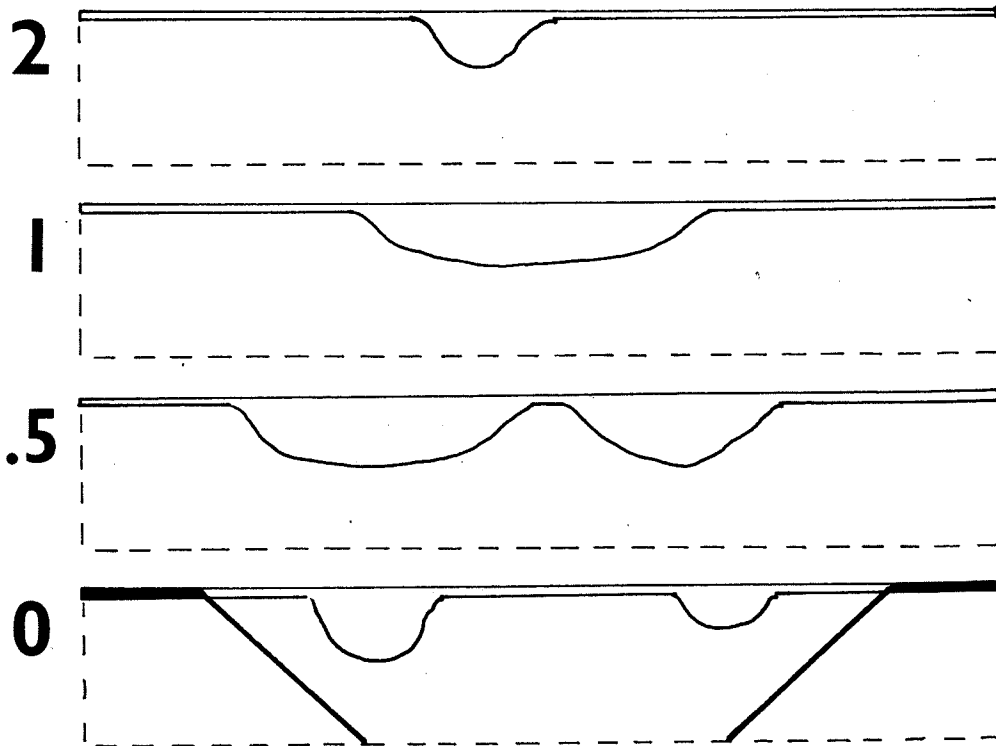




$s = .08$ cu. ft.
of ice

PHOTOGRAPH OF HANGING DAM

HANGING DAM CROSS-SECTIONS



PLAN VIEW

STATION FT.

WATER SURFACE
ELEVATION
1.290
1.295
1.3
1.305
1.31

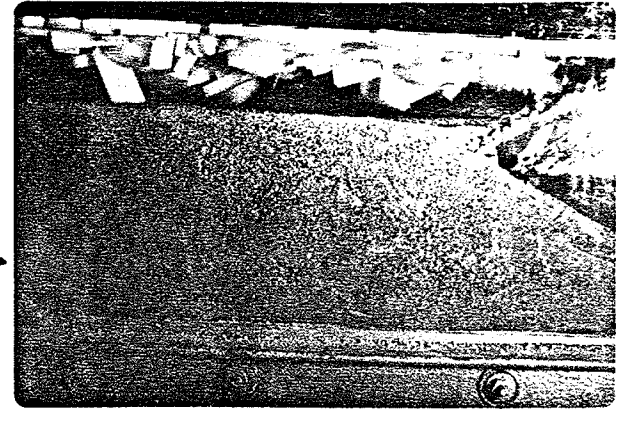
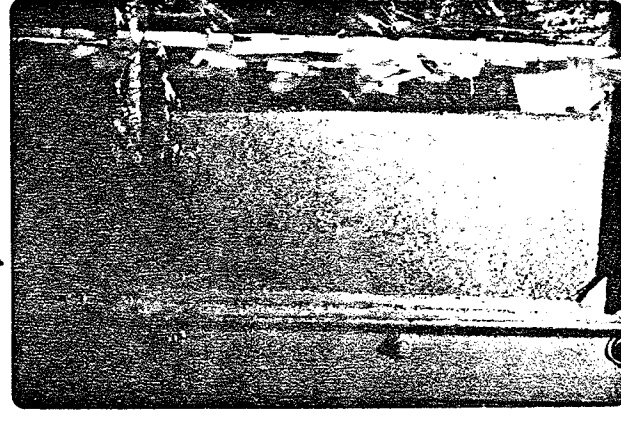
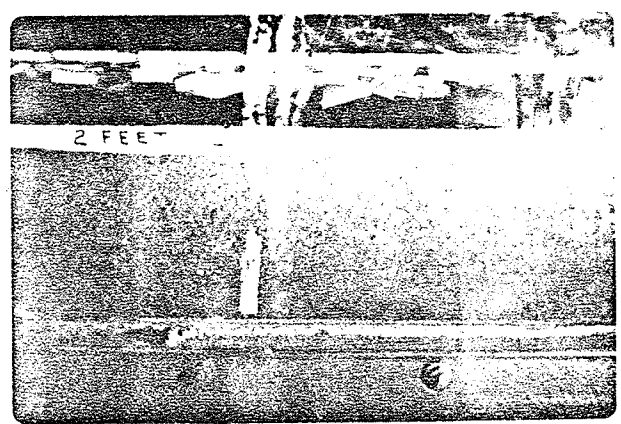
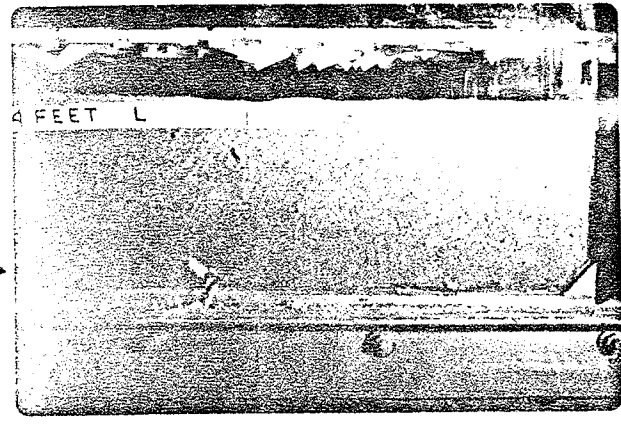
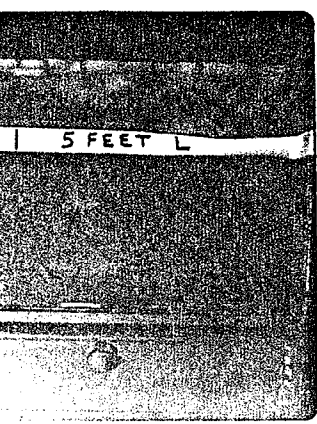
C3

$m = .46$

AVERAGE DOWNSTREAM F = .07

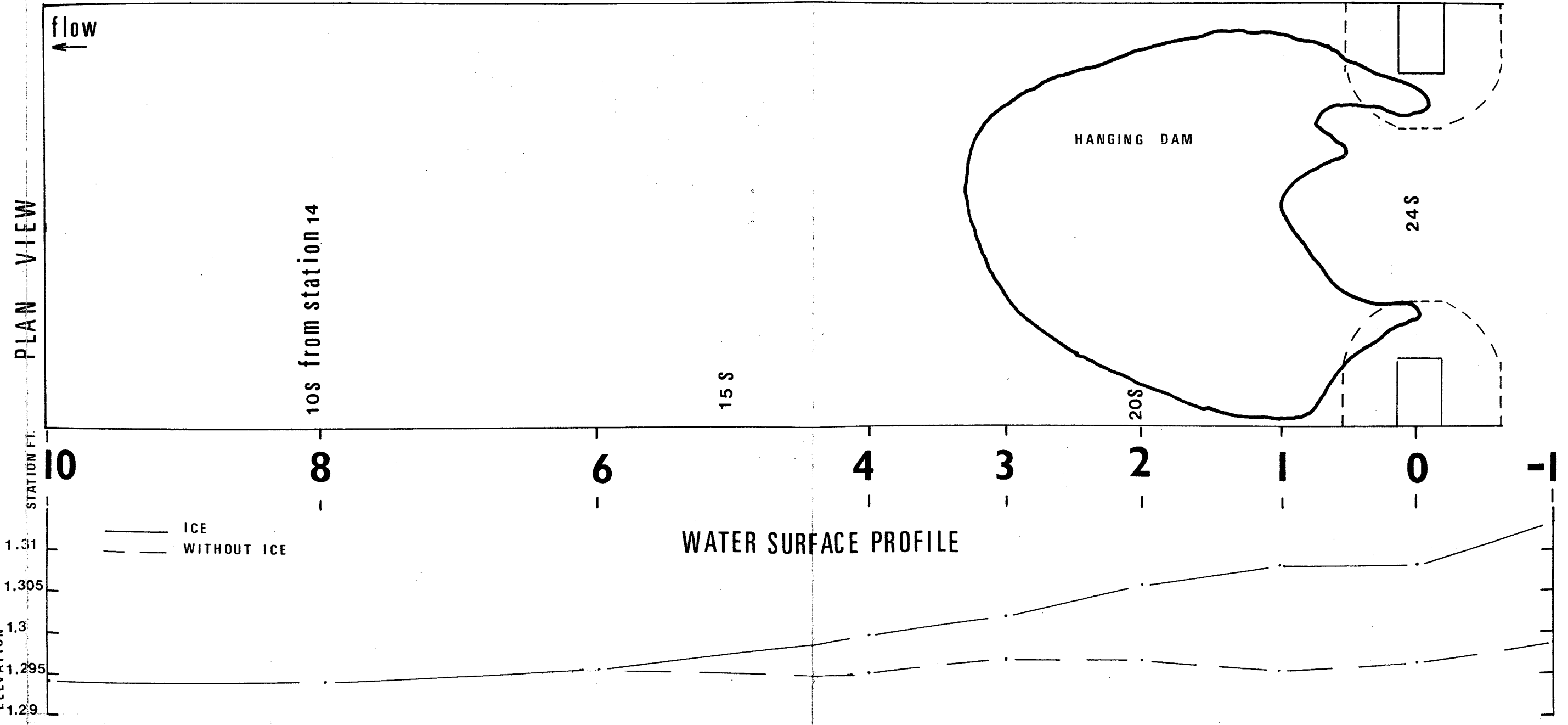
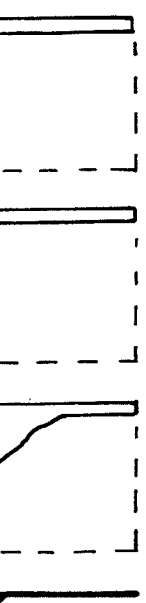
$d = .2 \text{ ft}$

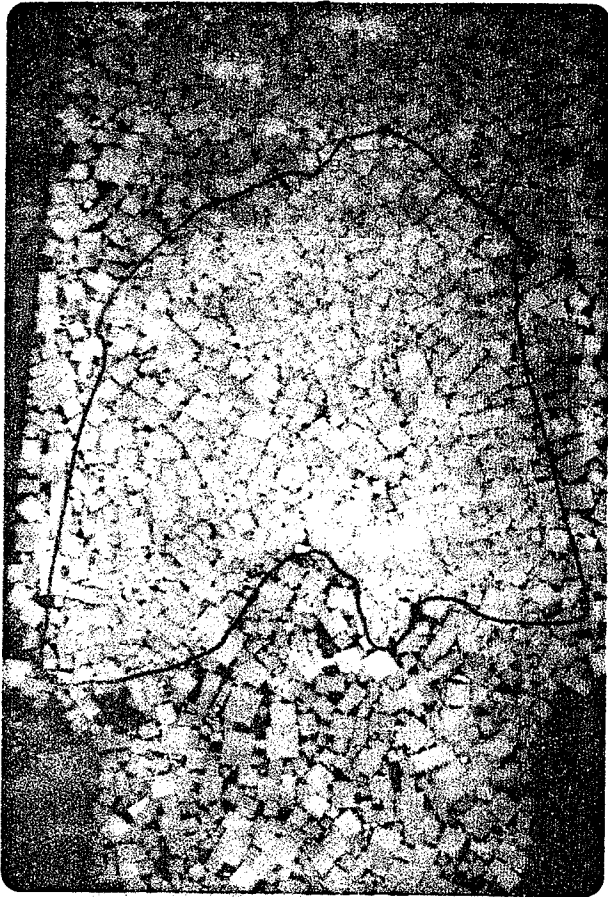
RUN HD - 11



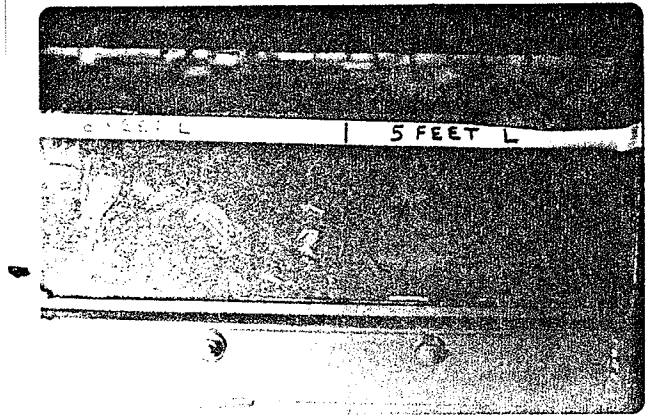
PHOTOGRAPHS

$S = .08$ cu. ft.
of ice





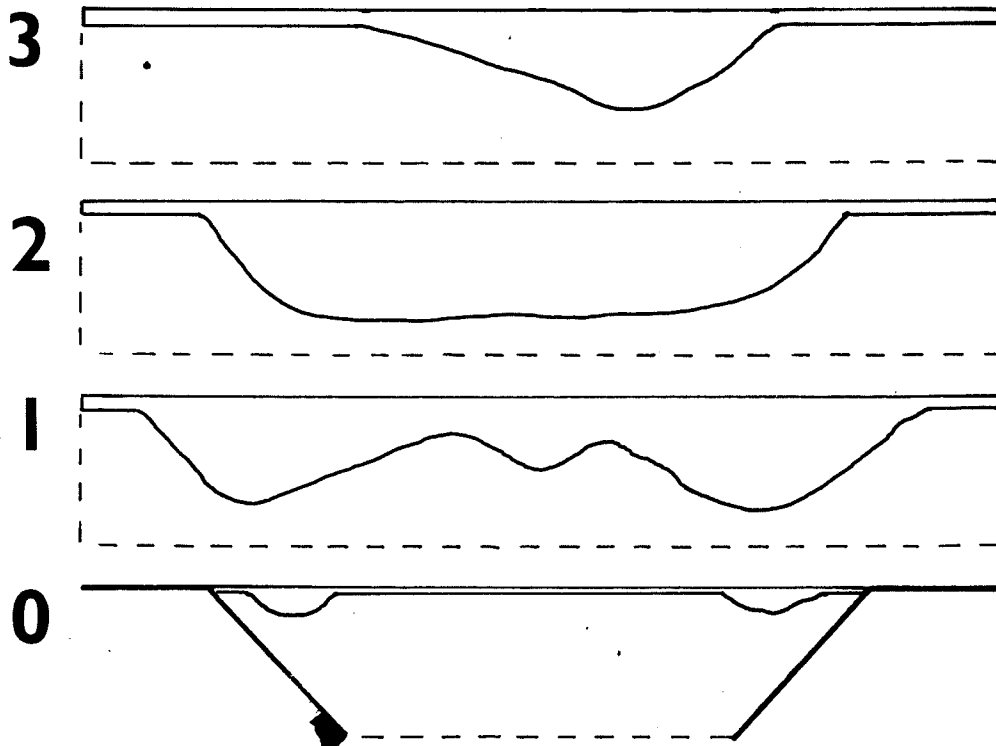
PHOTOGRAPH OF HANGING DAM



SIDE PHOTOGRAPHS

$s = .08$ cu. ft.
of ice

HANGING DAM CROSS-SECTIONS



PLAN VIEW
 STATION FT.
 ELEVATION
 1.31
 1.305
 1.3
 1.295
 1.29

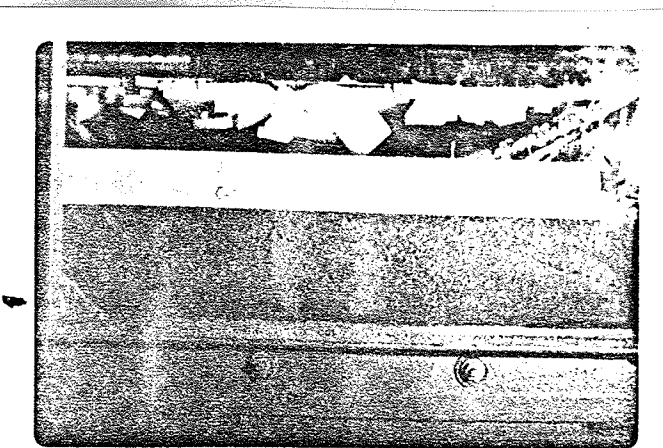
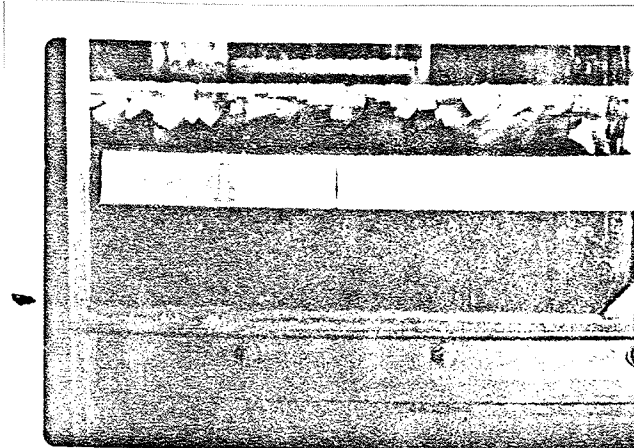
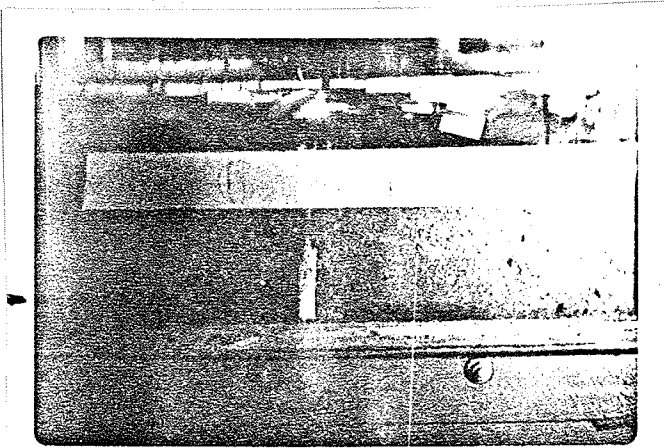
C4

$m = .46$

AVERAGE DOWNSTREAM F = .089

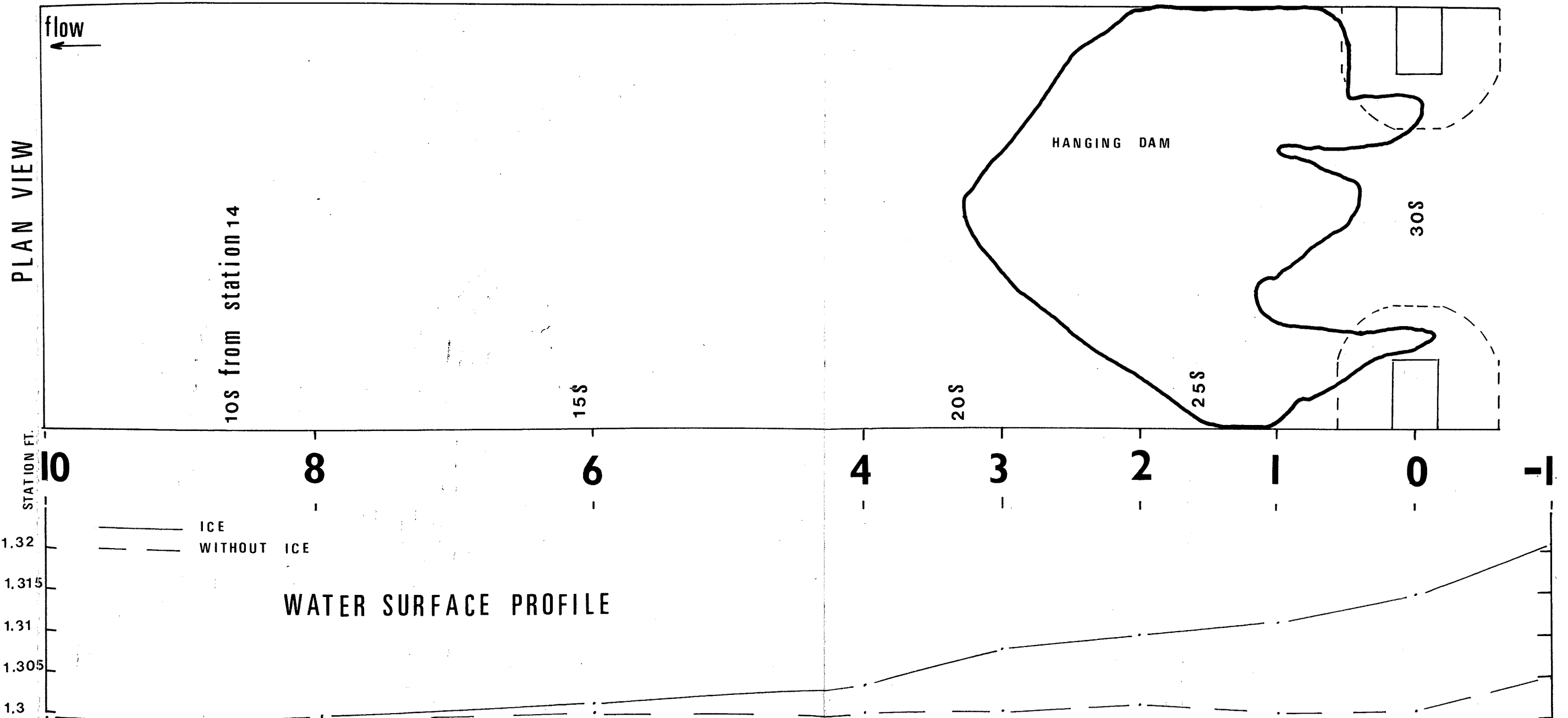
$\bar{d} = .2 \text{ ft.}$

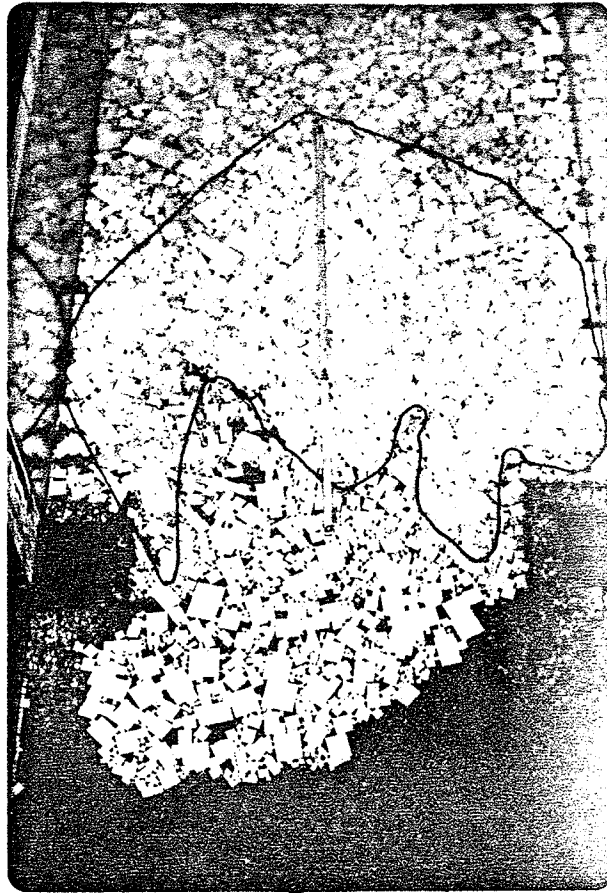
RUN HD - 14



SIDE PHOTOGRAPHS

s=.08 cu. ft.
of ice

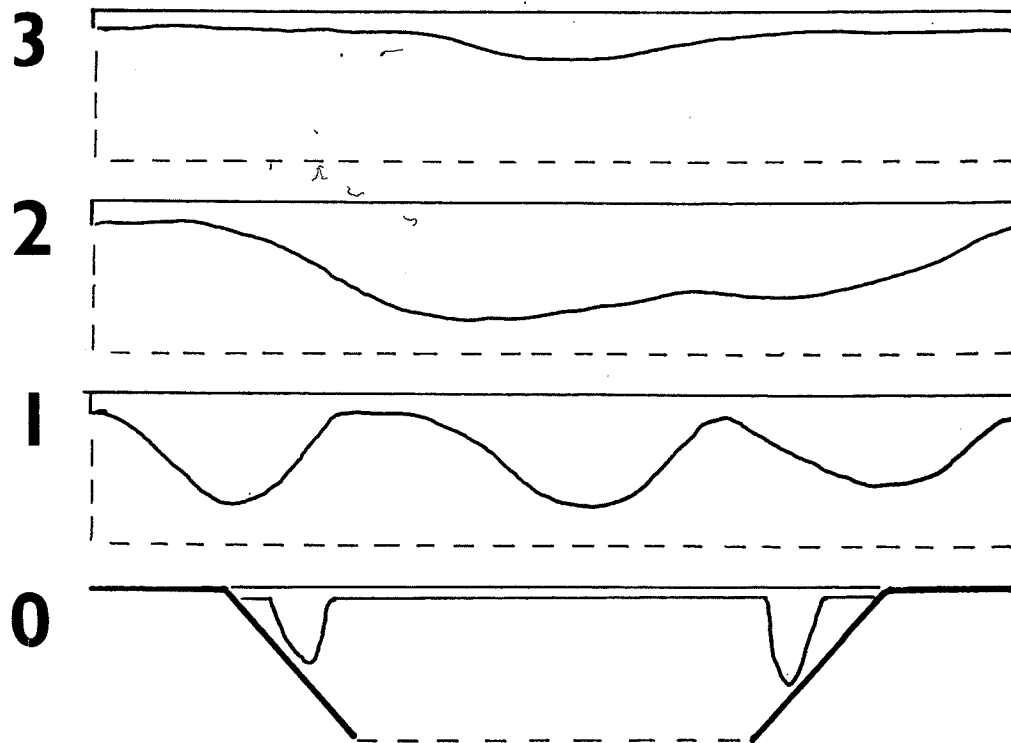




$S = .08$ cu. ft.
of ice

PHOTOGRAPH OF HANGING DAM

HANGING DAM CROSS-SECTIONS



PLAN VIEW

STATION FT.

WATER SURFACE
ELEVATION
1.32
1.315
1.31
1.305
1.3

C5 - C7 m = .40

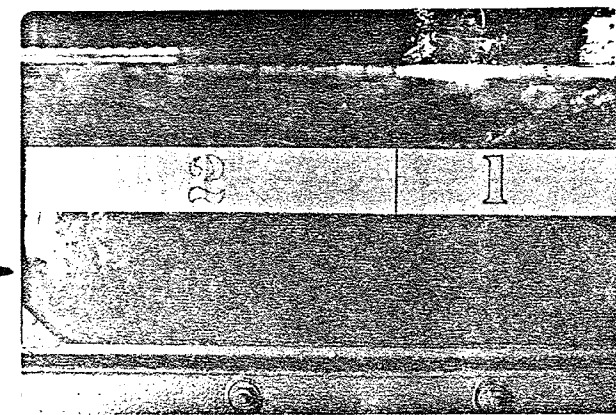
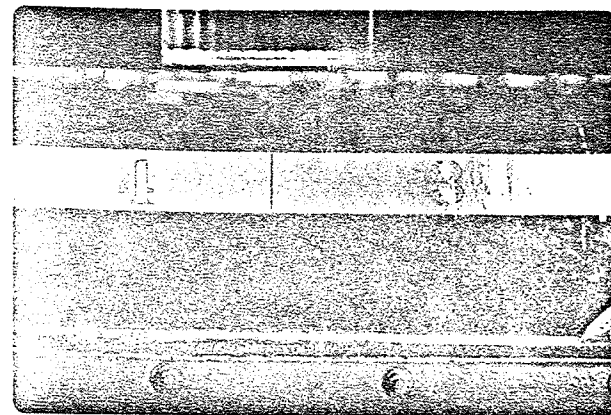
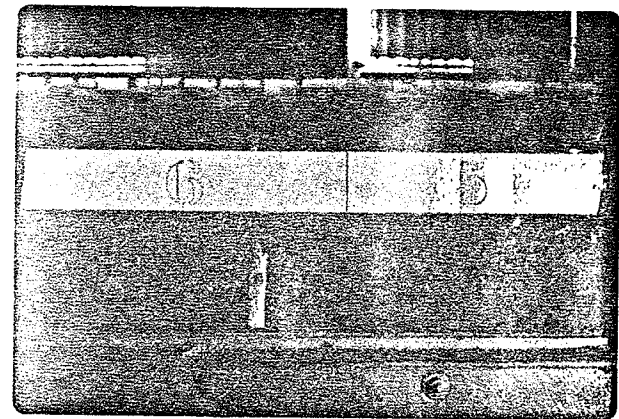
d = .2 ft.

C5

m = .4

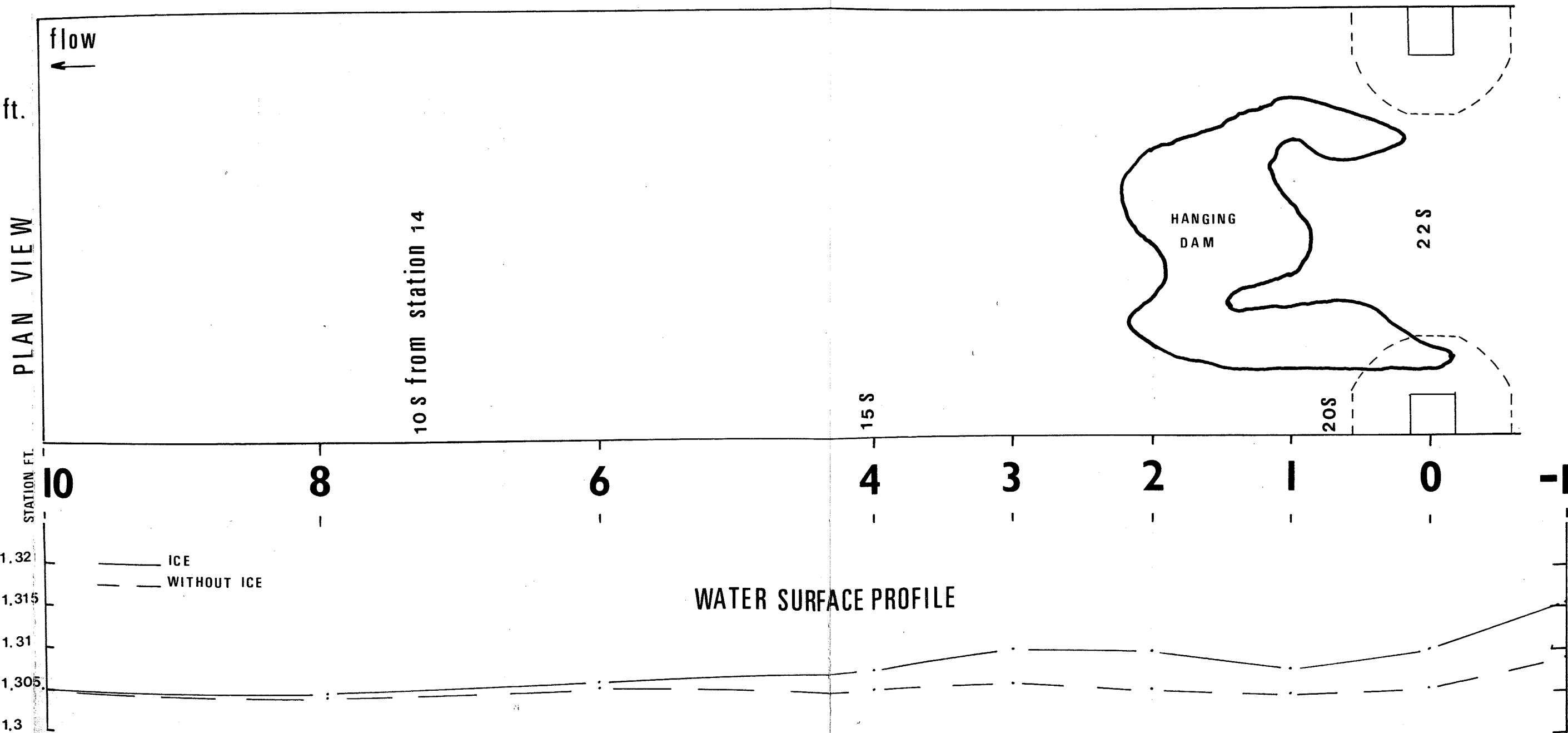
AVERAGE DOWNSTREAM F = .067

RUN HD - 21



SIDE PHOTOGRAPHS

$s = .08$ cu. ft.
of ice

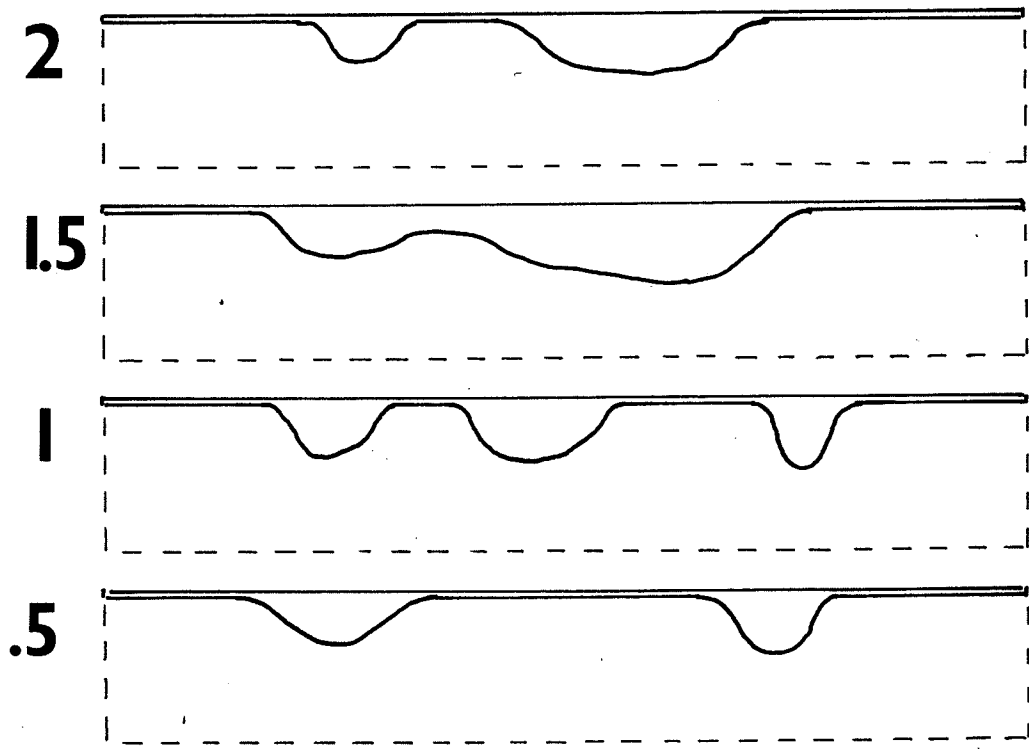




$s = .08$ cu. ft.
of ice

PHOTOGRAPH OF HANGING DAM

HANGING DAM CROSS-SECTIONS



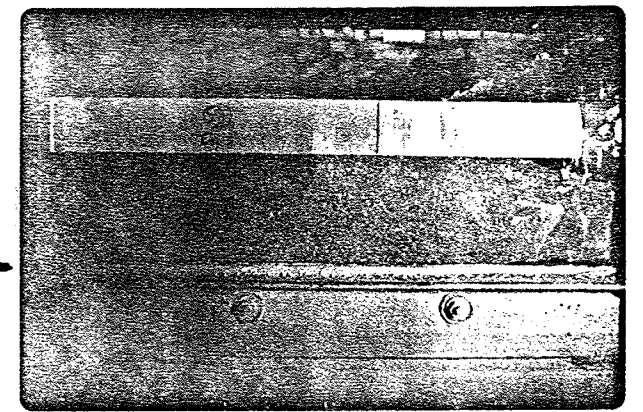
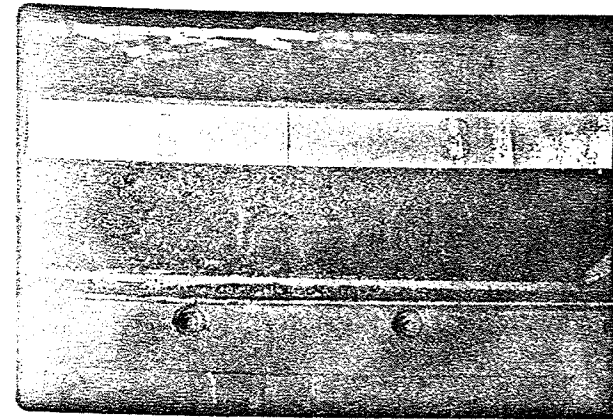
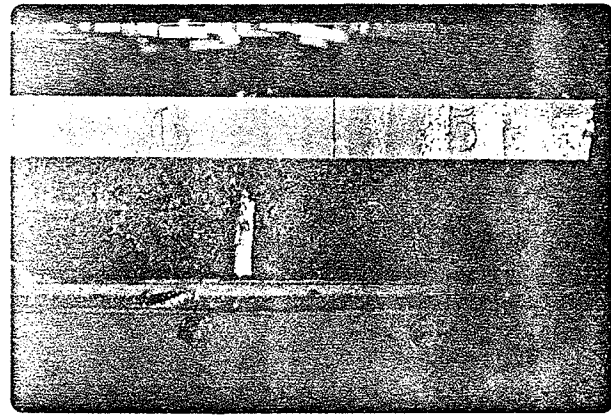
PLAN VIEW
 STATION FT.
 1.32
 1.315
 1.31
 1.305
 1.3
 WATER SURFACE
 ELEVATIONS

C6

$m = .4$

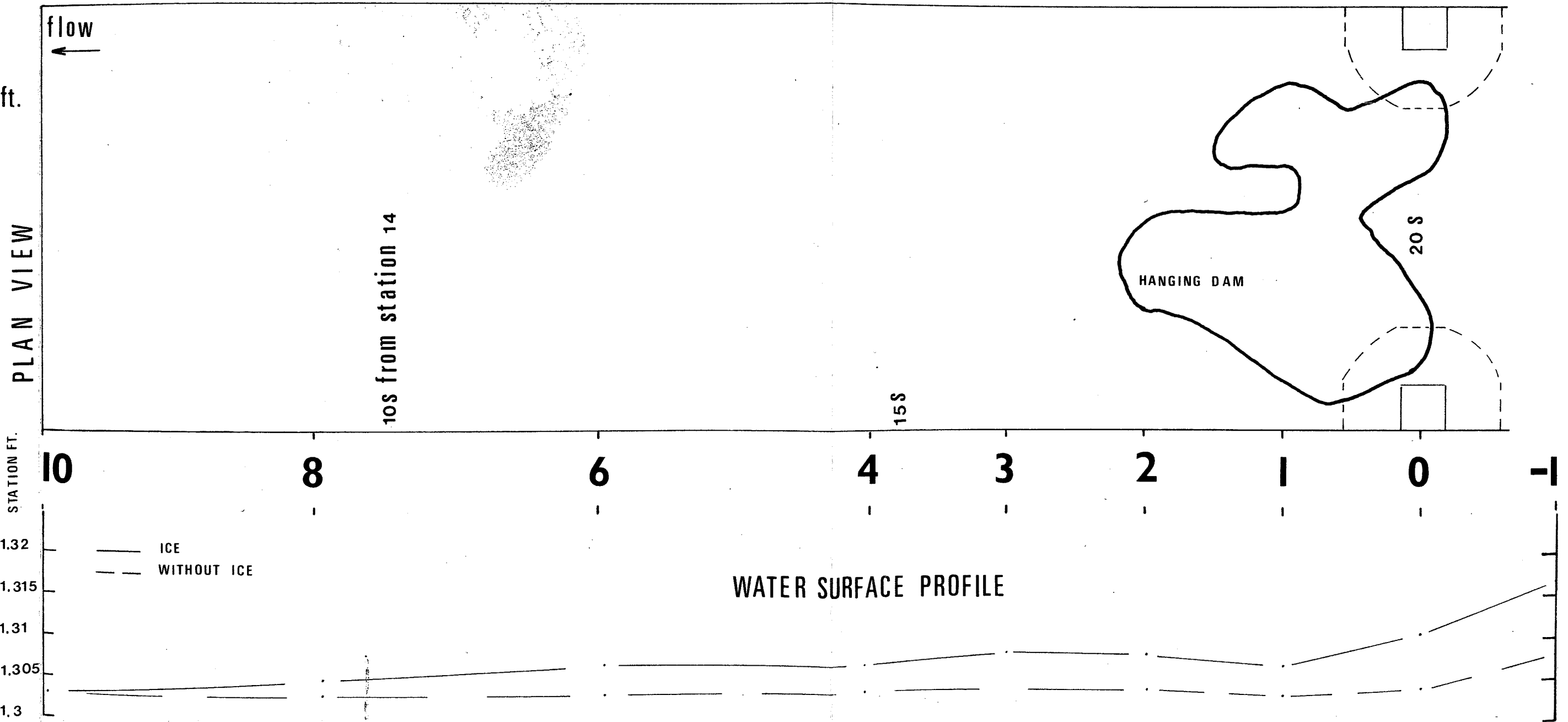
AVERAGE DOWNSTREAM F = .074

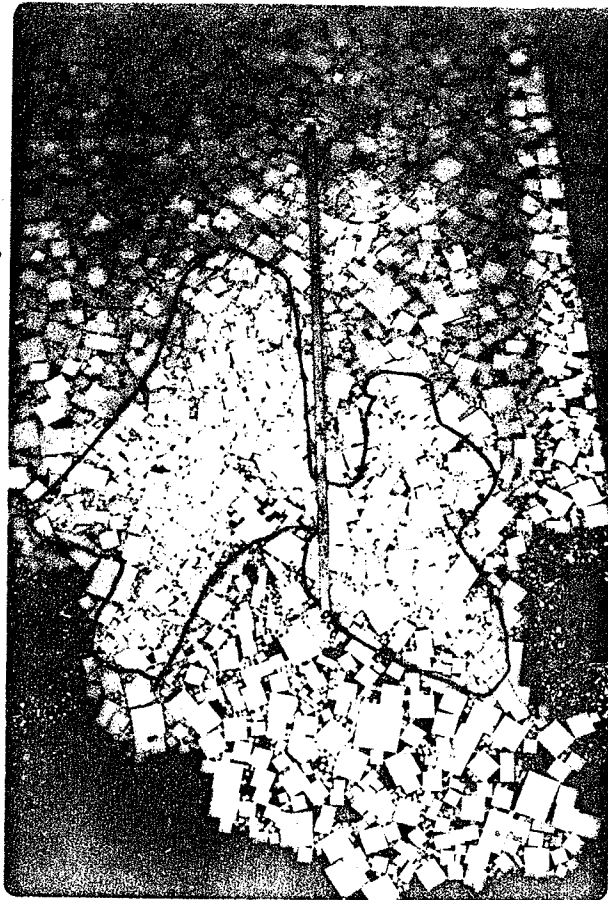
RUN HD - 23



SIDE PHOTOGRAPHS

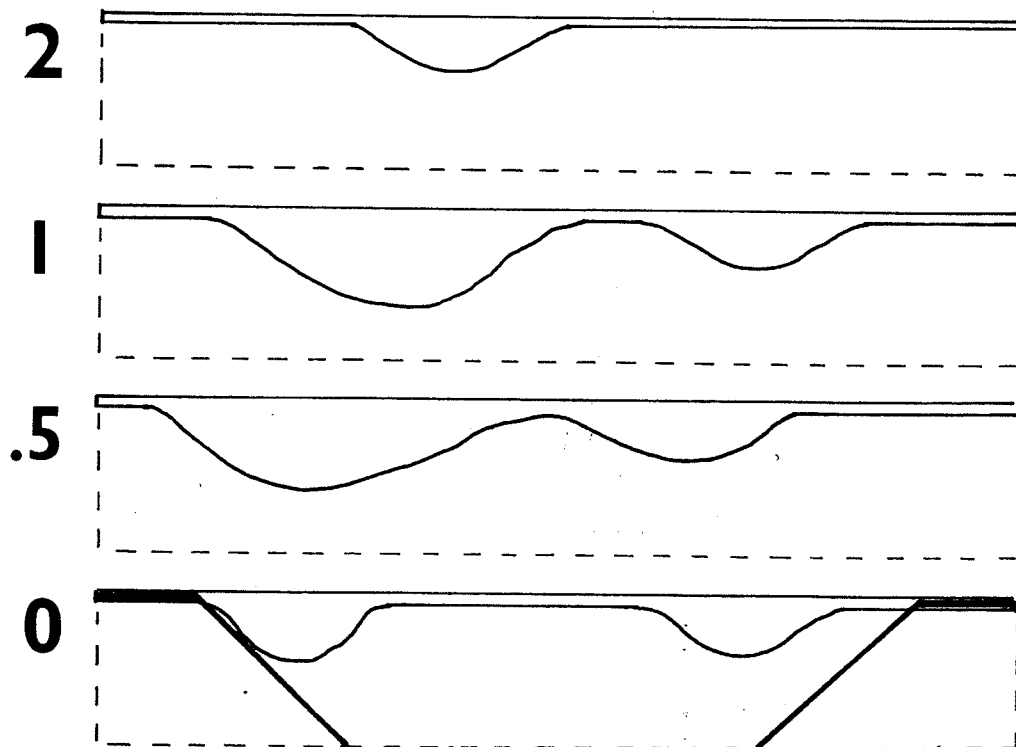
$S = .08$ cu. ft.
of ice





$S = .08 \text{ cu. ft.}$
of ice

PHOTOGRAPH OF HANGING DAM
HANGING DAM CROSS-SECTIONS



PLAN VIEW

STATION FT.
1.32
1.315
1.31
1.305
1.3
WATER SURFACE
ELEVATION

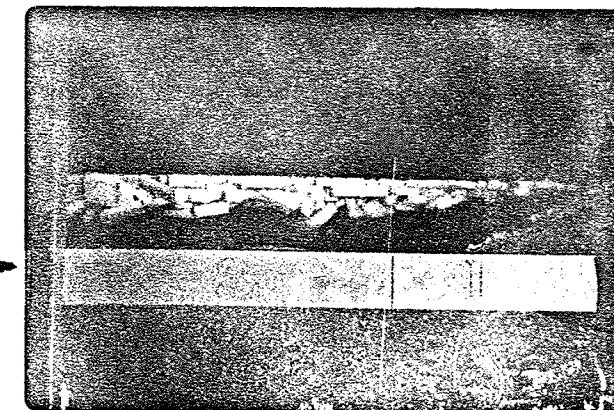
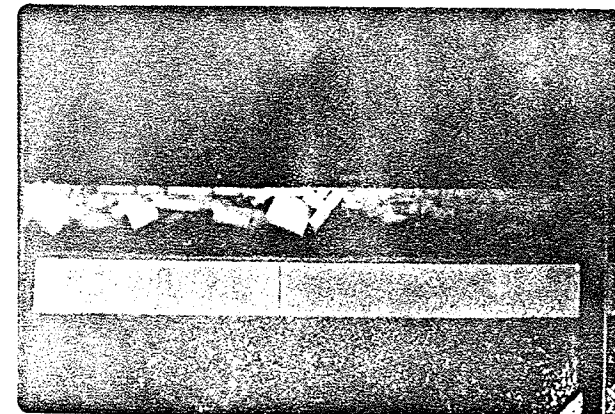
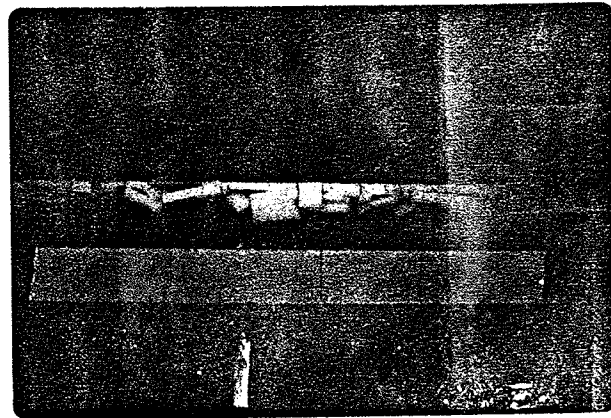
C7

m = .4

AVERAGE DOWNSTREAM F = .08

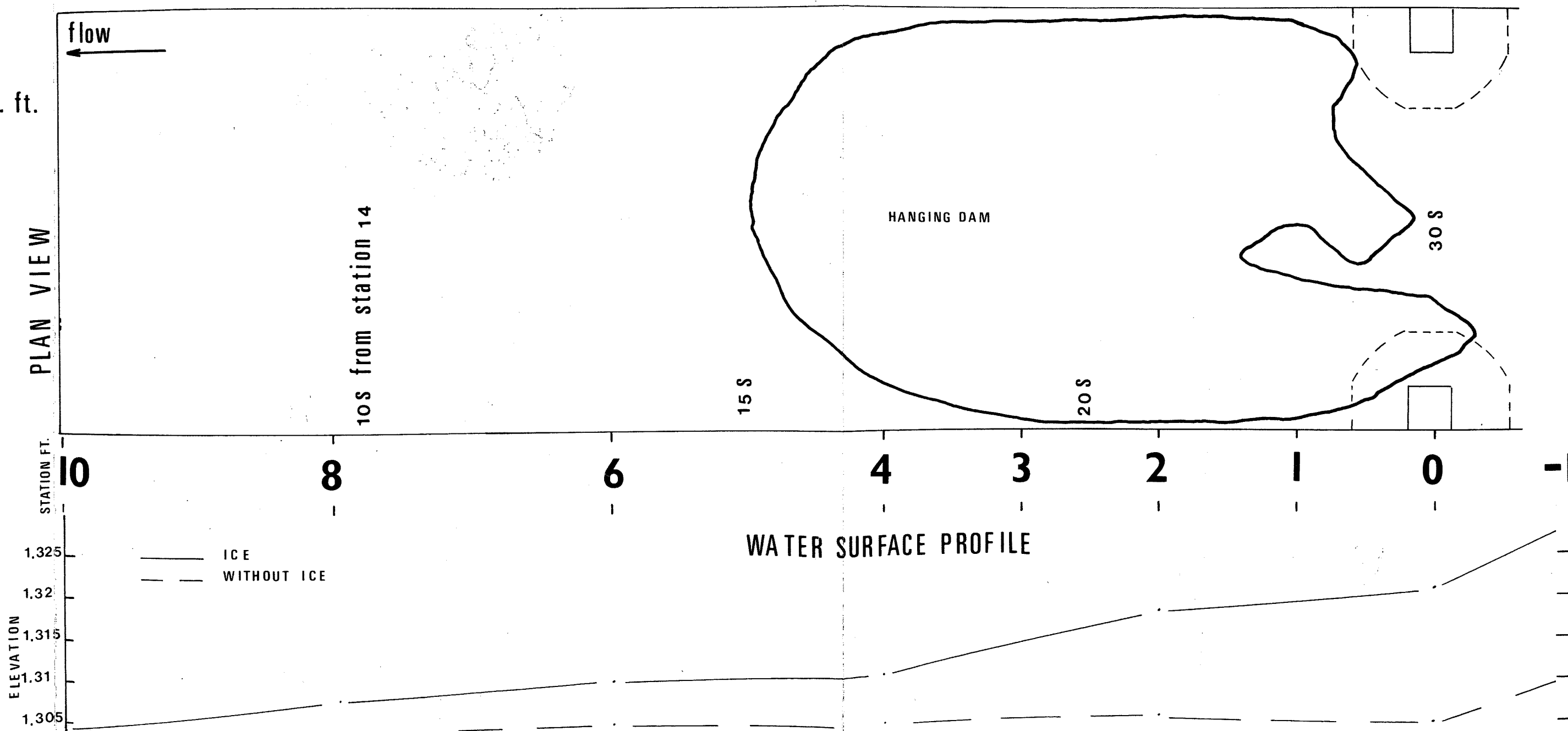
d = .2 ft.

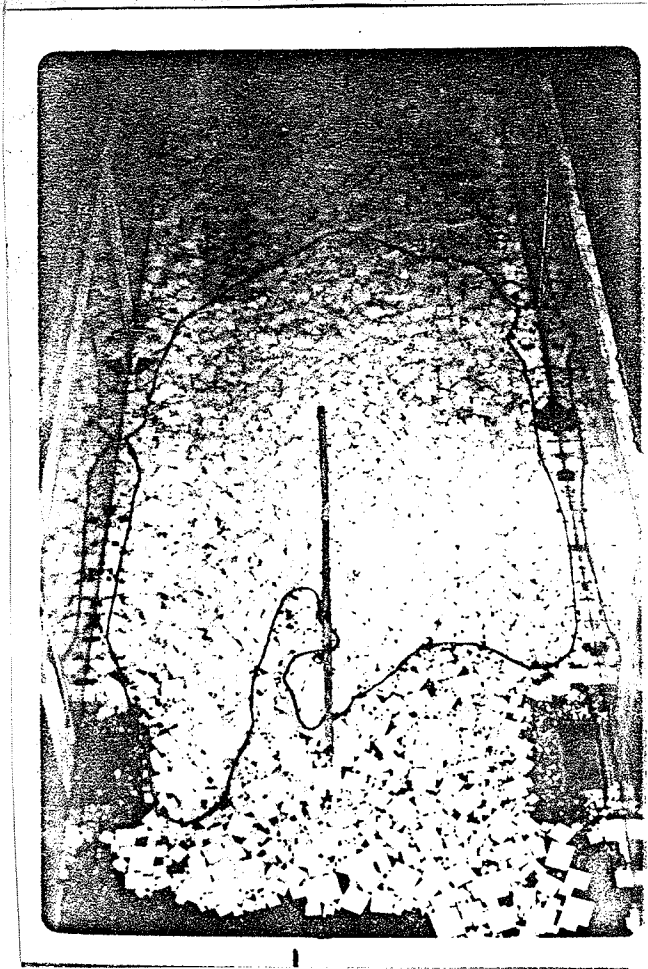
RUN HD - 25



SIDE PHOTOGRAPHS

$s = .08$ cu. ft.
of ice

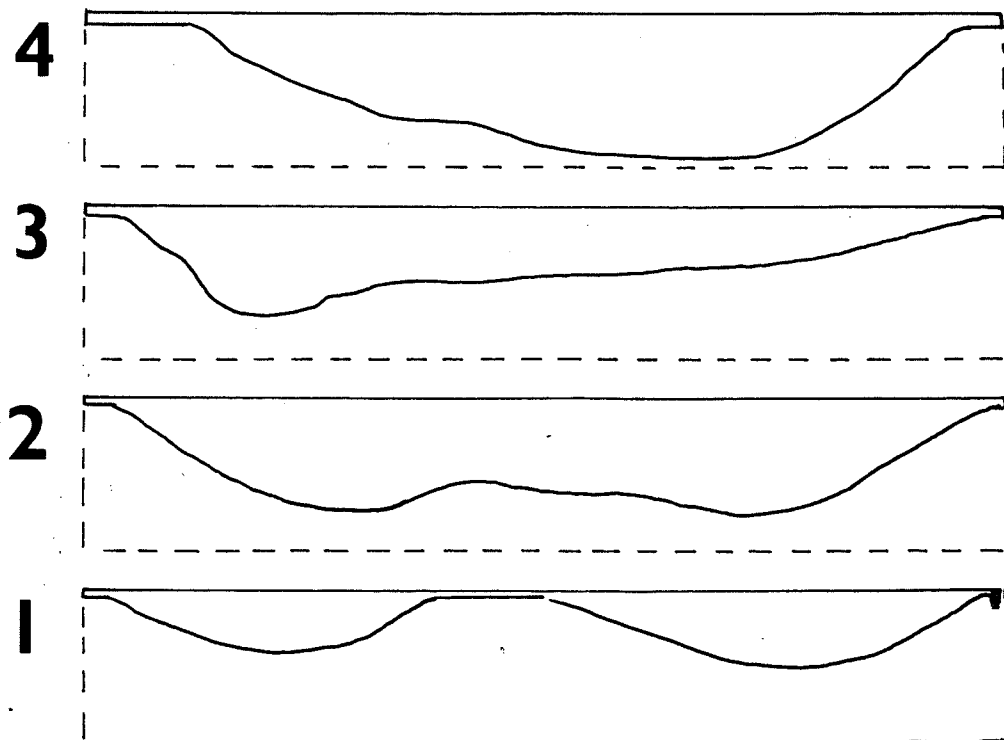




s = .08 cu. ft.
of ice

PHOTOGRAPH OF HANGING DAM

HANGING DAM CROSS-SECTIONS



PLAN VIEW
 STATION FT.
 ELEVATION
 1,325
 1,32
 1,315
 1,31
 1,305

C8 - C10 m = .36

d = .2 ft.

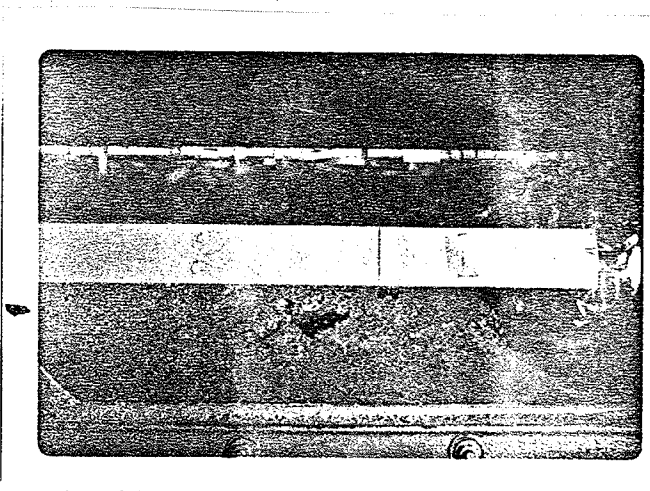
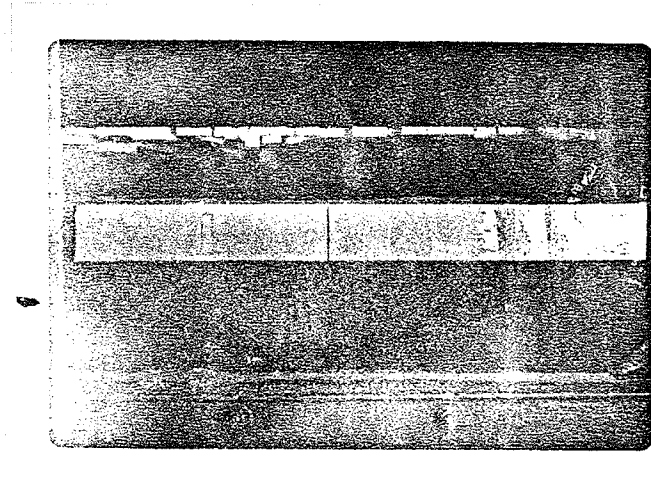
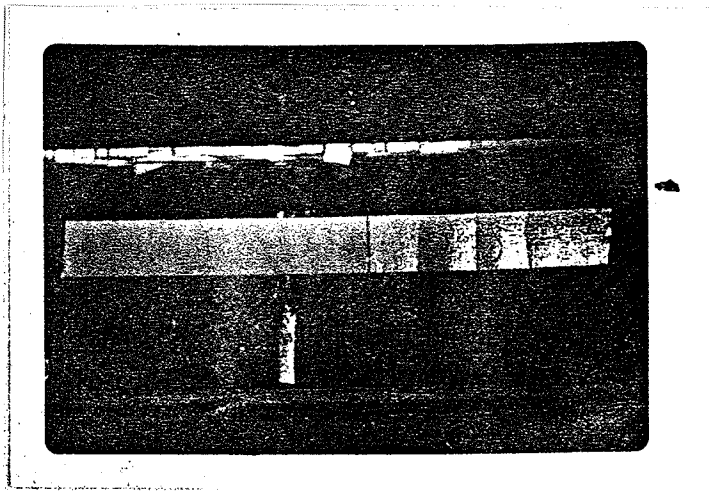
C8

$m = .36$

AVERAGE DOWNSSTREAM F = .082

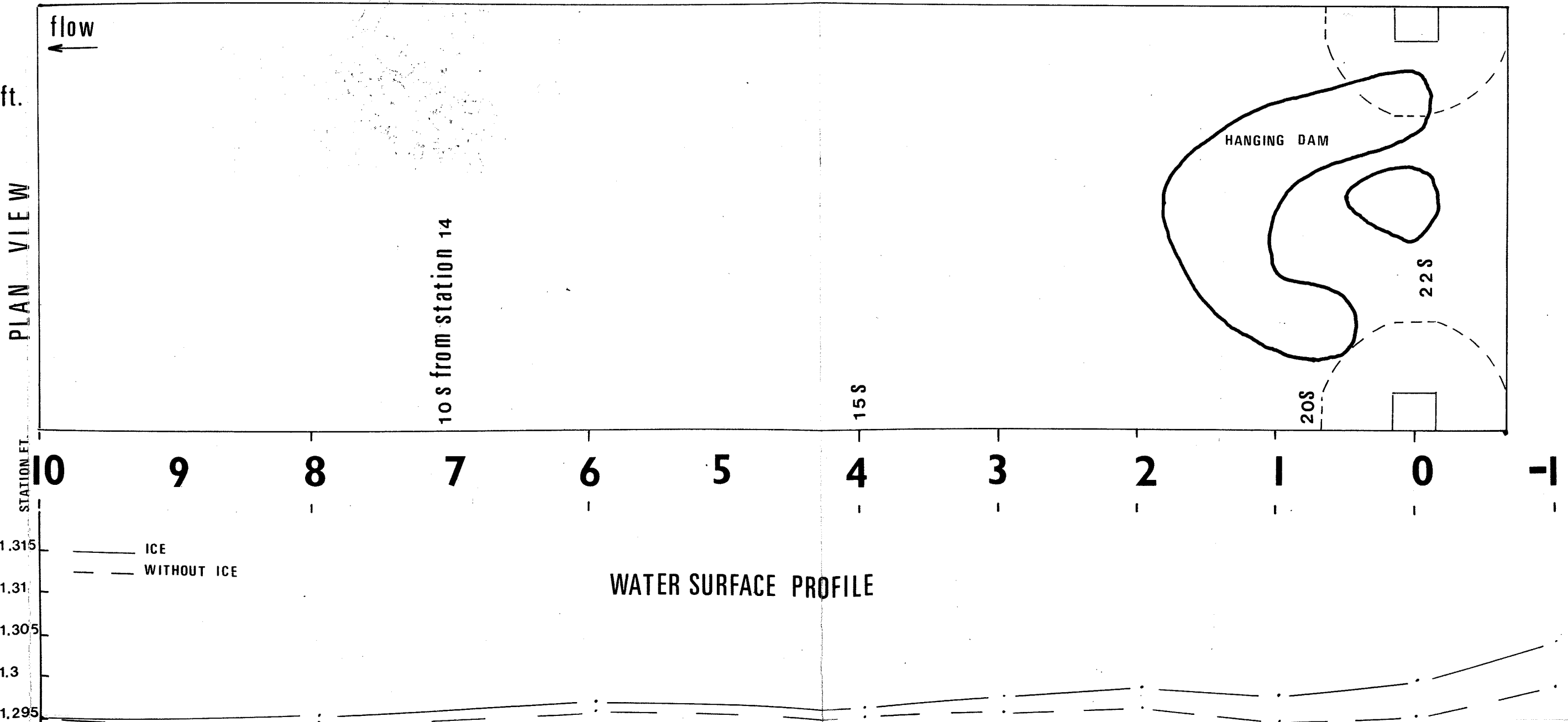
$d = .2 \text{ ft.}$

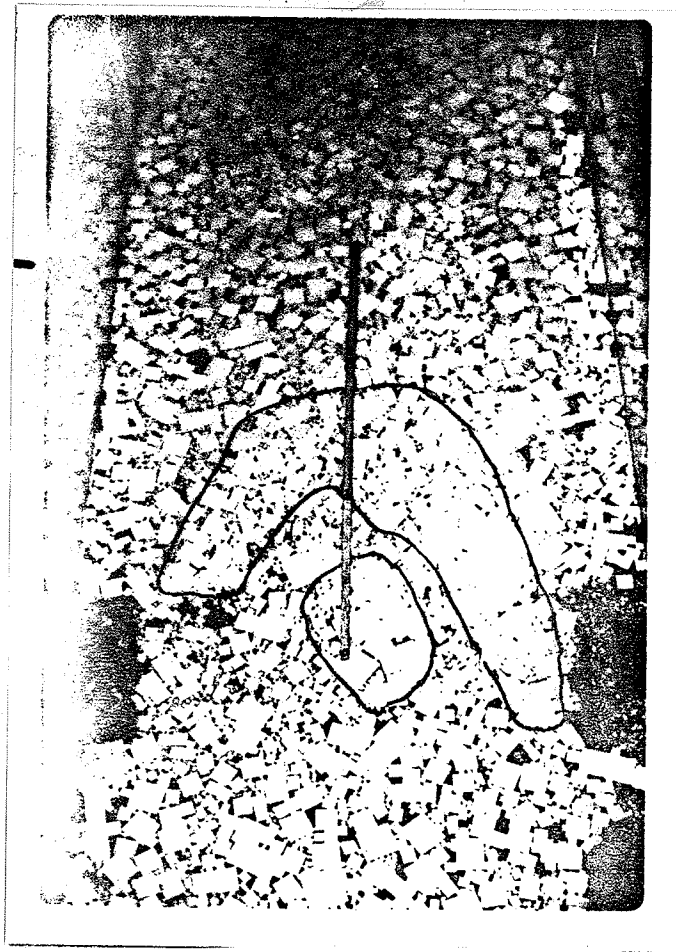
RUN HD - 19



SIDE PHOTOGRAPHS

$s = .08$ cu. ft.
of ice

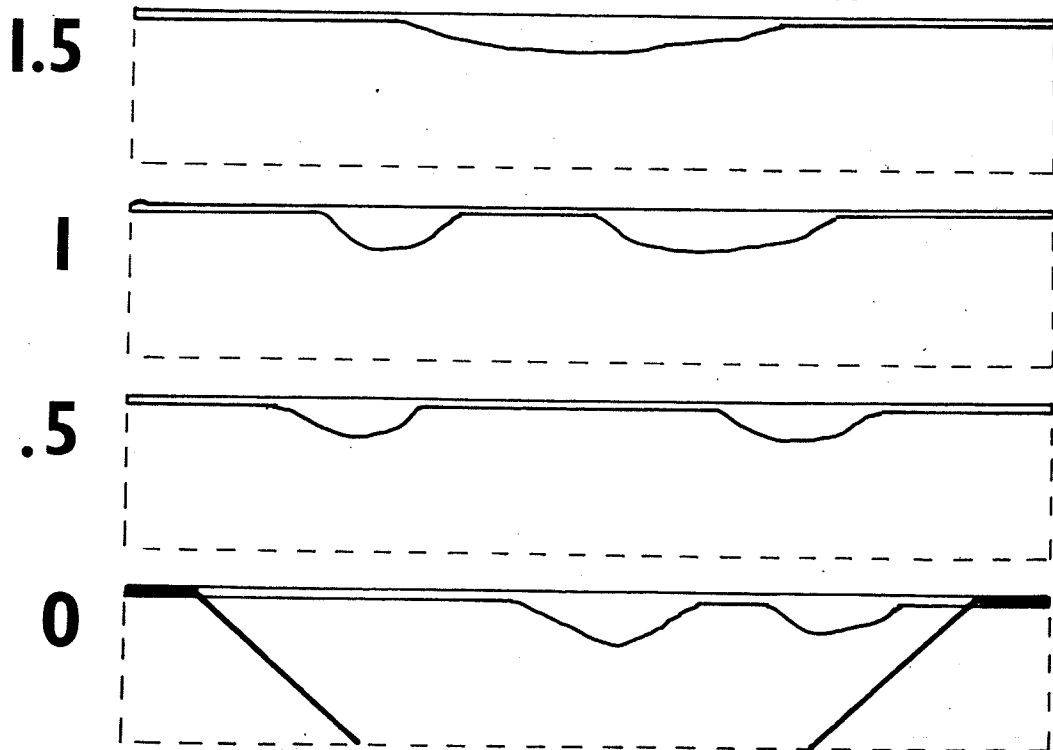




PHOTOGRAPH OF HANGING DAM

S = .08 cu. ft.
of ice

HANGING DAM CROSS-SECTIONS



PLAN VIEW

STATION FT.

ELEVATION OF WATER SURFACE

1.315

1.31

1.305

1.3

1.295

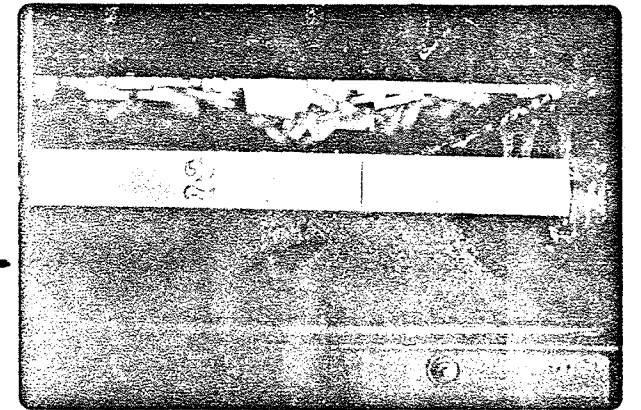
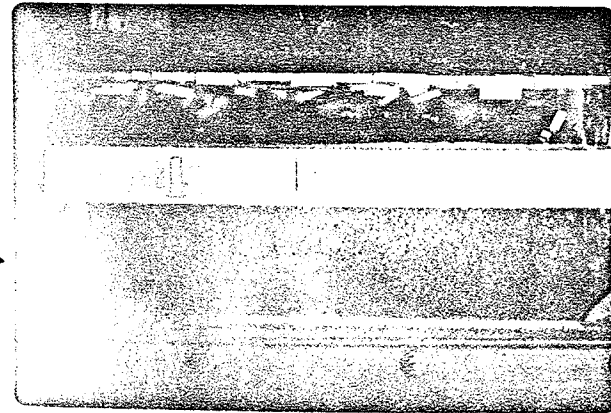
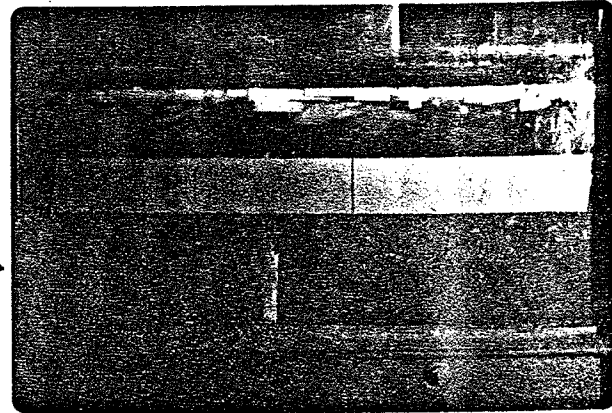
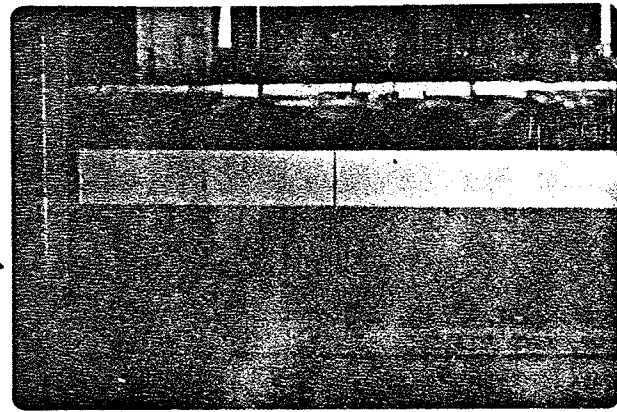
C9

$m = .36$

AVERAGE DOWNSTREAM F = .093

$d = .2 \text{ ft.}$

RUN HD - 16



PHOTOGRAPHS

S = .08 cu. ft.

of ice

PLAN VIEW

flow
←

10s from station 14

15s

HANGING DAM

20s

28s

STATION FT.

10

9

8

7

6

5

4

3

2

1

0

-1

WATER SURFACE PROFILE

ELEVATION

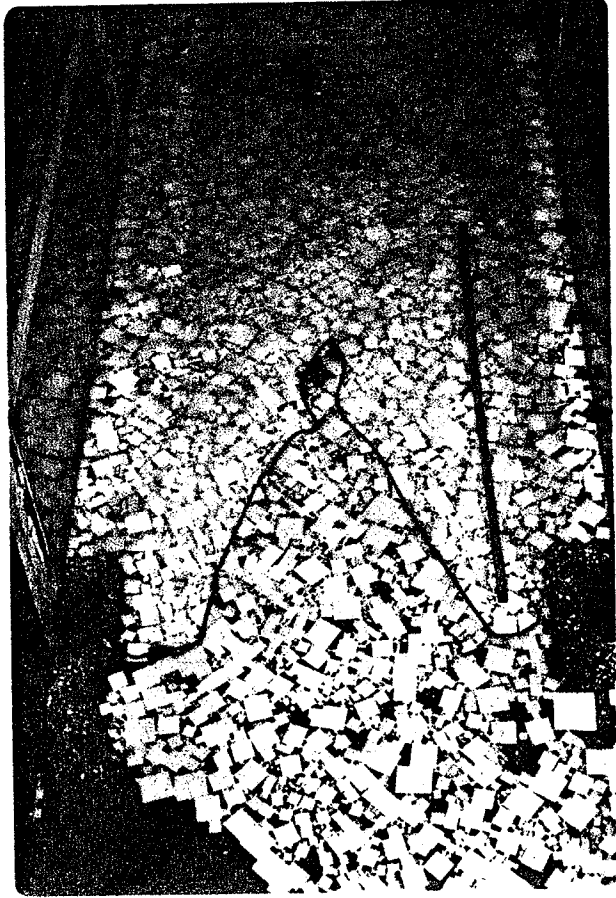
1.32

1.315

1.31

1.305

1.3

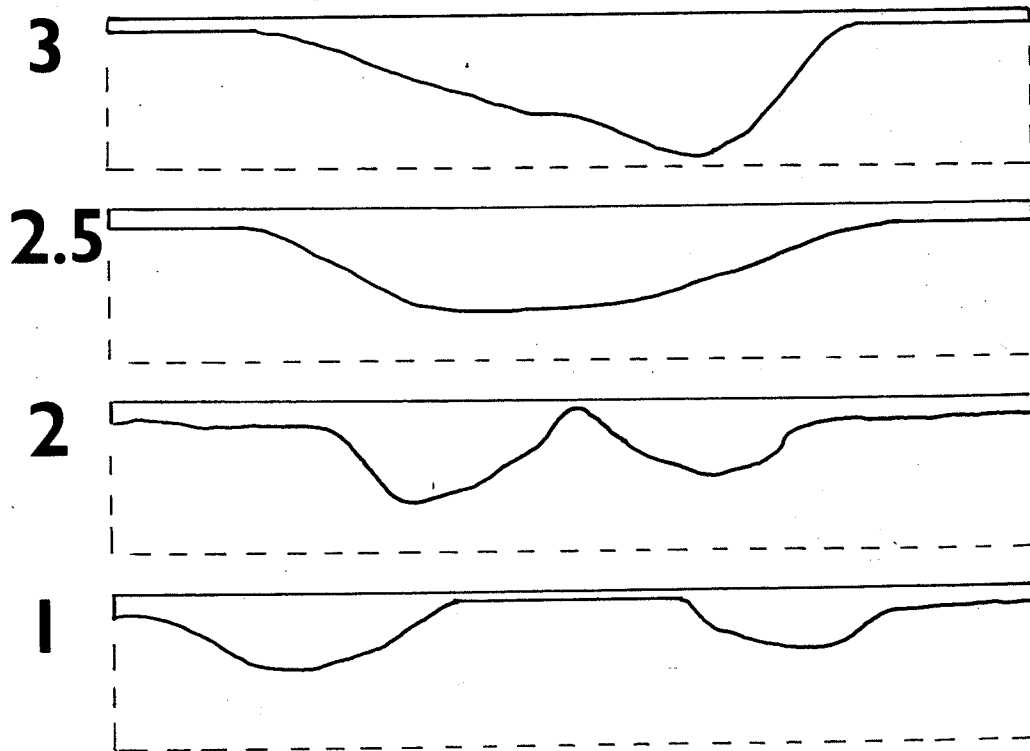


PHOTOGRAPH OF HANGING DAM

SIDE PHOTOGRAPHS

$S = .08$ cu. ft.
of ice

HANGING DAM CROSS-SECTIONS



ELEVATION

STATION FT.

PLAN VIEW

1.32
1.315
1.31
1.305
1.3

C10

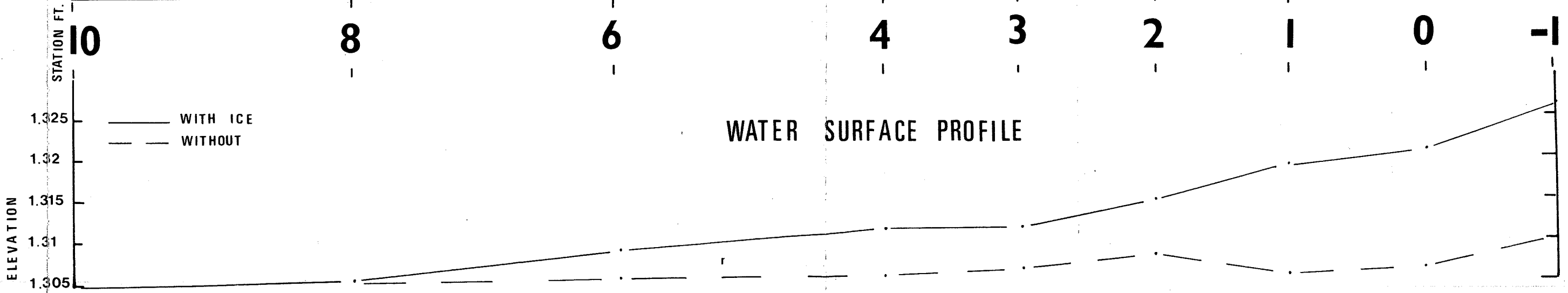
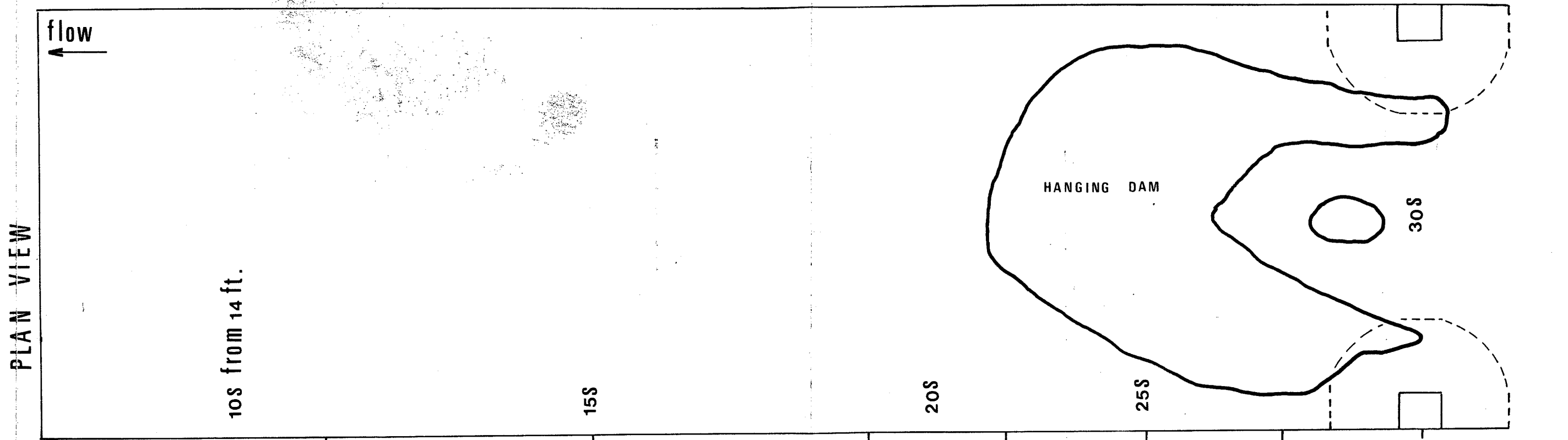
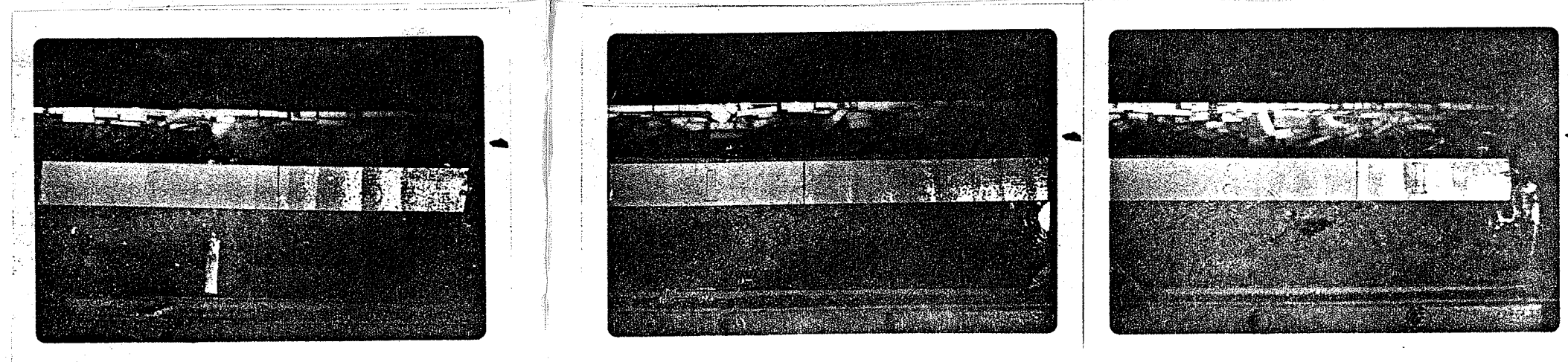
m = .36

AVERAGE DOWNSTREAM F = .098

d = .2 ft.

RUN HD - 20

S = .08 cu. ft.
of ice

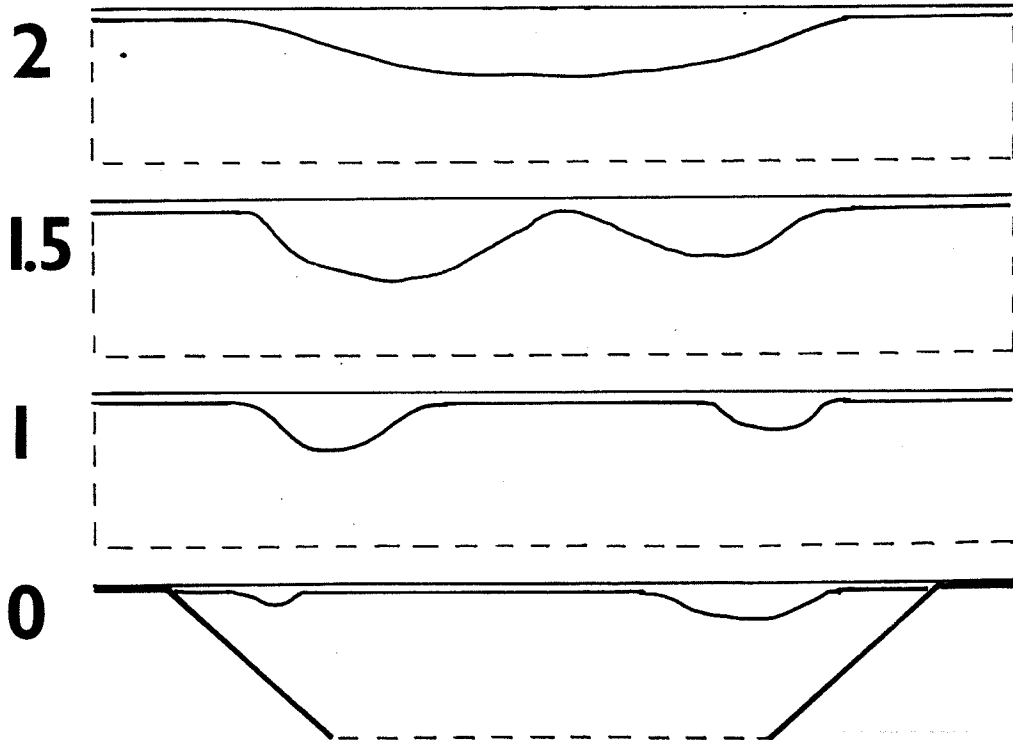




S = .08 cu. ft.
of ice

PHOTOGRAPH OF HANGING DAM

HANGING DAM CROSS-SECTIONS



PLAN VIEW
 STATION FT.
 1.32
 1.32
 1.315
 1.31
 1.30
 ELEVATION

C - 11 m = .46

d = .33 ft.

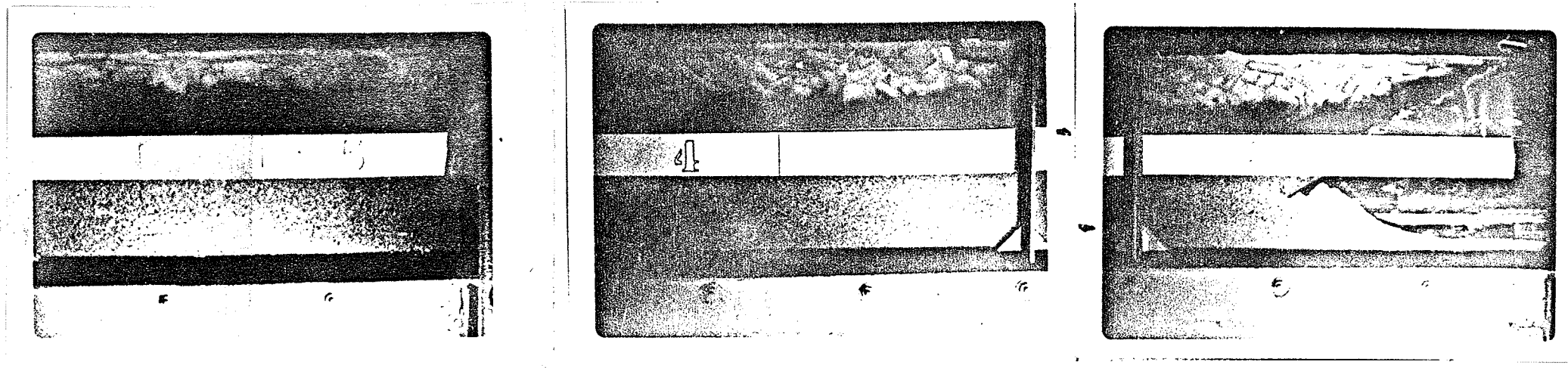
C11

m = .46

AVERAGE DOWNSTREAM F = .07

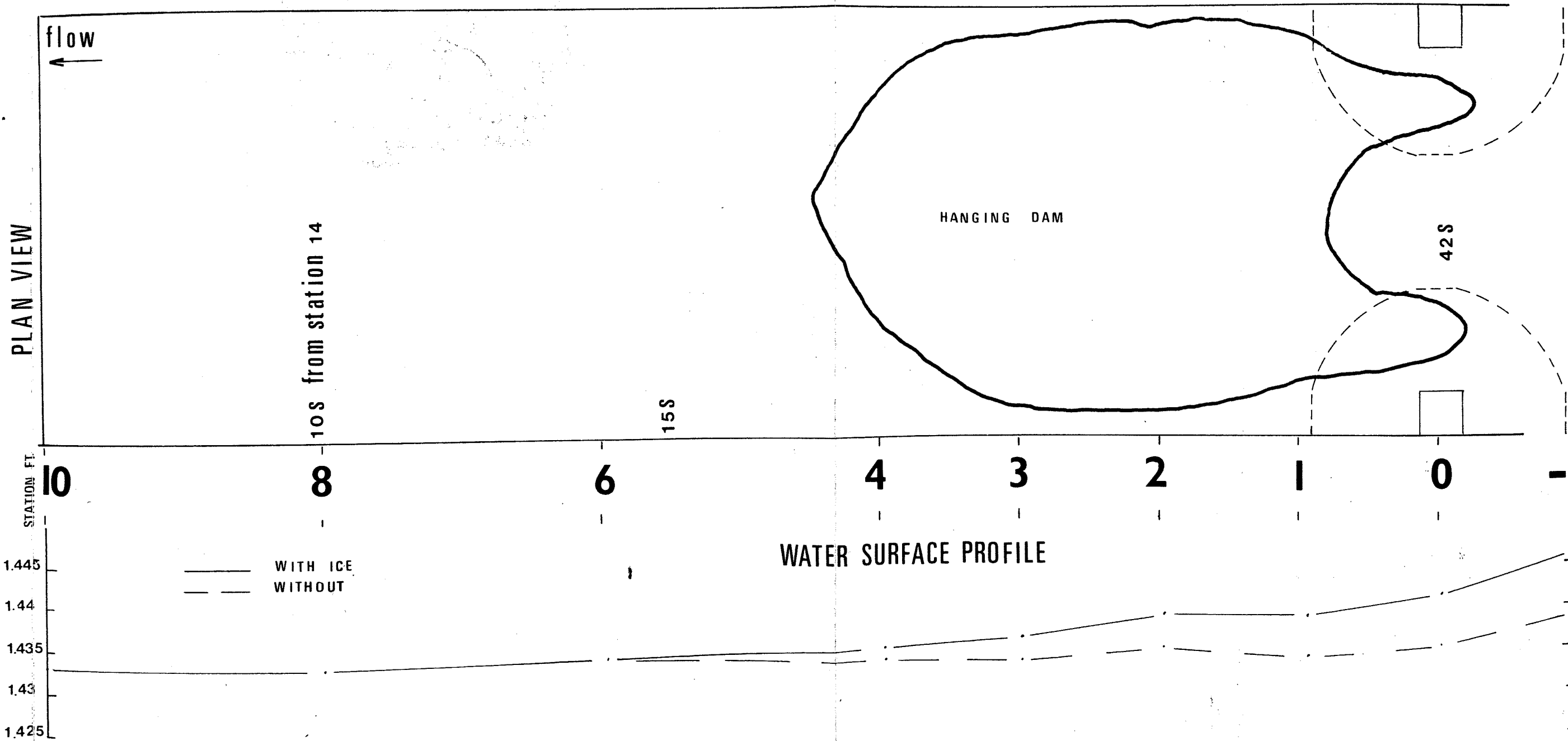
d = .33 ft.

RUN HD - 26



SIDE PHOTOGRAPHS

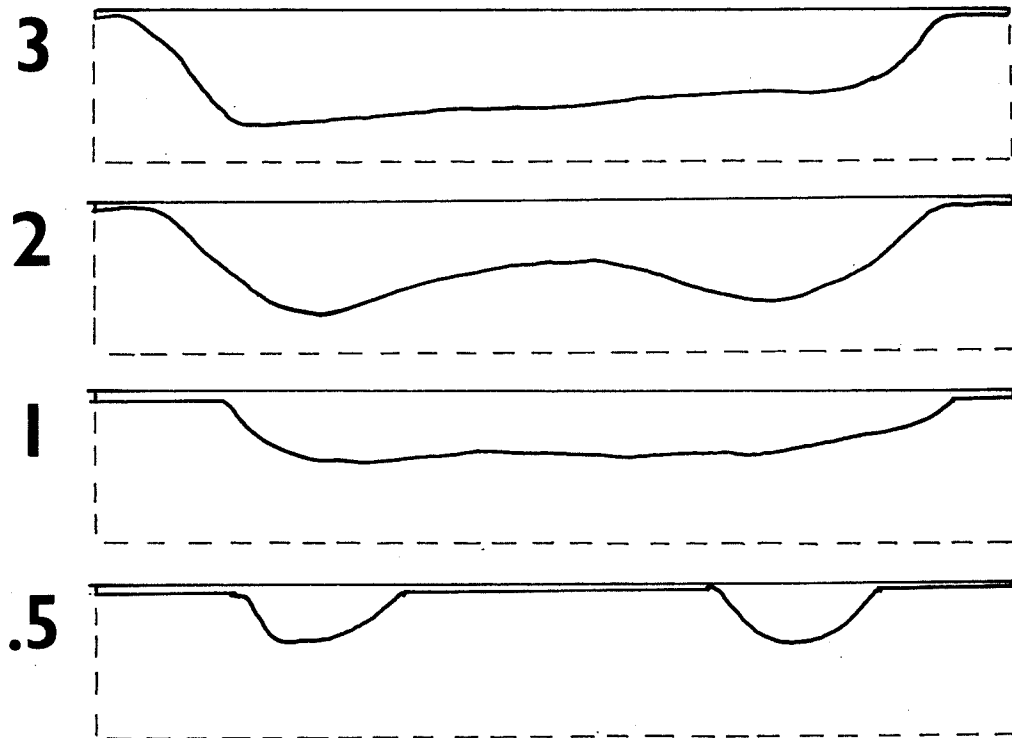
s = .08 cu. ft.
of ice





s=.08 cu. ft.
of ice

PHOTOGRAPH OF HANGING DAM
HANGING DAM CROSS-SECTIONS



PLAN VIEW

STATION FT.

ELEVATION
1.445
1.44
1.435
1.43
1.425